LACK OF PHOSPHATIDATE PHOSPHATASE CAUSES REDUCED CHRONOLOGICAL LIFE SPAN THROUGH INCREASED ENERGY EXPENDITURE AND OXIDATIVE STRESS

By

YEONHEE PARK

A dissertation submitted to the

Graduate School-New Brunswick

Rutgers, The State University of New Jersey

In partial fulfillment of the requirements

For the degree of

Doctor of Philosophy

Graduate Program in Food Science

Written under the direction of

George M. Carman

And approved by

_____

_____

_____

_____

New Brunswick, New Jersey

May, 2015

ABSTRACT OF THE DISSERTATION

Lack of Phosphatidate Phosphatase Causes Reduced Chronological Life Span through Increased Energy Expenditure and Oxidative Stress

By YEONHEE PARK

Dissertation Director:

Dr. George M. Carman

In *Saccharomyces cerevisiae*, Pah1 phosphatidate phosphatase, which catalyzes the dephosphorylation of phosphatidic acid (PA) to yield diacylglycerol (DAG), plays a major role in the synthesis of the storage lipid triacylglycerol. The evolutionarily conserved enzyme also regulates *de novo* phospholipid synthesis by controlling the level of PA, a precursor of membrane phospholipids. In this work, we showed that the *pah1*Δ mutant is defective in growth on non-fermentable carbon sources. Despite its apparent phenotype for respiratory deficiency, the *pah1*Δ mutant exhibited typical mitochondrial attributes, and even had an elevated mitochondrial membrane potential at the post-diauxic shift. Although oxidative phosphorylation was not compromised, the cellular levels of ATP in quiescent *pah1*Δ mutant cells were reduced by two-fold, which correlated with a four-fold increase in membrane phospholipids. Furthermore, the quiescent mutant cells exhibited three-fold elevations in mitochondrial superoxide and cellular lipid

hydroperoxides, and acute sensitivity to hydrogen peroxide. Consequently, the *pah1*Δ mutant had a shortened chronological life span. This phenotype, along with the inability to grow on non-fermentable carbon sources and sensitivity to hydrogen peroxide was complemented by loss of the *DGK1*-encoded DAG kinase indicating that the underpinning of *pah1*Δ defects in quiescence was the imbalance of PA/DAG. These results indicate that Pah1 PAP plays a crucial role in energy conservation and chronological life span through its regulation of lipid synthesis.

ACKNOWLEDGEMENTS

First and foremost, I would like to express sincere gratitude and appreciation to my advisor, Dr. George M. Carman for his encouragement, patience, and support throughout my graduate program. As a mentor, he guided and motivated me to develop my scientific way of thinking and fulfill my research. He always welcomed me with a smile and gave various directions to overcome difficulties and improve my knowledge and insight.

I thank sincerely my dissertation committee members, Dr. Gil-Soo Han, Dr. Loredana Quadro, and Dr. Peter Gillies for their valuable suggestions, comments and feedback for my dissertation.

I am also grateful to passionate and brilliant Carman laboratory members, former members, and the department of food science friends; Stylianos Fakas, Hyeon-Son Choi, Minjung Chae, Florencia Pascual, Wen-Min Su, Lu-Sheng Hsieh, Yixuan Qiu, Younkyung Kim, Yang-Jin Jung, Hyein Jang, and Jiin Jung. They were willing to share their experimental skills and scientific knowledge for my research and I had pleasant and enjoyable days with them during my graduate study.

I would like to thank my loving family. They always prayed for me and encouraged me when I was exhausted. With their love and support, I could successfully finish my research.

Finally, I thank God for meeting valuable people and gaining a lot of experience.

TABLE OF CONTENTS

LIST OF TABLES

LIST OF ILLUSTRATIONS

LIST OF ABBREVIATIONS

ATP	adenosine triphosphate
CDP-DAG	cytidine diphosphate diacylglycerol
CL	cardiolipin
CTP	cytidine triphosphate
DGK	diacylglycerol kinase
DHAP	dihydroxyacetone phosphate
ETC	electron transport chain
ER	endoplasmic reticulum
FAD	flavin adenine dinucleotide
GPDH	glycerol-3-phosphate dehydrogenase
NADH	nicotinamide adenine dinucleotide
PA	phosphatidic acid
PAP	phosphatidate phosphatase
PC	phosphatidylcholine
PE	phosphatidylethanolamine
PG	phosphatidylglycerol
PGP	phosphatidylglycerophosphate
PI	phosphatidylinositol
PKA	protein kinase A
PKC	protein kinase C
PS	phosphatidylserine

ROS	reactive oxygen species
SC	synthetic complete
TAG	triacylglycerol
TLC	thin layer chromatography
TMRM	tetramethylrhodamine methyl ester
UAS_{INO}	inositol-responsive upstream activating sequence

INTRODUCTION

The synthesis of lipids is an energy (e.g., ATP) consuming process that cells engage in throughout growth (1-4). In our laboratory, we utilize the unicellular eukaryote yeast *Saccharomyces cerevisiae* to study the regulation of lipid synthesis. Yeast synthesizes lipids that are typical of multicellular higher eukaryotes (5-7). Compared with other eukaryotic organisms, its genetic manipulation is easily accomplished for gene knockout and overexpression. In addition, the entire genome sequence information of *S. cerevisiae* allows for the genomic and proteomic analyses of lipid metabolism (5-7). Furthermore, with its short doubling time (ca, 90 min), yeast are easily grown to a large quantity for isolation of enzymes for biochemical studies (5-7).

Pah1 Phosphatidate Phosphatase

In exponentially growing yeast, phospholipids are synthesized from the precursor phosphatidic acid (PA) via the liponucleotide intermediate cytidine diphosphate diacylglycerol (CDP-DAG) for the formation of cellular membranes (2, 3). As cells progress into the stationary phase, PA is channeled to DAG for the formation of the neutral storage lipid triacylglycerol (TAG) (8, 9). The PA phosphatase (PAP), which catalyzes the dephosphorylation of PA to produce DAG and inorganic phosphate (P_i), has emerged as a key enzyme that controls the synthesis of phospholipids and TAG (Fig. 1) (2, 3, 10-12). Since the discovery of PAP activity in chicken liver by Smith *et al.* in 1957, the enzyme activity has been known to be of two types based on the requirement of magnesium ion (Mg^{2+})as a cofactor, i.e., Mg^{2+}-dependent and Mg^{2+}-independent (10, 13).

FIGURE 1. Reaction catalyzed by phosphatidate phosphatase. The figure shows the reaction catalyzed by the PAP enzyme. In yeast, two forms of the enzyme exist; one form requires Mg^{2+} as a cofactor and the other enzyme has no cofactor requirement.

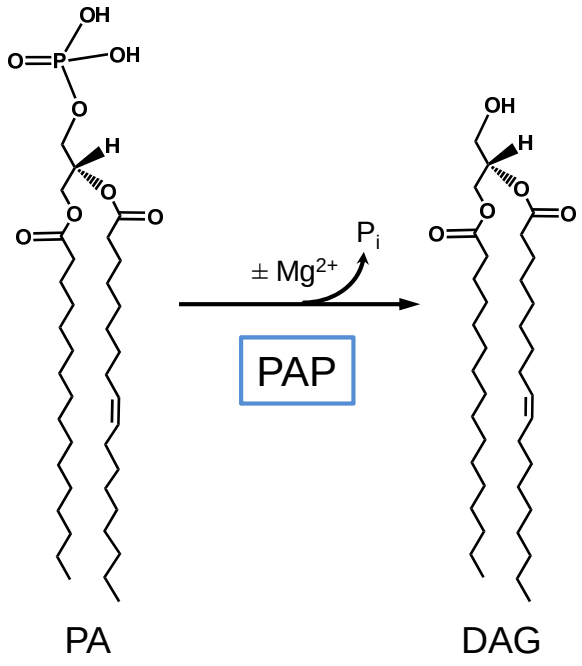
OH
O=P
OH
O
H
O
O
O
O
O
± Mg2+
Pi
PAP
OH
H
O
O
O
O
PA
DAG

In *S. cerevisiae*, all of the genes encoding of PAP enzymes have been identified mainly through their purification (12). The Mg^{2+}-independent PAP is encoded by the *DPP1* (diacylglycerol pyrophosphate phosphatase) and *LPP1* (lipid phosphate phosphatase) genes (14, 15). The *DPP1* gene was identified using the sequence information of the purified enzyme that catalyzes the dephosphorylation of diacylglycerol pyrophosphate (DGPP) to produce PA (14, 16). Subsequently, the *LPP1* gene was identified by its sequence similarity to the *DPP1* gene (15). Dpp1 (33.5 kDa) and Lpp1 (31.6 kDa) are integral membrane enzymes that are localized to the vacuole and the endoplasmic reticulum (ER) compartments, respectively (17, 18). These enzymes have broad substrate specificity and catalyze the dephosphorylation of diverse lipid phosphate molecules including PA, DGPP, lyso-PA (14-16, 19). They contain a conserved three-domain lipid phosphatase motif that is composed of the consensus sequences KX_6RP, PSGH, and SRX_5HX_3D (20). The Mg^{2+}-independent enzymes are implicated to play roles in lipid signaling rather than in lipid (e.g., TAG) synthesis.

The Mg^{2+}-dependent PAP is encoded by the *PAH1* (phosphatidic acid phosphohydrolase) and *APP1* (actin patch protein) genes. The *APP1* gene was identified from the sequence information of the PAP enzyme purified from yeast cells lacking the PAP-encoding genes *PAH1*, *DPP1*, and *LPP1* (21, 22). App1 (66 kDa) is a peripheral membrane enzyme containing the D*X*D*X*(T/V) catalytic motif in a domain that is weakly similar to a haloacid dehalogenase (HAD)-like domain (22, 23). App1p is conserved only in fungi and catalyzes the dephosphorylation of PA and other lipid phosphate molecules such as lyso-PA and DGPP (22). That App1 is shown to interact with many actin patch proteins implicates the role of the enzyme in endocytosis (22). The *PAH1*

gene was identified by the reverse genetic approach using the sequence information of the purified enzyme that catalyzes the Mg^{2+}-dependent dephosphorylation of PA (21). Pah1 (95 kDa) does not have a transmembrane region and thus functions on the membrane as a peripheral membrane enzyme (21). This enzyme, which translocates from the cytosol to the nuclear/ER membrane, plays a major role in *de novo* lipid synthesis, particularly in the synthesis of the storage lipid TAG. Pah1 PAP is specific for PA, and its enzymatic activity is based on the D*X*D*X*(T/V) catalytic motif within the HAD-like domain that is evolutionarily conserved in eukaryotes (21, 24). The genetic and biochemical studies of Pah1 and its orthologs in mammalian cells have revealed that the PAP enzyme is a major regulator in lipid homeostasis and cell physiology (10, 11, 25-30).

Roles of Pah1 Phosphatidate Phosphatase in the Synthesis of Phospholipids and Triacylglycerol

In the exponential phase, Pah1 PAP activity is relatively low and PA is primarily partitioned to CDP-DAG by the Cds1 CDP-DAG synthase (Fig. 2A) (31, 32). CDP-DAG is a high-energy liponucleotide intermediate found at a branch point in phospholipid synthesis, and is converted to diverse phospholipids. CDP-DAG reacts with inositol to produce phosphatidylinositol (PI), which is catalyzed by the Pis1 PI synthase (Fig. 3) (33, 34). CDP-DAG also reacts with serine to produce phosphatidylserine (PS), which is catalyzed by the Cho1 PS synthase (35). The PS is then decarboxylated to phosphatidylethanolamine (PE) by the Psd1/Psd2 PS decarboxylases (Fig. 3). In yeast, most PE is produced by the Psd1 PS decarboxylase

localized to the inner mitochondrial membrane, whereas a minor portion of PE is synthesized by the Psd2 PS decarboxylase localized in Golgi and vacuole membranes (36-38). PE is then converted to phosphatidylcholine (PC) through three sequential methylations in which the first reaction is catalyzed by the Cho2 PE methyltransferase and the next two reactions are catalyzed by the Opi3 phospholipid methyltransferase in the ER (Fig. 3) (39-42). When cells are supplemented with ethanolamine or choline, PE and PC are synthesized via the Kennedy pathway (Fig. 3). These lipid precursors are phosphorylated by the Eki1ethanolamine kinase and the Cki1 choline kinase, respectively, to produce phosphoethanolamine and phosphocholine, which are then converted to CDP-ethanolamine and CDP-choline by the Ect1 phosphoethanolamine cytidylyltransferase and the Pct1 phosphocholine cytidylyltransferase, respectively (43-46). CDP-ethanolamine and CDP-choline may then react with DAG (generated by the Pah1 PAP reaction) to produce PE and PC by the Ept1 ethanolamine phosphotransferase and the Cpt1 choline phosphotransferase, respectively (47, 48). The synthesis of PC and PE via the Kennedy pathway becomes essential in yeast cells defective in the *de novo* phospholipid synthesis via the CDP-DAG pathway (5, 49, 50). In mitochondria, CDP-DAG is also generated from PA by Tam41 CDP-DAG synthase (51). Here, the CDP-DAG reacts with glycerol-3-phosphate to produce phosphatidylglycerophosphate (PGP) by the Pgs1 PGP synthase (52, 53) (Fig. 3). The PGP is then dephosphorylated to phosphatidylglycerol (PG) by the Gep4 PGP phosphatase (54). The PG then combines with another molecule of CDP-DAG to produce cardiolipin (CL) in a reaction catalyzed by the Crd1 CL synthase (55, 56). The CL is then subject to remodeling of its acyl chains: it is deacylated by the Cld1 CL-specific deacylase to produce monolysoCL

(MLCL), which is then reacylated by the Taz1 taffazin acyltransferase to produce the mature form of CL (57, 58).

FIGURE 2. Synthesis of phospholipids and triacylglycerol during the growth of *S. cerevisiae*. *A*, CDP-DAG pathway predominates during exponential phase. *B*, TAG synthesis is elevated by Pah1 PAP activity as cells progress to stationary phase. *C*, TAG is hydrolyzed to DAG, and then the DAG is phosphorylated by Dgk1 DAG kinase activity for the phospholipid synthesis during growth resumption. The bold type indicates the predominate pathway during each growth phase.

A.

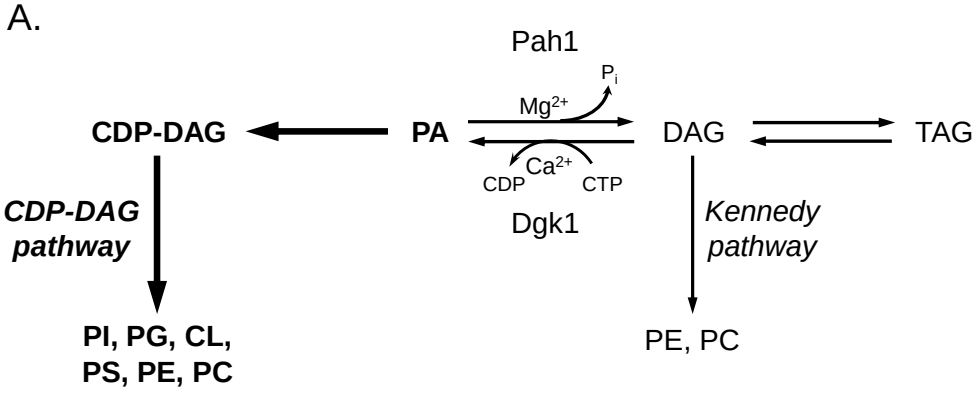
Pah1
P_i
Mg^{2+}
CDP-DAG
PA
DAG
TAG
Ca^{2+}
CDP
CTP
Dgk1
CDP-DAG pathway
Kennedy pathway
PI, PG, CL, PS, PE, PC
PE, PC

B.

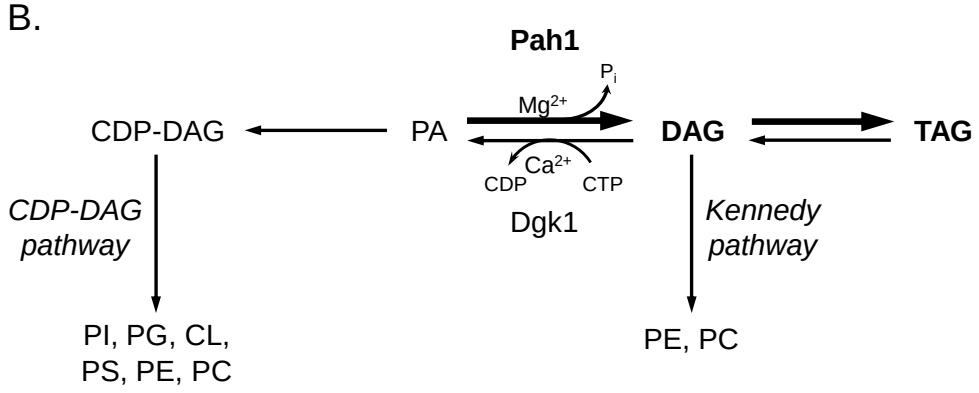
Pah1
P_i
Mg^{2+}
CDP-DAG
PA
DAG
TAG
Ca^{2+}
CDP
CTP
Dgk1
CDP-DAG pathway
Kennedy pathway
PI, PG, CL, PS, PE, PC
PE, PC

C.

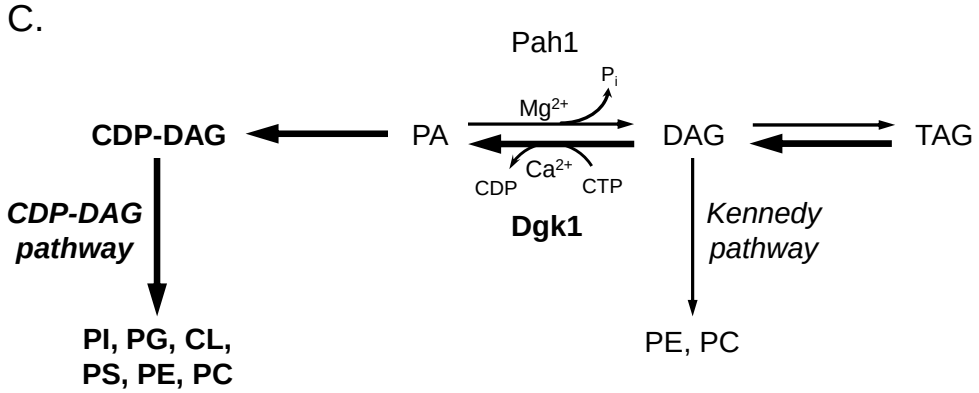
Pah1
P_i
Mg^{2+}
CDP-DAG
PA
DAG
TAG
Ca^{2+}
CDP
CTP
Dgk1
CDP-DAG pathway
Kennedy pathway
PI, PG, CL, PS, PE, PC
PE, PC

FIGURE 3. Pathways for the conversion of phosphatidic acid to phospholipids and triacylglycerol in *S. cerevisiae*. Red color, lipids and enzymes involved in the CDP-DAG pathway; Blue color, lipids and enzymes involved in the Kennedy pathway.

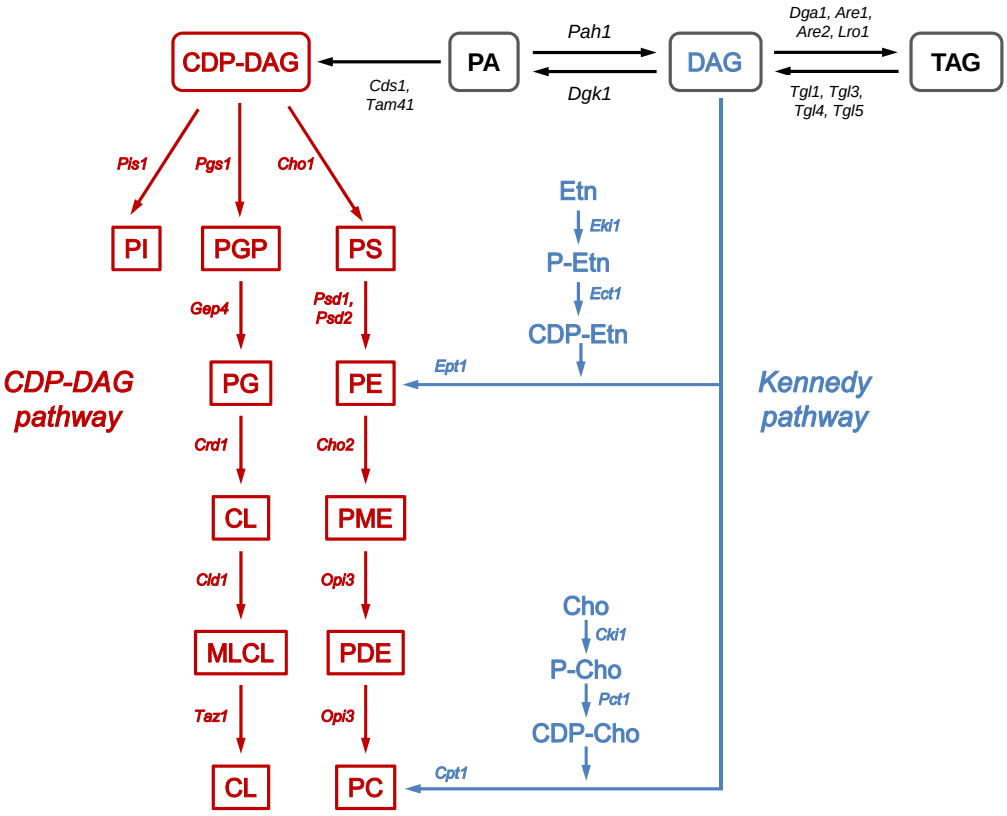
CDP-DAG
PA
DAG
TAG
Pah1
Dga1, Are1, Are2, Lro1
Cds1, Tam41
Dgk1
Tgl1, Tgl3, Tgl4, Tgl5
Pis1
Pgs1
Cho1
PI
PGP
PS
Etn
Eki1
P-Etn
Ect1
CDP-Etn
Gep4
Psd1, Psd2
Ept1
CDP-DAG pathway
PG
PE
Kennedy pathway
Crd1
Cho2
CL
PME
Cld1
Opi3
Cho
Cki1
P-Cho
Pct1
CDP-Cho
MLCL
PDE
Taz1
Opi3
Cpt1
CL
PC

As the cells progress into the stationary phase, PAP activity is increased and PA is primarily converted to DAG (Fig. 2B) (8, 59, 60). The DAG is then acylated to produce TAG in a reaction catalyzed by the Dga1/Are1/Are2 acyl-CoA-dependent DAG acyltransferases or by the Lro1 acyl-CoA-independent DAG acyltransferase (Fig. 3) (61-65).

Quiescent stationary phase cells may resume logarithmic if supplemented with fresh growth medium (Fig. 2C). The TAG synthesized during the transition to stationary phase is hydrolyzed by Tgl3/Tgl4 TAG lipases to produce fatty acid and DAG (Fig. 3) (66, 67). The fatty acid can be used for *de novo* phospholipid synthesis through the acylations of glycerol-3-phosphate to form PA and the DAG produced from the lipase reaction can be converted back to PA by Dgk1 DAG kinase (68, 69). In either case, the PA produced is converted to CDP-DAG for phospholipid synthesis as discussed above.

In addition to their roles as lipid intermediates, the substrate PA and product DAG of the Pah1 PAP reaction also function as signaling molecules in diverse cellular processes. For example, PA is implicated in membrane proliferation, secretion, and vesicular trafficking, whereas in higher eukaryotes, DAG is involved in the activation of protein kinase C (70-79). In yeast, PA plays a role in regulating the expression of the UAS_{INO}-containing phospholipid synthesis genes through its affinity with the transcriptional repressor Opi1 (80). When the level of PA is increased in the nuclear/ER membrane, Opi1 becomes inactive by being tethered to the membrane through its interaction with PA and Scs2. In contrast, when the level of PA is decreased, Opi1 is dissociated from the interaction and translocates into the nucleus where it represses the transcription of the UAS_{INO}-containing genes by binding to the Ino2 subunit of the Ino2-

Ino4 transcriptional activator complex (80, 81).

Phenotypes of *pah1*Δ

The importance of Pah1 PAP in TAG synthesis as well as in the regulation of phospholipid synthesis is indicated by diverse phenotypes of cells lacking the enzyme, many of which are intimately related to the increased level of PA and the decreased levels of DAG and TAG (21, 24, 59, 82, 83). The lack of Pah1 in the cell causes the accumulation of its substrate PA as well as the increased conversion of PA to phospholipids. The increased level of PA in the *pah1*Δ mutant induces the expression of the UAS_{INO}-containing lipid synthesis genes (as mediated by the repressor Opi1), resulting in an increase in phospholipid synthesis (82). Considering that Pah1 PAP activity is elevated as yeast cells progress to the stationary phase, the effect of the enzyme loss on phospholipid synthesis is greater in the stationary phase when compared with the exponential phase (59). The increased levels of phospholipids in the *pah1*Δ mutant are responsible for aberrant expansion of the nuclear/ER membrane (24, 82). The reduction of TAG levels in the *pah1*Δ mutant correlates with reduced number of lipid droplets when compared with wild type cells (59, 83). The *pah1*Δ mutant defective in DAG acylation accumulates unincorporated fatty acids, and thereby becomes sensitive to exogenously supplemented fatty acids (59). Moreover, the *pah1*Δ mutant exhibits the apoptotic phenotype in the stationary phase of growth (59).

The *pah1*Δ mutant also exhibits phenotypes whose molecular basis in connection with its altered lipid metabolism is not yet clear. It is defective in cell wall integrity and easily ruptured by sonication (84, 85). In addition, the *pah1*Δ mutant exhibits a high

mannose-to-glucose ratio, a high level of *N*-acetyl-glucosamine (GlcNAc) in cell wall, and hypersensitivity to K1 killer toxin (84). Moreover, it is defective in vacuole fusion, and exhibits small fragmented vacuoles as opposed to large vacuoles in the stationary phase (86). Furthermore, the *pah1*Δ mutant is sensitive to high temperature (37 °C) (21). Finally, the *pah1*Δ mutant cannot utilize the non-fermentable carbon source glycerol, suggesting a respiratory deficiency (24).

Effects of Dgk1 Diacylglycerol Kinase on the *pah1*Δ Phenotypes

Some of the phenotypes caused by the *pah1*Δ mutation require Dgk1 DAG kinase activity to produce PA, and consequently, its loss complements some *pah1*Δ phenotypes (see below). The *dgk1*Δ single mutation does not lead to remarkable phenotypes (87). However, the overexpression of *DGK1* gene causing the increase in the level of PA, like that occurring in the *pah1*Δ mutant, results in the temperature sensitivity at 37 °C and the abnormal nuclear/ER membrane expansion (68). Furthermore, Dgk1 activity is increased in the *pah1*Δ mutant when compared with that of wild type cells (87). The deletion of *DGK1* gene in the *pah1*Δ mutant affects lipid composition displaying the normal level of PA, and the decrease in the level of phospholipids (87). However, the phospholipid levels are still higher than that of wild type cells because of the low level of TAG in the *dgk1*Δ *pah1*Δ mutant (87). The aberrant expansion of the nuclear/ER membrane and lipid droplet morphology of the *pah1*Δ mutant are complemented by the deletion of the *DGK1* gene (87). The inositol auxotrophy caused by the overexpression of *PAH1* gene (because of the PA connection with the repressor Opi1) is also complemented by the overexpression of the *DGK1* gene (87).

Mammalian Orthologs of Pah1

In mammals, lipin-1 is a Pah1 ortholog (21). *Lpin1* was found as a mutated gene in the fatty liver dystrophy (*fld*) mouse displaying hypertriglyceridemia and insulin resistance due to diminished adipose tissue development (88). The molecular function of *Lpin1*-encoded protein was revealed through the discovery of Pah1 PAP in *S. cerevisiae* (21). Pah1 and lipin-1 share the conserved NLIP at the N-terminus and the HAD-like domain at the C-terminus (21, 88). Like a Pah1, all lipins require Mg^{2+} as a cofactor for the enzyme activity, and are specific for PA (89). In mammals, lipin-2 and lipin-3 also exhibit PAP activity (89). The *Lpin-1* mutation in mice results in reduced adipose tissue mass and insulin resistance (88, 90). In addition, the deletion of *Lpin-1* in Schwann cells causes peripheral neuropathy by demyelination due to endoneurial accumulation of PA (91, 92). On the other hand, the tissue-specific overexpression of *Lpin-1* in transgenic mice promotes obesity (90). Furthermore, lipin-1 and lipin-2 mutations in humans exhibit childhood rhabdomyolosis and cardiac dysfunction, and Majeed syndrome, respectively (93, 94).

Regulation of Pah1 Phosphatidate Phosphatase by Phosphorylation/Dephosphorylation

The function of Pah1 PAP as a peripheral membrane enzyme is regulated by its phosphorylation and dephosphorylation for its subcellular localization, catalytic activity, and abundance (82, 95-102). The enzyme in its phosphorylated state is cytosolic and inactive. The cytosolic Pah1 PAP translocates to the nuclear/ER membrane via its dephosphorylation, and the dephosphorylated enzyme associated with the membrane is

physiologically active. In addition to its subcellular localization, the catalytic activity and protein stability of Pah1 PAP are also regulated by phosphorylation and dephosphorylation (12).

Pah1 PAP is one of the most highly phosphorylated proteins in *S. cerevisiae*, and is shown to be phosphorylated by multiple protein kinases presumably in the cytosol (96-98, 103). Previous studies on Pah1 PAP showed that it is a physiological target for phosphorylation by Pho85-Pho80, Cdc28-cyclin B, protein kinase A (PKA), and protein kinase C (PKC) (96-99). Pah1 PAP is phosphorylated by Pho85-Pho80 at seven residues (Ser^{110}, Ser^{114}, Ser^{168}, Ser^{602}, Thr^{723}, Ser^{744}, and Ser^{748}), that are contained within the minimal Ser/Thr-Pro motifs (95, 97). In Pah1 PAP, simultaneous mutations of the seven phosphorylation sites to non-phosphorylatable alanine residues (7A mutant) results in a 1.8-fold increase in its PAP activity (95). In contrast, phosphorylation of *E. coli*-expressed Pah1 PAP at the seven sites causes a 6-fold reduction in its catalytic efficiency (V_{max}/K_m). Compared with wild type Pah1 PAP, the phosphorylation-deficient form of the enzyme is lower in its overall abundance, but shows a much higher level of the membrane association (97). Of the seven phosphorylation sites, three sites (Ser^{602}, Thr^{723}, and Ser^{744}) are also catalyzed by the Cdc28-cyclin B complex (96). The alanine mutations of Pah1 PAP on these phosphorylation sites have little effect on its PAP activity *in vitro* (96). The phosphorylation of Pah1 PAP by PKA occurs at Ser^{10}, Ser^{677}, Ser^{773}, Ser^{774}, and Ser^{788}. The PKA-mediated phosphorylation of Pah1 PAP at Ser^{10} has an inhibitory effect on its PAP activity, and affects the localization and function of the PAP enzyme in conjunction with phosphorylation by Pho85-Pho80 and Cdc28-cyclin B (98). Furthermore, Pah1 is phosphorylated by PKC at Ser^{677}, Ser^{769}, Ser^{773}, and Ser^{788}.

Of these residues, Ser^{677}, Ser^{773}, and Ser^{788} are common target sites for phosphorylation by PKA. Unlike Pho85-Pho80 and PKA, PKC has no major effect on the catalytic activity and the subcellular localization of Pah1 PAP (99). However, phosphorylation of Pah1 PAP by PKC has the effect of reducing the enzyme level when it is not pre-phosphorylated by Pho85-Pho80 (99).

The translocation of Pah1 PAP from the cytosol to the membrane surface requires its dephosphorylation that is catalyzed by the Nem1 (catalytic subunit)-Spo7 (regulatory subunit) phosphatase complex localized in the nuclear/ER membrane (100, 104). Like Pah1 PAP, Nem1 has the D*X*D*X*T(T/V) catalytic motif in the HAD-like domain (104-106). In the process of the membrane translocation, Pah1 PAP interacts with the Nem1-Spo7 phosphatase complex through its acidic tail, and once dephosphorylated, Pah1 PAP interacts with the membrane through its N-terminal amphipathic helix. The membrane-associated Pah1 PAP catalyzes the dephosphorylation of PA to produce DAG, and then it is degraded by proteasomes (82, 96, 100, 102, 104).

Regulation of Pah1 Phosphatidate Phosphatase by Other Factors

Pah1 PAP activity is also regulated by negatively charged phospholipids including CDP-DAG and PI or positively charged sphingoid bases such as sphinganine and phytosphingosine (107, 108). Negatively charged phospholipids enhance Pah1 PAP activity, resulting in increased TAG synthesis or PE/PC synthesis via the Kennedy pathway (107). CDP-DAG and PI decrease the K_m of Pah1 PAP for PA, and the reduced PA level by Pah1 PAP activity represses UAS_{INO}-containing genes that encode enzymes for phospholipid synthesis via the CDP-DAG pathway (81, 107). On the other hand,

positively charged sphingoid bases decrease Pah1 PAP activity in a parabolic competitive manner, leading to the elevated PA level, which is not converted to DAG by Pah1 PAP, derepresses UAS_{INO}-containing genes (107, 108).

In addition, nucleotides, ATP, and CTP affect Pah1 PAP activity by a decrease in the catalytic efficiency and the chelation of the cofactor, Mg^{2+} (109). The elevated cellular ATP level favors increases in the PA level and phospholipid synthesis (109). High CTP level also favors the increase in PA level and derepression of UAS_{INO}-containing genes (110). On the other hand, the low ATP level favors TAG synthesis than phospholipids synthesis (109).

Pah1 PAP is genetically regulated at the transcriptional level by growth phase and nutrient availability (60, 111). The expression of *PAH1* gene is induced in the stationary phase more than in the exponential phase (8). Accordingly, during the exponential phase, membrane phospholipid synthesis occurs for cell growth, and then TAG synthesis is progressed at the expense of phospholipid synthesis in the stationary phase. Furthermore, transcriptional regulation of Pah1 PAP by the growth phase is enhanced by inositol supplementation in the stationary phase cells (60). The regulation of the *PAH1* expression in response to growth phase is also mediated by Ino2/Ino4/Opi1 regulatory circuit and transcriptional factors, Gis1 and Rph1 (2, 3, 60). The essential mineral zinc, which serves as a cofactor for various enzymes, controls the expression of *PAH1* gene (111, 112). In the zinc depletion, the zinc-sensing and zinc-inducible transcriptional activator Zap1 is induced, and then Zap1 binds to the zinc-responsive *cis*-acting element (UAS_{ZRE}) which is located in the *PAH1* promoter (111). Accordingly, Pah1 PAP activity is induced, resulting in the increase in TAG synthesis (111).

Mitochondria

The mitochondria is a double membrane–bound organelle found in most eukaryotic cells, and consist of several compartments including the outer membrane, the inner membrane, the intermembrane space, the cristae space, and the matrix. This organelle, which contains its own DNA (mtDNA) and a transcription/translation system, is required for essential cellular processes such as respiration, apoptosis, lipid synthesis, calcium signaling, and aging (113-115). The integrity of mitochondrial structure is crucial, and its alterations in humans, are shown to be intimately associated with neurodegenerative diseases such as Parkinson's and Alzheimer's diseases, ischemia, and peripheral neuropathy from AIDS (113, 116, 117). Furthermore, mitochondrial dysfunction contributes to the outbreak of metabolic syndromes including obesity, cardiovascular disease, and diabetes (118, 119).

Oxidative Phosphorylation in Mitochondria

Mitochondria produce ATP using an electron transport chain (ETC) localized in the inner mitochondrial membrane. In higher eukaryotic organisms, the ETC is comprised of four complexes: NADH-ubiquinone oxidoreductase (complex I), succinate-ubiquinone oxidoreductase (complex II), ubiquinol-cytochrome *c* oxidoreductase or cytochrome bc_1 complex (complex III), and cytochrome *c*-O_2 oxidoreductase (complex IV) (Fig. 4) (113). *S. cerevisiae* possesses external (encoded by *NDE1* and *NDE2*) and internal (encoded by *NDI1*) NADH dehydrogenases instead of complex I (120-123). The external NADH dehydrogenases facing the mitochondrial intermembrane space catalyze the oxidation of cytosolic NADH to NAD^+, whereas internal NADH dehydrogenase

facing the mitochondrial matrix oxidizes mitochondrial matrix NADH (120-123). Additionally, various systems involving the NAD-dependent and FAD-dependent glycerol-3-phosphate dehydrogenases (GPDH) and the ethanol-acetaldehyde shuttles also oxidize cytosolic NADH, providing electrons to the ubiquinone (coenzymeQ, or Q) (124-127). Complex II, which catalyzes the conversion of succinate to malate in the TCA cycle of the mitochondrial matrix, also transports electrons to the ubiquinone (128, 129). In the next step, ubiquinone reduced by electrons (ubiquinol) carries electrons to the cytochrome bc_1 complex and cytochrome *c* (130). Cytochrome *c* transfers electrons to the final acceptor (O_2), simultaneously creating an electrochemical gradient that is used by the F_1F_O-ATP synthase to drive the production of ATP from ADP (131-133). During the oxidative phosphorylation, complex III and IV pump protons into the mitochondrial intermembrane space in *S. cerevisiae*, creating the electrochemical gradient, whereas complex I as well as complexes III and IV functions as a proton pump in mammals (124).

FIGURE 4. ATP synthesis by oxidative phosphorylation in *S. cerevisiae*. Nde1/Nde2, external NADH dehygrogenase; Ndi1, internal NADH dehydrogenase; Gpd1/Gpd2, NADH-dependent GPDH; Gut2, FAD-dependent GPDH; II, succinate dehydrogenase; Q, ubiquinone; III, cytochrome bc_1 complex; Cyt *c*, cytochrome *c*; VI, cytochrome *c* oxidase; OMM, outer mitochondrial membrane; IMM, inner mitochondrial membrane; black arrow, electron pump; blue arrow, proton flow.

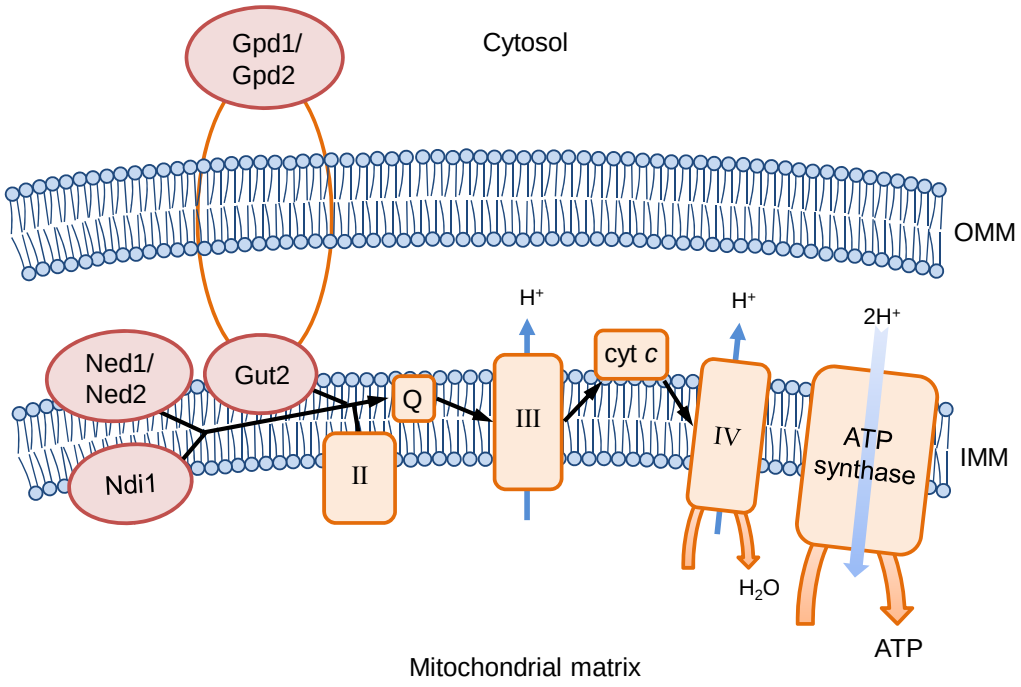
Gpd1/
Gpd2
Cytosol
OMM
Ned1/
Ned2
Gut2
Ndi1
Q
II
III
cyt c
IV
ATP
synthase
IMM
H+
H+
2H+
H2O
ATP
Mitochondrial matrix

Respiratory Supercomplexes in Mitochondria

The ETC exists in the cell as supramolecular structures termed respiratory supercomplexes. Complexes I, III, IV, and F_1F_o-ATP synthase are organized into respiratory supercomplexes that exhibit different combinations among organisms (134-139). Although the role of the supercomplex organization is still unclear, it is considered to be an important factor to understand oxidative phosphorylation of mitochondria. The formation of respiratory supercomplexes may increase the efficiency of electron transfer, but decrease the production of reactive oxygen species (ROS) (140-143). In the aging rat heart, the levels of respiratory supercomplexes have been shown to decrease without a reduction in levels of individual electron transport chain complexes (140). In cells of Barth syndrome patients, respiratory supercomplexes are shown to be less stable due to the lack of mature cardiolipin species (144). In addition, the supercomplex formation of F_1F_O-ATP synthase is related to inner mitochondrial membrane morphology (145).

Reactive Oxygen Species in Mitochondria

ROS such as superoxide anion ($O_2^{-}\cdot$), hydroxyl radical ($HO\cdot$), and hydrogen peroxide (H_2O_2) are highly reactive molecules generated from mitochondria, peroxisome, ER, and other compartments of cells (146-148). In particular, during oxidative phosphorylation, superoxide is formed by electron leakage from the ETC of mitochondria (149-151). ROS cause oxidative damage to surrounding molecules (e.g., DNA, protein, and lipid), which can lead to gene mutations, the loss of enzymatic activities and alterations in protein structure, the formation of toxic products, and eventually cell death (152-154). To minimize the detrimental damages of ROS, cells effectively remove them

by antioxidant enzymes such as superoxide dismutase (SOD), peroxidase, and catalase as well as by non-enzymatic systems (155). Cu, Zn-SOD (encoded by *SOD1*) localized in the cytosol/mitochondria and Mn-SOD (encoded by *SOD2*) localized in mitochondria convert superoxide anion into hydrogen peroxide (156-158). The hydrogen peroxide produced by SOD or other oxidative stresses is removed by catalases and glutathione peroxidases that convert it to oxygen and water. In *S. cerevisiae, CTT1*-encoded catalase T is localized in cytoplasm, whereas *CTA1*-encoded catalase A is localized in mitochondria and peroxisomes (159-162). Glutathione peroxidases (Gpx1, Gpx2, and Gpx3) remove not only hydrogen peroxide but also organic hydroperoxides to protect cells effectively from oxidative stress (163). In addition, a wide variety of antioxidants remove ROS to alleviate oxidative stress (154, 164).

In yeast, a mutation in Cu, Zn-SOD results in an increase in the rate of spontaneous mutation under aerobic condition, but not under anaerobic condition (165). In addition, cells lacking Cu, Zn-SOD exhibit a poor growth in the presence of non-fermentable carbon sources, cell death, and an increase in carbonylation damage to mitochondrial proteins (166). Moreover, deficiency of the enzyme leads to the vacuole fragmentation by an elevation of iron-mediated oxidation (167). The *sod2*Δ mutant exhibits sensitivity to pure oxygen on YEPD (3% glucose) and YPEG (3% ethanol and 3% glycerol) (168). Additionally, the lipid peroxidation of mitochondria caused by hydrogen peroxide decreases the activity of the complex III, leading to the stimulation of superoxide anion production and iron release (169). Moreover, yeast cells lacking the *CTT1* and *CTA1* genes exhibit an increase in sensitivity to hydrogen peroxide in the stationary phase, but do not show a noticeable growth defect under normal growth

conditions (170). In mice, overexpression of human catalase targeted to the mitochondria protects from the age-induced decrease in mitochondrial function and lipid-induced muscle insulin resistance (171). By contrast, other studies show that the inactivation of catalases extends chronological life span in *S. cerevisiae* by increasing the level of hydrogen peroxide which activates SOD (172). Although the relationship between ROS and cell survival is still a controversial issue, it is established that ROS is one of the critical factors for cell viability.

Lipid Synthesis in Mitochondria

Mitochondria also participate in lipid synthesis along with the ER, and have a distinct lipid composition when compared with other organelle membranes (131, 132, 173, 174). The major phospholipids constituting the mitochondrial membrane are imported from the ER, while CL, PE, and PG are synthesized at the inner mitochondrial membrane. CL plays a key role in mitochondrial functions such as respiratory supercomplex stabilization, mitochondrial protein import, ceramide synthesis, aging, and cell wall and vacuolar biogenesis (175-179). In yeast, the loss of Crd1 leads to a decrease in life span at 37 °C, respiratory deficiency, a loss of mtDNA, and swollen vacuolar morphology (177, 179, 180, 180, 181). Additionally, the *pgs1*Δ mutant exhibiting no detectable levels of both PG and CL significantly decreases the replicative life span at 30 °C (177). Phenotypes of tafazzin-deficient cells, which exhibit a decrease in chronological life span and a fermentative growth defect, are alleviated by mutation of *CLD1* gene controlling CL/MLCL ratio (182). Moreover, overexpression of Cld1 affects respiration, leading to decrease in ATP production from oxidative phosphoryaltion (182).

In *Trypanosoma brucei*, deletion of PG synthase gene causing a loss of PG and decrease in the level of CL alters mitochondrial morphology, and reduces the amount of respiratory complexes III and IV (183). On the other hand, acyl chain remodeling of CL by tafazzin does not affect mitochondrial morphology and mitochondrial function of oxidative phosphorylation in yeast, indicating that unremodeled CL supports roles of remodeled CL (184).

Mitochondrial morphology and function are also regulated by PE, a non-bilayer-forming phospholipid. In yeast, PE and CL have overlapping functions in mitochondrial fusion, and the lack of both phospholipids in the *crd1*Δ *psd1*Δ double mutant causes a defect in mitochondrial fusion, the loss of mtDNA, and the decrease in the mitochondrial membrane potential (185). In CHO cells, the reduction of mitochondrial PE by RNAi-mediated knock down of PS decarboxylase results in decreased respiratory capacity, ATP production, and activities of ETC, as well as a defect in the supercomplex organization (186). Cells deficient in mitochondrial PE also exhibit a gross defect in the mitochondrial ultrastructure (186). Similarly, inactivation of PS decarboxylase in mice causes the production of aberrant mitochondrial morphology, leading to embryonic lethality (187).

The minor lipids PA and DAG are critical to control fusion and fission events in mitochondria (188). Mitochondrial fusion and fission, which regulate the tubular network morphology of mitochondria, are associated to mitochondrial inheritance, repairing mtDNA, efficiency of ATP production and dissipation, mitophagy, and apoptosis (113, 116, 189-195). In plants, the addition of exogenous PA into cells depleted of phospholipase D, which hydrolyzes phospholipids into PA, increases ROS

production in the cellular membrane (196, 197). Therefore, lipid metabolism in mitochondria is a crucial for the mitochondrial function.

HYPOTHESIS

The loss of Pah1 PAP activity causes striking changes in the lipid composition, such as a great reduction in the TAG level, an accumulation of fatty acids, and a significant increase in membrane phospholipids (21, 24). These changes in lipid contents are directly or indirectly coupled to other phenotypes of the *pah1*Δ mutant, such as marked vacuole fragmentation, temperature sensitivity, fatty acid-induced lipotoxicity, and an aberrant expansion of the nuclear/ER membrane (21, 24, 59, 82, 83, 86). In particular, the *pah1*Δ mutant exhibits the respiratory deficiency phenotype as indicated by the inability to grow on glycerol, a non-fermentable carbon source (24). It is the molecular basis of this phenotype that this research addresses. Based on the fact that mitochondrial phospholipids are essential to mitochondrial function, we hypothesized that the inability to grow on non-fermentable carbon sources is due to an effect of the *pah1*Δ mutation on mitochondrial lipid metabolism, which in turn, has an impact on mitochondrial structure and function. We also addressed the hypothesis mitochondrial metabolism, such as the production of ROS has an impact on cell viability and chronological life span.

EXPERIMENTAL PROCEDURES

Materials

All chemicals were reagent grade or better. Growth medium components were obtained from Difco Laboratories. Phusion high fidelity DNA polymerase and the DNA gel extraction kit were purchased from New England Biolabs and Qiagen, respectively. Carrier DNA for yeast transformation was from Clontech. Sodium DL-lactate solution, potassium acetate, ethanol, DL-dithiothreitol (DTT), lyticase, sorbitol, sucrose, aprotinin, benzamidine, bovine serum albumin, leupeptin, pepstatin, phosphoenolpyruvate (PEP) phenylmethylsulfonyl fluoride (PMSF), 30% hydrogen peroxide solution, xylenol orange, ammonium iron (II) sulfate hexahydrate, sodium azide, potassium cyanide (KCN), phenazine methosulfate (PMS), diethyl ether, hydrogen chloride-methanol solution, 2-(4,5-dimethyl-2-thiazolyl)-3,5-diphenyl-2H-tetrazolium bromide (MTT), DL-glycerol-3-phosphate, dihydroxyacetonephosphate (DHAP), ATP, and nitro blue tetrazolium (NBT) were purchased from Sigma-Aldrich. BacTiter-Glo^{TM} Microbial Cell Viability Assay was purchased from Promega. DNA size ladders, molecular mass protein standards, electrophoresis reagents, Triton X-100, and protein assay reagent were from Bio-Rad. Polyvinylidene difluoride (PVDF) membrane and the enhanced chemifluorescence Western blotting detection kit were from GE Healthcare. Alkaline phosphatase-conjugated goat anti-rabbit IgG antibodies and alkaline phosphatase-conjugated goat anti-mouse IgG antibodies were from Thermo Scientific and Pierce, respectively. MitoSOX™Red mitochondrial superoxide indicator and tetramethylrhodamine methyl ester (TMRM), anti-porin (Por1) monoclonal antibody, anti-carboxypeptidase Y (Prc1)

monoclonal antibody, anti-OxPhos monoclonal antibody against subunit III (Cox3) of Complex IV, anti-phosphoglycerate kinase (Pgk1) antibody, and 3-12% polyacrylamide gradient gels were purchased from Life Technologies. Radiochemicals and primulin were from Perkin-Elmer Life Sciences and MP Biomedicals, respectively. Acrylamide solutions and scintillation counting supplies were from National Diagnostics. Silica gel 60 thin-layer chromatography (TLC) plates and glycerol were obtained from EM Science. Lipids and heptadecanoic acid (C17:0) were from Avanti Polar Lipids and Alfa Aesar, respectively.

Strain and Growth Conditions

The yeast strains used in this study are listed in Table 1. Yeast cells were grown at 30 °C in synthetic complete (SC)-glucose (2%) or YEPD (1% yeast extract, 2% peptone, and 2% glucose) medium. For growth on a non-fermentable source, 2% glucose was replaced with 2% ethanol, 3% glycerol, 2% acetate, or 2% lactate. The sensitivity of yeast cells to hydrogen peroxide was assessed with the reagent at the concentration of 0-1 mM or 0-4 mM depended on growth medium. The growth of yeast cells in liquid medium was measured by absorbance at 600 nm ($A_{600\ nm}$) using a spectrophotometer. For measurement of growth on solid medium, liquid culture was adjusted to $A_{600\ nm}$ = 0.67, followed by 10-fold serial dilutions. The serially diluted cell suspensions were spotted onto solid medium and cell growth was scored after incubation for 2-3 days. For the growth of strain BY4741, the SC-glucose medium was modified (concentrations of histidine, methionine, and leucine were increased, glutamine, phenylalanine, and inositol were added) for optimum growth (198).

TABLE I. Strains and plasmids used in this study

Strains or plasmids	Genotype or relevant characteristics	Source or Reference
E. coli		
DH5α	F$^-$ ϕ80d*lacZ*ΔM15Δ (*lacZYA-argF*)U169 *deoR rec*A1 *end*A1 *hsd*R17(r_k^- m_k^+) *pho*A *sup*E44 λ$^-$ *thi*-1 *gyr*A96 *rel*A1	(199)
S. cerevisiae		
W303-1A	*MAT***a** *ade2-1 can1-100 his3-11,15 leu2-3,112 trp1-1 ura3-1*	(200)
GHY57	*pah1*Δ*::URA3* derivative of W303–1A	(21)
YPY3	*dgk1*Δ*::HIS3* derivative of W303–1A	This study
YPY4	*dgk1*Δ*::HIS3 pah1*Δ*::URA3* derivative of W303–1A	This study
BY4741	*MAT***a** *his3*Δ*1 leu2*Δ*0 met15*Δ*0 ura3*Δ*0*	(201)
GHY57-3	*pah1*Δ*::URA3* derivative of BY4741	This study
Plasmid		
pGH317	*pah1*Δ*::URA3* inserted into YEp351	(21)
pYX142-mtGFP	plasmid for expression of GFP fused with mitochondrial presequence	(202)

DNA Manipulations and Yeast Transformation

Standard methods were used for isolation of chromosomal and plasmid DNA, for digestion and ligation of DNA, and for PCR amplification of DNA (199, 203). The plasmids used in this study are listed in Table 1. Transformations of *E. coli* and yeast were performed as described previously (199, 204).

Construction of the *dgk1*Δ and *dgk1*Δ *pah1*Δ Mutants

Yeast deletion mutations were generated by the method of one-step gene replacement (205). For construction of the *dgk1*Δ mutant (YPY3), the strain W303-1A was transformed with the *dgk1*Δ*::HIS3* disruption cassette that was amplified by PCR from the genomic DNA of the *dgk1*Δ::*HIS3* mutant in the RS453 strain background (87). The yeast transformant exhibiting histidine prototrophy was confirmed for the deletion of *DGK1* by PCR analysis. For construction of the *dgk1*Δ *pah1*Δ mutant (YPY4), YPY3 was transformed with the *pah1*Δ*::URA3* disruption cassette that was produced from pGH317 by digestion with XbaI and SphI (21). The *dgk1*Δ transformant exhibiting uracil prototrophy was confirmed for the deletion of *PAH1* by PCR analysis.

Preparation of Yeast Cell Extracts

All steps for preparation of yeast cell extracts were performed at 4 °C. Yeast cultures were harvested at 1,500 × g for 5 min, washed with water, resuspended in lysis buffer (50 mM Tris-HCl, pH 7.5, 0.3 M sucrose, 10 mM β-mercaptoethanol, 0.5 mM PMSF, 1 mM benzamidine, 5 μg/ml aprotinin, 5 μg/ml leupeptin, and 5 μg/ml pepstatin). The cell suspension was added with glass beads (0.5-mm diameter) and then subjected to

five repeats of 1 min burst and 2 min cooling using a BioSpec Product Mini-BeadBeater-16 (206). The disrupted cells were centrifuged at 1,500 × g for 10 min to separate unbroken cells and cells debris (pellet) from cell extracts (supernatant). The protein concentration of cell extracts was determined by the method of Bradford using bovine serum albumin as a standard (207).

Isolation of Mitochondria

Yeast mitochondria were prepared according to the method of Meisinger *et al*. (208). Exponential (4 L) and stationary phase (2 L) cultures were harvested, washed with water, and measured for cell wet weight. Cells were resuspended in 100 mM Tris-H_2SO_4 (pH 9.4) buffer containing 10 mM DTT (2 ml/g wet weight cells). After incubation for 20 min at 30°C with gentle shaking, the cell suspension was centrifuged at 3,000 × *g* for 5 min. The cell pellet was washed with 20 mM potassium phosphate (pH 7.4) buffer containing 1.2 M sorbitol, resuspended in the same buffer containing lyticase (3680 U/g wet cell), and incubated for 1.5 h at 30 °C with gentle shaking. The resulting spheroplasts were harvested by centrifugation for 5 min at 3,000 × *g*, washed, and resuspended with pre-cooled homogenization buffer (10 mM Tris-HCl buffer, pH 7.4, 0.6 M sorbitol, 1 mM EDTA, and 1 mM PMSF) at 6.5 ml/g wet cell weight, followed by disruption using a Dounce glass homogenizer with 15 strokes on ice. The homogenized spheroplasts were diluted 2-fold in the same buffer, and centrifuged at 1,500 × *g* for 5 min at 4 °C to remove cell debris and nuclei. The supernatants were centrifuged at 4,000 × *g* for 5 min at 4 °C, and the resulting supernatant was centrifuged at 12,000 × *g* for 15 min at 4 °C to collect crude mitochondria. The crude mitochondria (0.2 ml/mg) were

resuspended in SEM buffer (250 mM sucrose, 1 mM EDTA, 10 mM MOPS-KOH, pH 7.2), and homogenized with 10 strokes on ice (208). The homogenized mitochondria were layered on a gradient consisting of 15%, 23%, 32%, and 60% sucrose in 10 mM MOPS-KOH (pH 7.2) buffer containing 1 mM EDTA, and centrifuged at 134,000 × *g* (Beckman SW28 rotor) for 1 h at 4 °C. The mitochondrial fraction at the interface between the 32% and 60% sucrose layers was collected and diluted with 2 volumes of SEM buffer, followed by centrifugation at 10,000 × *g* for 15 min at 2 °C. Protein concentration of the purified mitochondria was determined by the method of Bradford using bovine serum albumin as a standard (207).

SDS-PAGE and Western Blot Analysis

SDS-PAGE using 10% slab gels and Western blotting using PVDF membrane were performed as described previously (209-211). Mouse anti-porin monoclonal antibodies, rabbit anti-PS synthase antibodies, mouse anti-carboxypeptidase Y monoclonal antibodies, and mouse anti-phosphoglycerate kinase antibodies were used at dilution of 1:1,000. Alkaline phosphatase-conjugated goat anti-mouse IgG antibodies and goat anti-rabbit IgG antibodies were used at a dilution of 1:5,000. Immune complexes were detected using the enhanced chemifluorescence Western blotting detection kit. Fluorimaging was used to acquire images from immunoblots, and the relative densities of the images were analyzed using ImageQuant software.

Blue Native Polyacrylamide Gel Electrophoresis

Mitochondria (200 μg) were isolated from yeast cultures ($A_{600\ nm}$ = 1.0-1.2) in

YPEG (1% yeast extract, 2% peptone, 0.95% ethanol, and 3% glycerol) medium, and were incubated for 1 h at 4 ºC with gentle shaking in 40 µl of digitonin buffer (30 mM HEPES-KOH, pH=7.4, 1.875% (w/v) digitonin, 50 mM potassium acetate, 2% glycerol, 1/50 volume protease inhibitor cocktail, and 1 mM PMSF). The lysed mitochondria were centrifuged at 125,000 × *g* (TLA-55 rotor) for 20 min at 4 ºC, and the supernatant was subjected to blue native-polyacrylamide gel electrophoresis (BN-PAGE) using a 3-12% linear gradient slab gel at 4 ºC for 20 h under a high voltage in the XCell Superlock Mini-Cell (212). Following electrophoresis, the polyacrylamide gel was stained with Coomassie blue or electroblotted onto a PVDF membrane. The protein complexes on the PVDF membrane were detected by immunoblotting with anti-OxPhos monoclonal antibody against subunit III of Complex IV (175). Data were analyzed using QuantityOne software from Bio-Rad.

Analysis of Mitochondrial Tubulation

Yeast strains transformed with pYX142–mtGFP (from M. Greenberg), and the transformants harboring the plasmid were selected for leucine prototrophy (202). The yeast transformants were grown at 30 °C in SC-glucose medium to the post-diauxic and the stationary phases, and were analyzed for green fluorescence by the Zeiss LSM 710 confocal microscope.

Electron Microscopy

Samples were prepared according to the method of Bozzola and Russell (213). The purified mitochondria were fixed with glutaraldehyde, washed with Millonig

phosphate buffer for 5 min, and then drawn off and placed in 2% osmium tetroxide for 60 min at 4 °C. Samples were rinsed with deionized water for 5 min and dehydrated at room temperature with ethanol (50% for 5 min, 70% for 10 min, 95% for 10 min, and 100% for 10 min (the 100% incubation was repeated 3 times)) and with propylene oxide (100 % for 10 min, repeated 3 times). Dehydrated samples were infiltrated with 50% mixture of epoxy resin and propylene oxide for 3 h followed by 100% epoxy resin for 2 h, embedded in 100% resin in a flat mold for orientation and allowed to polymerize overnight at 70 °C. 500 nm thick sections were cut using a glass knife and Leica Ultracut-R Ultramicrotome. They were heat-fixed to glass slides and stained for 20 seconds with Toluidine Blue to select the most appropriate areas for imaging. The selected block was trimmed and 120 nm thin sections were cut using Leica UC6 Ultramicrotome and diamond knife (Diatome-U.S.). 120 nm thin sections were placed on 100 and 150 mesh copper grid (EMS) and stained for 15 min with 2% uranyl acetate, rinsed with deionized water and further stained with Reynold's lead citrate for 5 min. The grids were imaged using JEOL 1200EX transmission electron microscope at 60 kv and captured with Gatan Orius 830 Digital imaging System.

Lipid Analysis

Lipids were extracted from purified mitochondria (500 μg) according to the method of Bligh and Dyer, and phospholipids were analyzed by two-dimensional TLC with HPTLC plates. The first dimension was separated using the solvent system of chloroform/methanol/ammonium hydroxide/water (45:25:2:3, v/v) for 40 min (214, 215). After drying the plate in the vacuum, the solvent system of chloroform/methanol/glacial

acetic acid/water (32:4:5:1, v/v) were used for phospholipid separation in the second dimension (215). After spraying with 0.05% primulin in acetone/water (80:20), phospholipids on the plates were visualized by fluoroimaging followed by quantification with ImageQuant software.

For fatty acid analysis by gas chromatography, extracted lipids from 1.5 mg of mitochondria were dried by nitrogen gas and resuspended in hexane. Mixture including sample, 1 ml of hydrogen chloride-methanol, 100 μg of heptadecanoic acid (C17:0) for standard were incubated for transmethylation at 70 °C for 1 h, and then cooled down at room temperature. 1 ml of 1N Sodium chloride and 2 ml of hexane were added to the mixture. After centrifugation, the upper phase was collected and added 2 volumes of toluene for preventing lipid oxidation, dried by nitrogen gas, and then resuspended in hexane. The analysis of fatty acid methyl esters was performed by a Hewlett Packard 5890 gas chromatography equipped with a 30-m X 0.32-mm Supelco MDN-55 column and a flame ionization detector; helium was the carrier gas (10 p.s.i.). The column temperature was programmed as follows: 100 °C for 10 min and then increased to 300 °C at 10 °C/min. The injector and detector temperatures were 250 °C. Fatty acid methyl esters were identified by reference standards.

For radiolabeling of lipids, yeast cells were grown in SC-glucose medium to the late exponential phase ($A_{600\,nm} \sim 1$). The cells were harvested, washed, and resuspended in SC-glycerol (3%) medium and [2-^{14}C]acetate (1 μCi/ml). After incubation for 4 h, the radiolabeled cells were harvested and lipids were extracted by the method of Bligh and Dyer (214). Radiolabeled lipids were separated by one-dimensional TLC on silica gel 60 plates using the solvent system of hexane/diethyl ether/gracial acetic acid (40:10:1, v/v)

(216). The radiolabeled lipids on the TLC plates were dried in a vacuum system, visualized by PhosphorImaging analysis, and quantified by ImageQuant software. [2-^{14}C]acetate was used as a standard to calculated the radioactivity of the radiolabeled lipids.

Measurement of Oxygen Consumption

For measurement of oxygen consumption, yeast cells were grown in SC-glucose medium to the post-diauxic and the stationary phases (217). The cultures were diluted 10-fold in the fresh medium, and were measured for oxygen consumption using an oxygen electrode (Vernier Labpro) in a 500 μl chamber. The cultures containing 0.05% sodium azide, which is one of ETC inhibitors, were used as controls to confirm mitochondrial oxygen consumption.

Measurement of Mitochondrial Membrane Potential

Mitochondrial membrane potential was measured using TMRM, which is a cationic red-orange fluorescent dye that is readily sequestered by active mitochondria. Yeast strains were grown to the post-diauxic and the stationary phases. The cultures corresponding to 1 $A_{600\ nm}$ unit of cells were harvested, washed twice with phosphate-buffered saline (PBS, pH 7.0), and then incubated for 30 min at 30 °C in the buffer containing 40 μM TMRM. After washing with PBS, the TMRM-labeled cells were diluted in PBS at $A_{600\ nm}$ = 0.1, and 10,000 cells were measured for fluorescence by C6 flow cytometer (BD Biosciences).

Mitochondrial ATP Synthase Activity

Mitochondrial F_1F_O-ATPase activity was measured by following the oxidation of NADH (extinction coefficient of 6,220 $M^{-1}cm^{-1}$) in the coupled reactions of pyruvate kinase and lactate dehydrogenase. The reaction mixture in a total volume of 1 ml contained 20 μg of mitochondria isolated from stationary phase cells, 50 μg/ml pyruvate kinase, 50 μg/ml lactate dehydrogenase, 50 mM HEPES-KOH (pH 8.0), 5 mM $MgSO_4$, 2.5 mM ATP, 2.5 mM PEP, 0.3 mM NADH, and 2 μg/ml antimycin. The enzyme reaction was initiated by addition of ATP into the reaction mixture, and $A_{340\ nm}$ was continuously measured for 2 min. The reaction was linear with time and protein concentration. Subsequently, the reaction mixture was added with 2 μg/ml oligomycin, an inhibitor for F_1F_O-ATPase activity, and the measurement was repeated to correct for non-mitochondrial ATPase activity. Specific activity was defined as nmol of NADH oxidized per min per mg of protein.

Measurement of ATP in Yeast Cells

Intracellular levels of ATP were measured by the luciferase assay using the BacTiter-Glo™ Microbial Cell Viability Assay kit. ATP reacts with luciferin by luciferase to generate adenyl-luciferin, which was then oxidized to generate light. Yeast cultures corresponding to 5 $A_{600\ nm}$ units of cells were harvested at indicated time points and resuspended in 80 μl sterile water, and mixed with an equal volume of BacTiter-Glo™ Reagent in 96 well opaque plates. After incubation for 3 min, luminescence produced from the cells was measured with a luminometer (Luminoskan Acent Microplate Leader). ATP (100 nM-100 μM) was used as a standard in the assay.

Measurement of Mitochondrial Superoxide

Intracellular superoxide levels were measured using MitoSOX Red, a mitochondrial superoxide indicator. Yeast cells were grown to the post-diauxic, and the stationary phases. The cultures corresponding to 1 $A_{600\ nm}$ units of cells were harvested, washed twice with PBS (pH 7.0), and then incubated for 30 min at 30 °C in the buffer containing 5 μM MitoSOX Red. After washing twice with PBS, the MitoSOX Red-labeled cells (10,000) were measured by C6 flow cytometer (BD Biosciences).

Measurement of Lipid Hydroperoxides

The levels of lipid hydroperoxides were measured by an assay using the ferrous oxidation-xylenol orange complex (218). Yeast cells were grown to the stationary phase in 500 ml of SC-glucose medium, and lipids were extracted by the method of Bligh and Dyer (214). The weight of extracted lipids were measured and dissolved in chloroform. 25 μl of lipid solution (1.25 mg of lipid) was mixed with an equal volume of a complex regent consisting of 2 M sorbitol, 3.9 mM ammonium iron (II) sulfate, 2.26 mM xylenol orange, and 2.8 % sulfuric acid. After incubation for 30 min, the reaction mixture was measured at $A_{560\ nm}$. The levels of lipid hydroperoxides were calculated using hydrogen peroxide as a standard.

Superoxide Dismutase Assay

SOD activity was determined in the polyacrylamide gel by NBT-negative staining (219, 220). For this assay, 10 μg of cell extracts was resolved by native PAGE with a 12% slab gel. The polyacrylamide gel was incubated for 10 min in 50 mM potassium

phosphate buffer (pH 7.8) and for 20 min in the buffer containing 0.5 mg/ml NBT, washed briefly, and then incubated for 15 min in the buffer containing 10 μg/ml of riboflavin and 0.25% TEMED. After washing, the polyacrylamide gel was illuminated on a light box for color development, and was subjected to image processing. The clear, unstained region, which indicates SOD activity, against a dark blue background was quantified by ImageQuant software.

Catalase Assay

Catalase activity was measured spectrophotometrically by following the decomposition of hydrogen peroxide (extinction coefficient of 40 $mM^{-1}cm^{-1}$) at $A_{240\ nm}$ (221). The reaction mixture in a total reaction volume of 250 μl contained 50 mM potassium phosphate buffer (pH 7.0), 20 mM hydrogen peroxide, 20 μg of cell extract or purified mitochondria. Specific activity was defined as the decomposition of 1 μmol of hydrogen peroxide per min per mg protein.

NADH-dependent Glycerol-3-Phosphate Dehydrogenase Assay

NADH-dependent GPDH activity was conducted with 40 μg of cell extract in 20 mM Imidazole-HCl (pH 7.0), 1 mM DTT, 1 mM $MgCl_2$, 0.09 mM NADH, 0.67 mM DHAP at room temperature using a spectrophotometer (222). An extinction coefficient of NADH is 6.22 $mM^{-1}\ cm^{-1}$ at $A_{340\ nm}$. Specific activity of NADH-dependent GPDH activity was defined as nmol of NADH oxidized per min per mg of protein.

FAD-dependent Glycerol-3-Phosphate Dehydrogenase Assay

Cells were grown in SC-ethanol (2%) medium at 30 °C with shaking overnight. The activity assay was performed for 10 min at $A_{562\ nm}$ using a spectrophotometer in a total volume of 1 ml containing 50 mM Hepes (pH 7.5), 10 mM KCN, 0.5 mM MTT, 0.2 mM PMS, 0.05% Triton X-100, 50 mM DL-glycerol-3-phosphate, 50 μM FAD, and 50 μg purified mitochondria at room temperature (223, 224). An extinction coefficient for reduced MTT at $A_{562\ nm}$ is 8.1 $mM^{-1}cm^{-1}$. Specific activity of FAD-dependent GPDH activity was defined as 1 nmol of MTT reduced per min per mg protein.

Analysis of Yeast Chronological Life Span

For analysis of chronological life span, yeast cultures saturated in SC-glucose medium were diluted in the fresh medium at $A_{600\ nm}$ = 0.01 and grown to the late exponential phase ($A_{600\ nm}$ ~ 1) (225). The exponential phase cells were diluted in the fresh medium at $A_{600\ nm}$ = 0.1, and grown for 2 days with shaking at 250 rpm. The cultures reached at the stationary phase (day 0) were continuously incubated for two weeks during which aliquots were taken daily and plated onto YEPD agar plates. Colonies formed after 2-day incubation were counted as being produced from viable cells. The viability of yeast cells at day 0 in the stationary phase was set 100%.

Analyses of Data

Statistical analyses were performed with SigmaPlot software. The p values < 0.05 were taken as a significant difference.

RESULTS

The *pah1*Δ Mutant Is Defective in Growth on Non-fermentable Carbon Sources

One of the distinct phenotypes shown by the *pah1*Δ mutant is the lack of growth on glycerol (24). Since non-fermentable carbon sources are metabolized by mitochondrial respiration, the growth defect on glycerol indicates that the *pah1*Δ mutant is respiratory deficient. To confirm this phenotype, we also examined the growth of wild type and the *pah1*Δ mutant on other non-fermentable carbon sources including acetate, ethanol, and lactate. Cells were grown in YEPD medium overnight and spotted on YP plates containing 2% ethanol, 2% acetate, 2% lactate, or 3% glycerol. As on glycerol, the *pah1*Δ mutant was not able to grow on acetate or lactate (Fig. 5A). Although it exhibited growth on ethanol, its growth was much slower than that of wild type. Consistent with the poor growth on ethanol, the *pah1*Δ mutant cultured in medium containing glucose showed a slower growth than wild type in the post-diauxic phase, i.e., when ethanol produced by fermentation of glucose was metabolized (data not shown). A similar result was also obtained with the strain BY4741, which has a shorter life span than W303-1A (Fig. 5B) (226). The *pah1*Δ mutant derivative of BY4741 was not able to grow on media containing non-fermentable carbon sources, while the wild type BY4741 strain did not exhibit the growth defect.

FIGURE 5. Cell growth on non-fermentable carbon sources. Yeast strains (*A*, W303-1A; *B*, BY4741) were grown at 30 °C to saturation in YEPD medium. The saturated cultures were harvested, washed, and resuspended in water at $A_{600\ nm} = 0.67$. After 10-fold serial dilutions, 5 μl of each cell suspension was spotted onto YP agar medium containing the indicated carbon source, followed by incubation for 3 days (2% glucose) or 5 days (2% ethanol, 2% acetate, 2% lactate, or 3% glycerol).

.

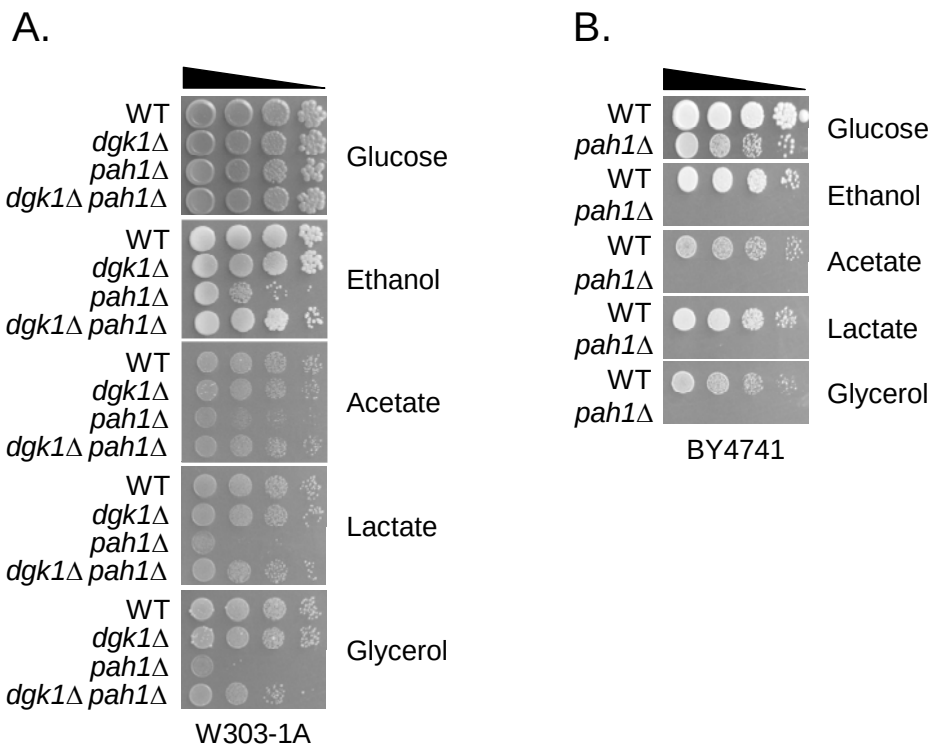
A.
WT
dgk1Δ
pah1Δ
dgk1Δ pah1Δ
Glucose
Ethanol
Acetate
Lactate
Glycerol
W303-1A
B.
WT
pah1Δ
Glucose
Ethanol
Acetate
Lactate
Glycerol
BY4741

The *pah1*Δ Mutant Is Not Defective in Mitochondrial Tubulation

Mitochondria exhibit a dynamic change in morphology through the process of fission and fusion, and they appear as small, fragmented units or as larger networks of elongated units (190, 227, 228). In nutrient-starved conditions, mitochondria form a tubular network to improve the efficiency of ATP production (229). The growth defect of the *pah1*Δ mutant on non-fermentable carbon sources raised a question about its mitochondrial morphology and function.

At first, we examined the mitochondrial morphology of wild type and the *pah1*Δ mutant in the post-diauxic and the stationary phases by using a mitochondria-targeted green fluorescence (GFP) protein. In fluorescence microscopy analysis, both wild type and the *pah1*Δ mutant in the stationary phase showed a tubular network of mitochondria, indicating that starvation induced mitochondrial tubulation (Fig. 6). In collaboration with Eugenia Mileykovskaya and William Dowhan, we also examined mitochondrial membrane structures by electron microscopy. This analysis indicated no major differences between the wild type and the *pah1*Δ mutant (Fig. 7).

FIGURE 6. Mitochondrial tubulation in wild type and the *pah1*Δ mutant. Wild type (W303-1A) and the *pah1*Δ mutant were transformed with pYX142–mtGFP, a plasmid that expresses the mitochondria-targeted GFP. The yeast transformants were grown to the post-diauxic and stationary phases, and were visualized by fluorescence microscopy.

.

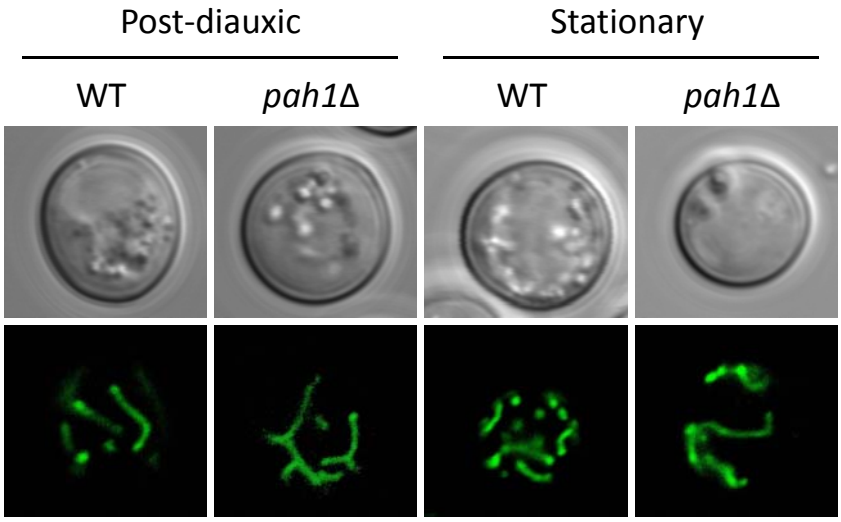
Post-diauxic
Stationary
WT
pah1Δ
WT
pah1Δ

FIGURE 7. Electron micrographs of mitochondria isolated from wild type and the *pah1*Δ mutant. Purified mitochondria from wild type (W303-1A) and the *pah1*Δ mutant were prepared for electron microscopy and visualized using JEOL 1200EX transmission electron microscope at 60 kv and captured with Gatan Orius 830 Digital imaging System.

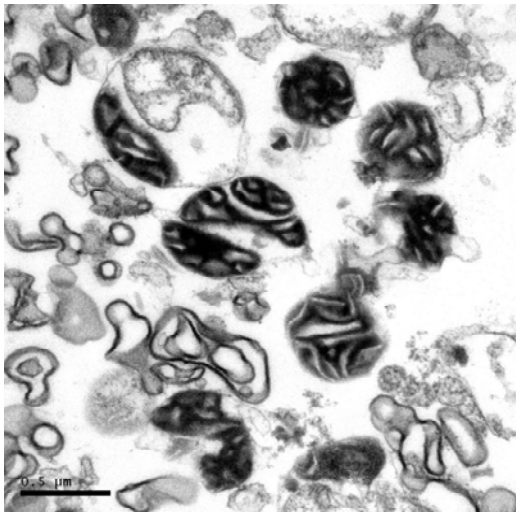

WT

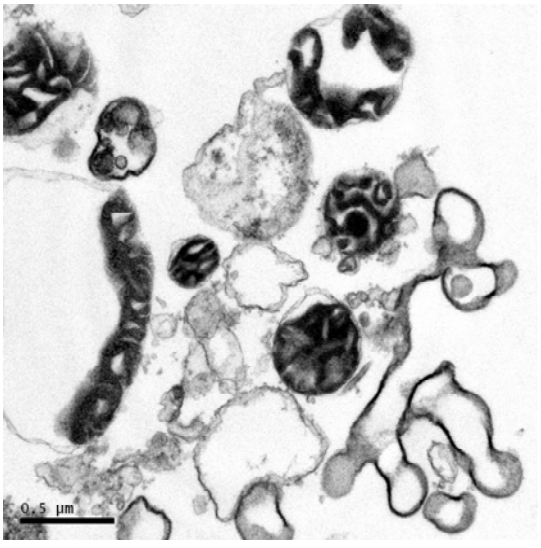

*pah1*Δ

The *pah1*Δ Mutant Exhibits a Reduction in Respiratory Supercomplex Levels

Respiratory supercomplexes are major components for oxidative phosphorylation that transfer electrons and create a proton gradient for ATP synthesis (121). They assemble to form respiratory supercomplexes that are thought to play a role in enhancement of electron flow and thereby preventing the formation of excess oxygen radicals. In S. *cerevisiae*, the ETC complexes III and IV associate to form the supercomplexes III_2+IV (trimer) and III_2+IV_2 (tetramer). In collaboration with Eugenia Mileykovskaya and William Dowhan, the formation of the respiratory supercomplexes was determined from mitochondria purified from wild type and the *pah1*Δ mutant grown in the YPEG medium. The mitochondrial fraction was solubilized with digitonin, and then separated by BN-PAGE. Immunoblot analysis with anti-Complex IV polyclonal antibody showed the trimeric and tetrameric forms of respiratory supercomplexes, which exhibited migration at the expected size of the protein complexes (Fig. 8A). Compared with wild type, the *pah1*Δ mutant showed a 20% reduction in the levels of both trimeric and tetrameric forms of mitochondrial respiratory supercomplexes (Fig. 8B).

FIGURE 8. Respiratory supercomplexes III_2IV_2 and III_2IV in wild type and *pah1*Δ mitochondria. *A*, mitochondria (17.6 μg) purified from wild type (W303-1A) and the *pah1*Δ mutant were solubilized in digitonin and were subjected to BN-PAGE (left). Mitochondrial supercomplexes separated in the gel were transferred to a PVDF membrane, and were subjected to immunoblot analysis with anti-OxPhos polyclonal antibody against subunit III of Complex IV (right). *B*, relative amounts of III_2IV (timer) and III_2IV_2 (tetramer) supercomplexes in wild type (W303-1A) and *pah1*Δ strains. AU, arbitrary units.

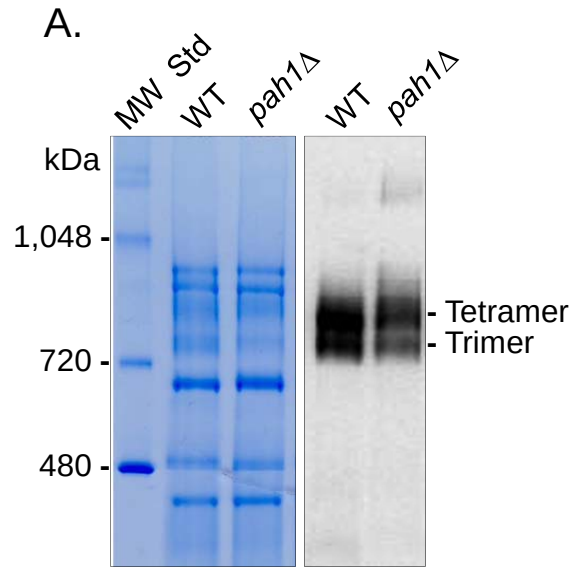
A.
MW Std
WT
pah1Δ
WT
pah1Δ
kDa
1,048
720
480
Tetramer
Trimer

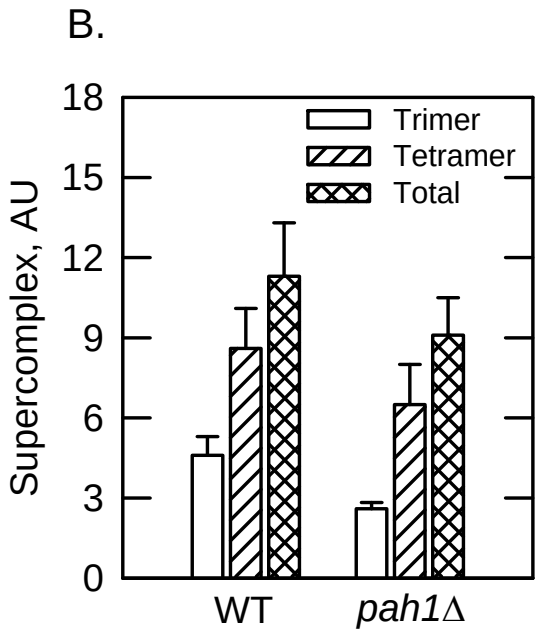
B.
Supercomplex, AU
18
15
12
9
6
3
0
Trimer
Tetramer
Total
WT
pah1Δ

Levels of Mitochondrial PS and PA Are Altered in the Stationary of the *pah1*Δ Mutant

The phospholipid synthesis in mitochondria plays an important role not only for mitochondrial functions but also for cellular functions (173, 174). CL, a signature phospholipid in mitochondria, is crucial for electron transport and oxidative phosphorylation as well as for the stability of respiratory chain complexes (175, 178). In *S. cerevisiae*, *de novo* synthesis of cellular PE mainly occurs from PS in mitochondria by Psd1 PS decarboxylase (36).

Accordingly, we examined whether the composition of mitochondrial phospholipids is altered in the *pah1*Δ mutant. Cells were harvested in the exponential and the stationary phases. Mitochondria were purified by centrifugation with sucrose gradient, and then the purity was confirmed by western blotting with anti-Por1 (mitochondrial marker), anti-Prc1 (vacuole marker), anti-Cho1 (ER marker) and anti-Pgk1 (cytosol marker) antibodies (Fig. 9). Phospholipids extracted by the method of Bligh and Dyer were separated by two dimensional TLC. Quantitation analysis showed that wild type and the *pah1*Δ mutant were very similar in the levels of the major mitochondrial phospholipids such as PC, PE, and PI in the exponential phase (Fig. 10). Notably, no significant difference was shown in the level of mitochondria-specific CL between the two strains. In contrast, the *pah1*Δ mutant showed alterations in the levels of the minor mitochondrial phospholipids PS and PA in the stationary phase (Fig. 10). Compared with wild type, the *pah1*Δ mutant showed a 40% increase of the PS level, and a 40% decrease of the PA level in mitochondrial phospholipids. These changes of the *pah1*Δ mutant in the levels of mitochondrial PS and PA were also confirmed by mass

spectrometry (data not shown). On the other hand, non-mitochondrial fraction of the *pah1*Δ mutant exhibited increase in the phospholipid level like a previously shown for the phospholipid level of whole cells (Fig. 10) (24, 59).

We also analyzed fatty acid composition of the mitochondrial fraction from stationary phase cells by the gas chromatography. This analysis showed that major fatty acid levels were similar to that of wild type cells (Fig. 11).

FIGURE 9. Isolation of mitochondria from wild type and the *pah1*Δ mutant. Wild type (W303-1A) and *pah1*Δ mutant cells were grown at 30 °C in SC-glucose medium to the exponential and the stationary phases. After treatment of lyticase**,** spheroplasts were disrupted by Dounce glass homogenizer. Crude mitochondria were collected by centrifugation at 12,000 × *g* for 15 min at 4 °C. Purified mitochondria were collected by sucrose gradient centrifuged at 134,000 × *g* for 1 h at 4 °C from the interface between the 32% and 60% sucrose layers. 10 μg cell extract and 2 μg purified mitochondrial fraction were subjected to SDS-PAGE and western blot analysis using anti-Por1 (porin), Prc1 (vacuolar carboxypeptidase), Cho1 (phosphatidylserine synthase), and Pgk1 (3-phosphoglycerate kinase) antibodies. C, cell extract; M, mitochondria.

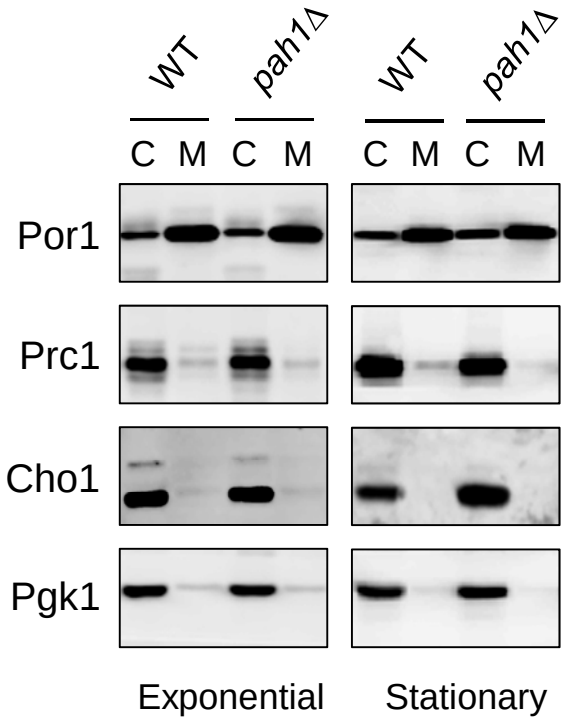
WT
pah1Δ
WT
pah1Δ
C M C M C M C M
Por1
Prc1
Cho1
Pgk1
Exponential
Stationary

FIGURE 10. Mitochondrial phospholipid composition of wild type and *pah1*Δ mitochondria. Wild type (W303-1A) and the *pah1*Δ mutant were grown at 30 °C in SC-glucose medium to the exponential and stationary phases. Mitochondria were purified from the yeast cultures, and were extracted for lipids by the method of Bligh and Dyer. Non-mitochondrial fraction was collected by centrifugation at 100,000 × *g*, for 1h at 4 °C from the supernatant after removing crude mitochondria. Phospholipids from 500 μg mitochondria were separated by two-dimensional TLC on silica gel 60 plates, stained with 0.05% primulin, and subjected to fluoroimaging and image quantification using ImageQuant software.

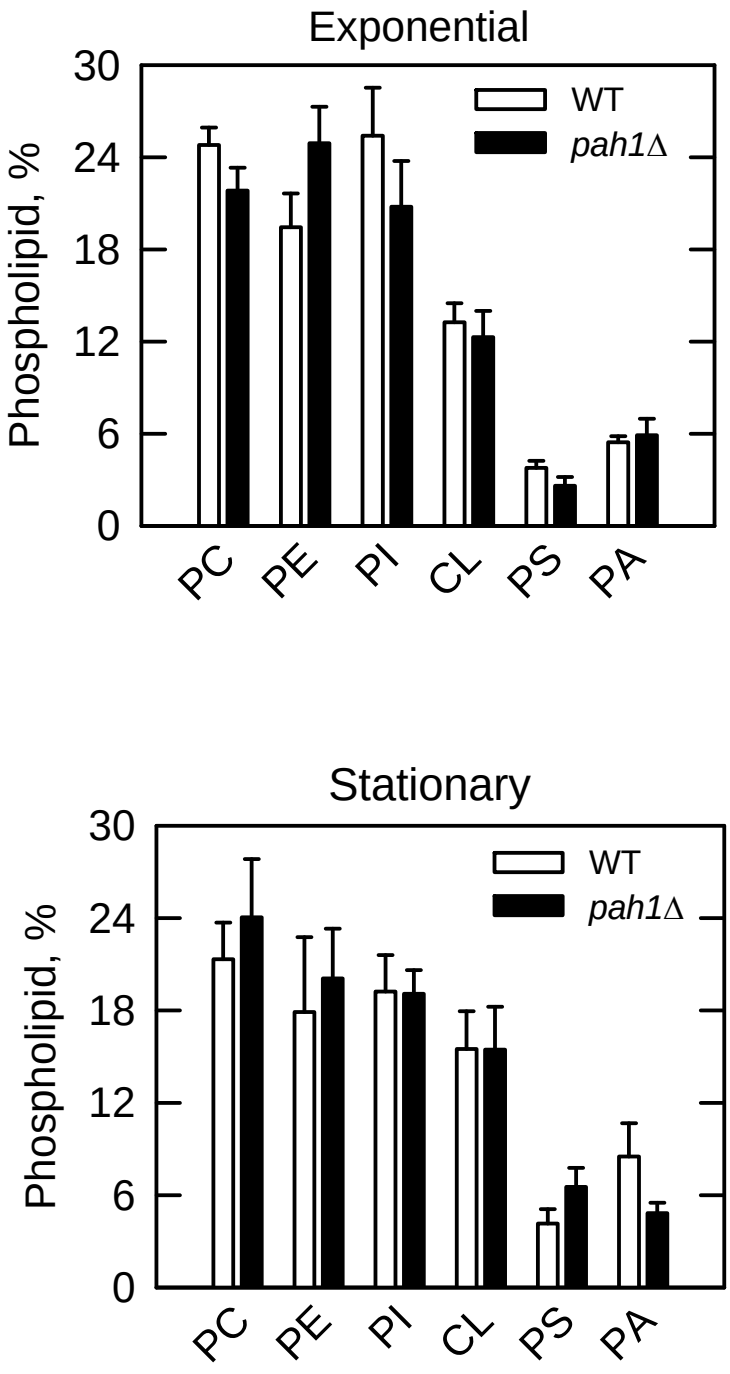
Exponential
Phospholipid, %
30
24
18
12
6
0
WT
pah1Δ
PC
PE
PI
CL
PS
PA
Stationary
Phospholipid, %
30
24
18
12
6
0
WT
pah1Δ
PC
PE
PI
CL
PS
PA

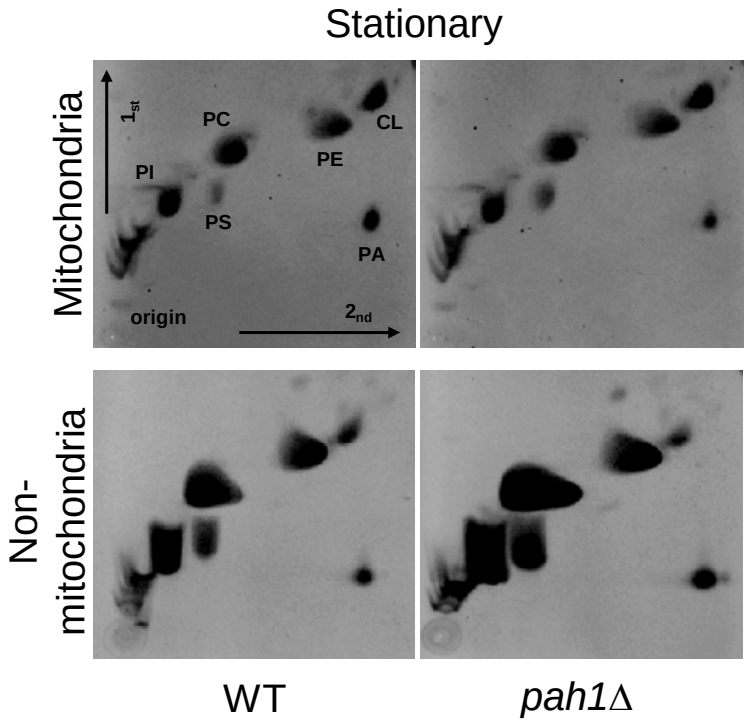
Stationary
Mitochondria
Non-mitochondria
1st
2nd
origin
PI
PC
PS
PE
PA
CL
WT
pah1Δ

FIGURE 11. Fatty acid composition of mitochondrial phospholipids in wild type and the *pah1*Δ mutant. Lipids were extracted from 1.5 mg of mitochondria by the method of Bligh and Dyer, and were methylated using 1 ml of hydrogen chloride - methanol at 70 °C for 1 h. Fatty acid methyl esters were analyzed by gas chromatography. *A*, the percentages shown for the individual fatty acid were normalized to the total fatty acids detected including palmitic acid (C16:0), palmitoleic acid (C16:1), stearic acid (C18:0), and oleic acid (C18:1). *B*, the amount of individual fatty acid was calculated by standard heptadecanoic acid (C17:0).

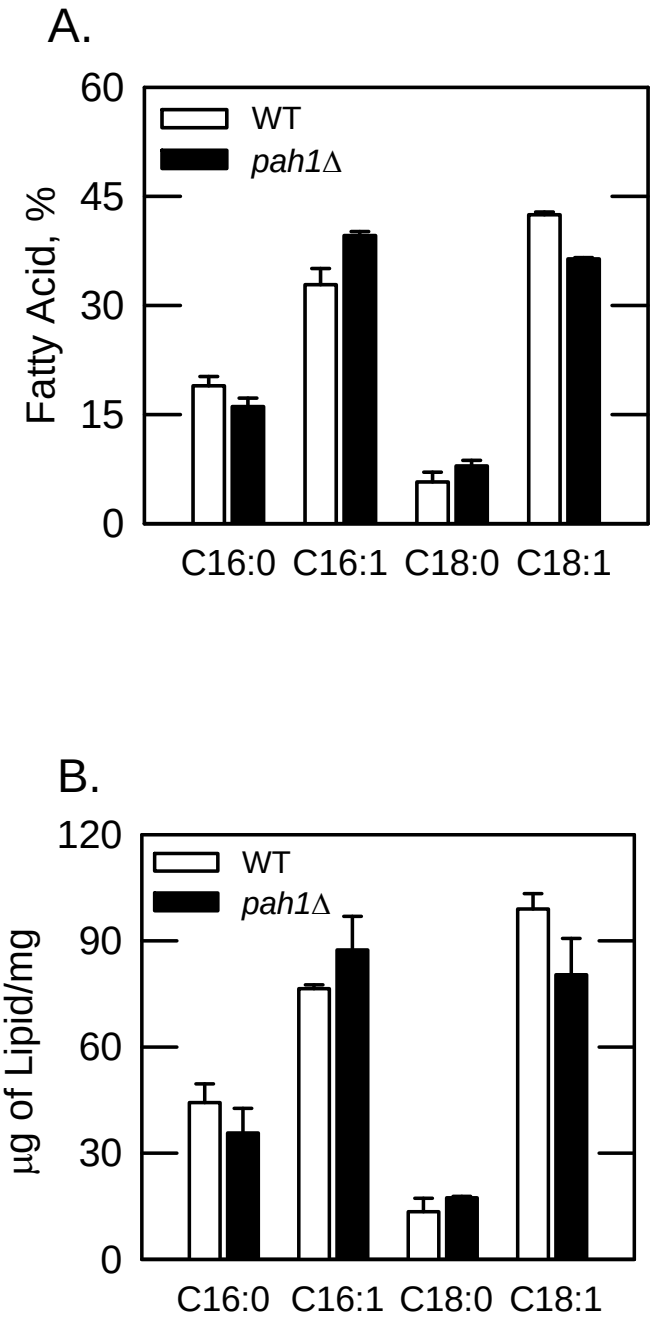
A.
60
45
30
15
0
Fatty Acid, %
WT
pah1Δ
C16:0
C16:1
C18:0
C18:1
B.
120
90
60
30
0
μg of Lipid/mg
WT
pah1Δ
C16:0
C16:1
C18:0
C18:1

The *pah1*Δ Mutant Exhibits an Elevated Mitochondrial Membrane Potential in the Post-diauxic Phase

We measured the oxygen consumption to examine the oxidative phosphorylation function during cell growth. In the exponential phase, wild type and the *pah1*Δ mutant showed the same rate of oxygen consumption (data not shown). Similarly, no significant difference was observed in the two yeast strains for oxygen consumption in the post-diauxic phase as well as in the stationary phase (Fig. 12A).

Next, we analyzed the mitochondrial membrane potential, which is required for ATP production, in wild type and the *pah1*Δ mutant by staining with TMRM, a potentiometric fluorescent dye that is readily sequestered by active mitochondria (230, 231). To figure out the proper concentration of TMRM for dyeing the 1 $A_{600\ nm}$ unit of cells, we treated wild type cells with different concentration of TMRM for 30 min. As a result, we decided to choose 40 μM TMRM to the 1 $A_{600\ nm}$ unit of cells. Wild type and the *pah1*Δ mutant were stained with TMRM, and the fluorescence of the stained cells was analyzed by a flow cytometer. Compared with wild type, the *pah1*Δ mutant showed 2.7-fold higher levels of the TMRM fluorescence in the post-diauxic phase (Fig. 12B). In the stationary phase, however, no significance difference was shown for the TMRM fluorescence in wild type and the *pah1*Δ mutant. This result indicates that the membrane potential of the *pah1*Δ mutant is not defective, but is higher in the post-diauxic phase.

FIGURE 12. Oxygen consumption and mitochondrial membrane potential in wild type and the *pah1*Δ mutant. *A***,** wild type (W303-1A) and the *pah1*Δ mutant were grown in SC-glucose medium to the post-diauxic and the stationary phases. The cultures were diluted 10-fold in the fresh medium measured for oxygen consumption by oxygen electrode for 5 min. *B***,** wild type (W303-1A), the *dgk1*Δ mutant, the *pah1*Δ mutant, and the *dgk1*Δ *pah1*Δ mutant in the post-diauxic and the stationary phases were harvested, washed with PBS, and incubated for 30 min in the buffer containing TMRM, a potentiometric fluorescent dye to monitor the membrane potential of mitochondria. After washing with PBS, the TMRM-stained cells were measured for fluorescence by the flow cytometer.

A.

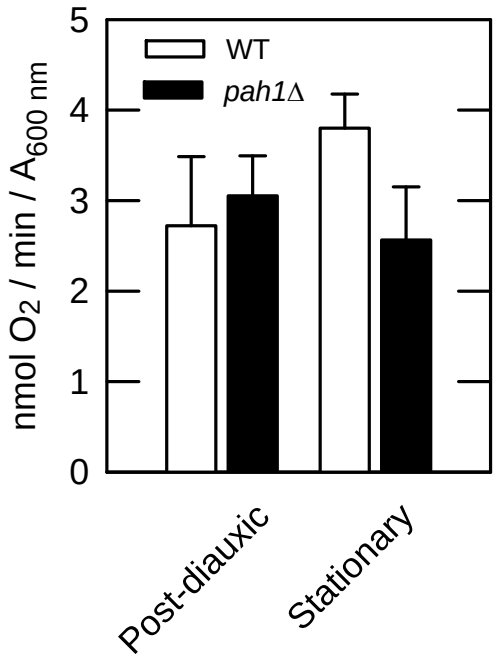
nmol O_2 / min / $A_{600\ nm}$
0
1
2
3
4
5
WT
*pah1*Δ
Post-diauxic
Stationary

B.

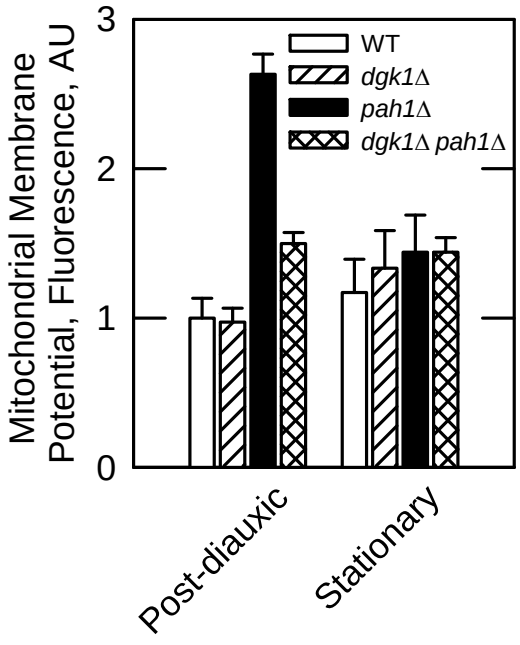
Mitochondrial Membrane Potential, Fluorescence, AU
0
1
2
3
WT
*dgk1*Δ
*pah1*Δ
*dgk1*Δ *pah1*Δ
Post-diauxic
Stationary

The *pah1*Δ Mutant Is not Defect in the Mitochondrial F_1F_O-ATP Synthase

In oxidative phosphorylation, the production of ATP occurs by mitochondrial F_1F_O-ATP synthase coupled with the H^+ flux (131-133). The enzyme also catalyzes the reverse reaction, i.e., ATP hydrolysis, in the absence of membrane potential or pH gradient (232). Accordingly, we measured the activity of F_1F_O-ATP synthase as its ATPase activity from the mitochondria of wild type and the *pah1*Δ mutant in the stationary phase. Mitochondria from the stationary phase cells were purified by sucrose gradient centrifugation. The ATPase activity was measured by the oxidation of NADH in the coupled reaction. Compared with wild type, the *pah1*Δ mutant showed the same level of mitochondrial F_1F_O-ATPase activity (Fig. 13). This result indicates that the mitochondrial F_1F_O-ATP synthase is functional in the *pah1*Δ mutant.

FIGURE 13. F_1F_O-ATP synthase activity of wild type and the *pah1*Δ mutant. 20 μg of mitochondria purified from the stationary phase cells were measured for F_1F_O-ATPase activity. A unit of ATP synthase activity was defined as nmol of NADH oxidized per min.

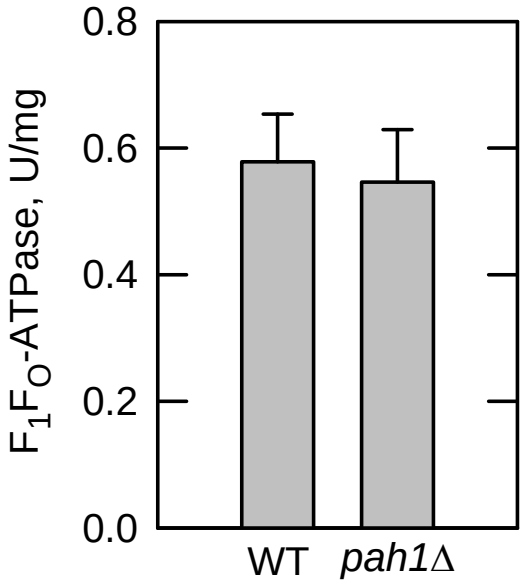
0.8
0.6
0.4
0.2
0.0
F1FO-ATPase, U/mg
WT
pah1Δ

The *pah1*Δ Mutant Exhibits a Decrease in Cellular ATP levels in the Post-diauxic Phase

One of important roles in mitochondria is to produce ATP needed for cell growth and survival by the oxidative phosphorylation (113). We measured its cellular levels by the ATP bioluminescence assay. In the assay, ATP reacts with luciferin to generate adenyl-luciferin, which is then oxidized by oxygen to generate light. The absolute requirement of ATP for the luciferase reaction is represented as the extent of bioluminescence. Cells were grown from the exponential (6 h) to the post diauxic phases (24 h) (Fig. 14A). At the indicated time points, cells were harvested and the level of ATP was measured ATP bioluminescence assay (Fig. 14B). This analysis showed that both wild type and the *pah1*Δ mutant had the same level of ATP in the exponential phase. In the post-diauxic phase, however, the *pah1*Δ mutant showed 45% lower levels of ATP when compared with the wild type control.

FIGURE 14. ATP levels of wild type and the *pah1*Δ mutant during cell growth. Wild type (W303-1A) and *pah1*Δ mutant cells were grown in SC-glucose medium, during which yeast cultures corresponding to 5 $A_{600\ nm}$ units of cells were harvested at the indicated time points from the exponential to the post-diauxic phases. Harvested cells were washed, and measured for the ATP levels by the luciferase assay. *A*, cell growth at $A_{600\ nm}$. *B*, cellular ATP levels

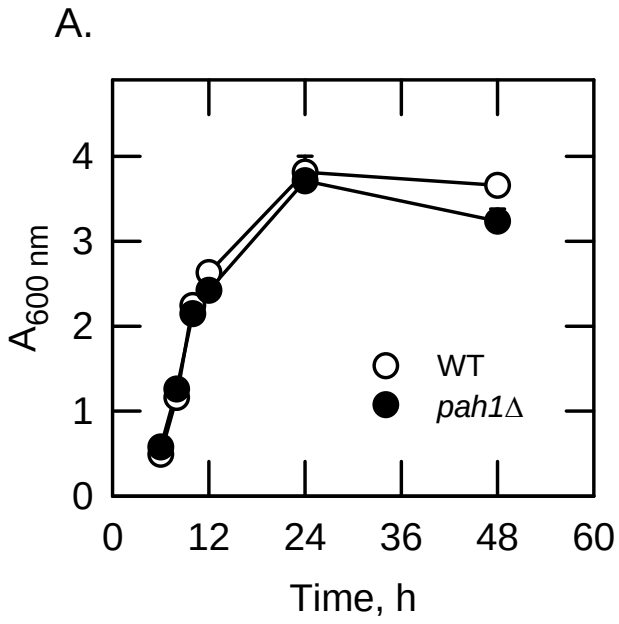
A.
$A_{600\ nm}$
0
1
2
3
4
0
12
24
36
48
60
Time, h
WT
pah1Δ

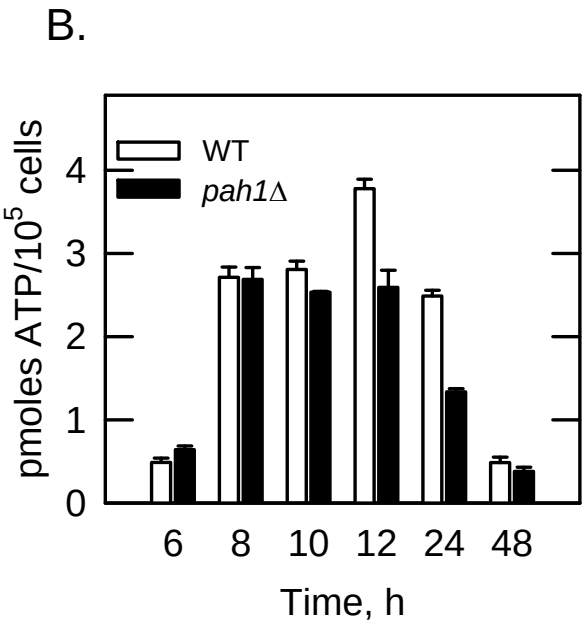
B.
pmoles ATP/10^5 cells
0
1
2
3
4
6
8
10
12
24
48
Time, h
WT
pah1Δ

The *pah1*Δ Mutant Exhibits Increased Lipid Synthesis in the Post-diauxic Phase

We examined wild type and the *pah1*Δ mutant for their ATP levels and lipid synthesis during growth on glycerol. This non-fermentable carbon source was chosen because of its pronounced effect on the growth of the *pah1*Δ mutant. Wild type and the *pah1*Δ mutant were first grown in SC-glucose medium to the exponential phase ($A_{600\ nm}$ =1). After transfer to SC-glycerol medium, the yeast cultures were incubated for 4 h in the absence (for ATP measurement) or presence (for lipid analysis) of [2-^{14}C]acetate. The ATP level was measured by the ATP bioluminescence assay. The [2-^{14}C]acetate labeled lipids were extracted by the method of Bligh and Dyer, and then separated by one dimensional TLC. When cultured in medium containing glucose, wild type and the *pah1*Δ mutant showed the same cellular ATP level (Fig. 15A). When cultured in SC-glycerol medium, however, the *pah1*Δ mutant showed 50% lower ATP level than wild type. By contrast, the *pah1*Δ mutant without a significant cell growth showed the 3- and 1.5-fold increases in phospholipid and fatty acid synthesis, respectively (Fig. 15B). Above all, the *pah1*Δ mutant exhibited 2.2-fold higher levels of lipid synthesis than wild type during growth on glycerol wild type.

FIGURE 15. ATP levels and lipid synthesis during growth of wild type and the *pah1*Δ mutant in SC-glycerol medium. *A*, wild type (W303-1A) and the *pah1*Δ mutant were grown at 30 °C to the late exponential phase ($A_{600\ nm}$ = 1) in SC-glucose medium. The yeast cells were harvested, washed with sterilized water, and incubated for 4 h in the medium containing non-fermentable glycerol as a carbon source. The cellular ATP levels were measured by the luciferase assay. *B*, the yeast strains were grown in the same way as described in *A* except for the addition of [2-^{14}C]acetate (1 μCi/ml) in the glycerol medium. Lipids were extracted from the radiolabeled cells and subjected to one dimensional TLC on silica gel 60. The radiolabeled lipids were visualized by phosphorimaging and were quantified by ImageQuant software with [2-^{14}C]acetate as a standard. PL, phospholipid; FA, fatty acid; Erg; ergosterol; ErgE; ergosterol ester separated on TLC.

A.

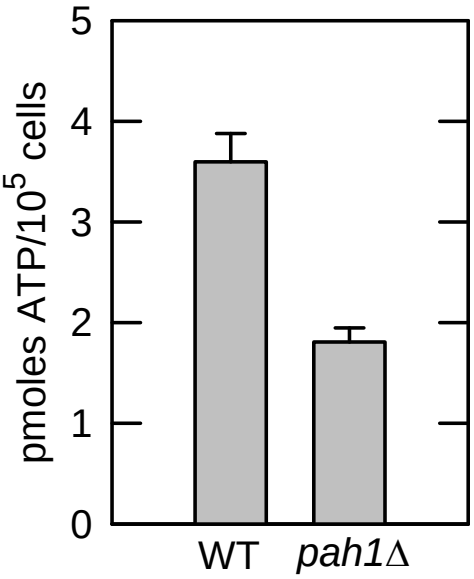
pmoles ATP/10^5 cells
0
1
2
3
4
5
WT
pah1Δ

B.

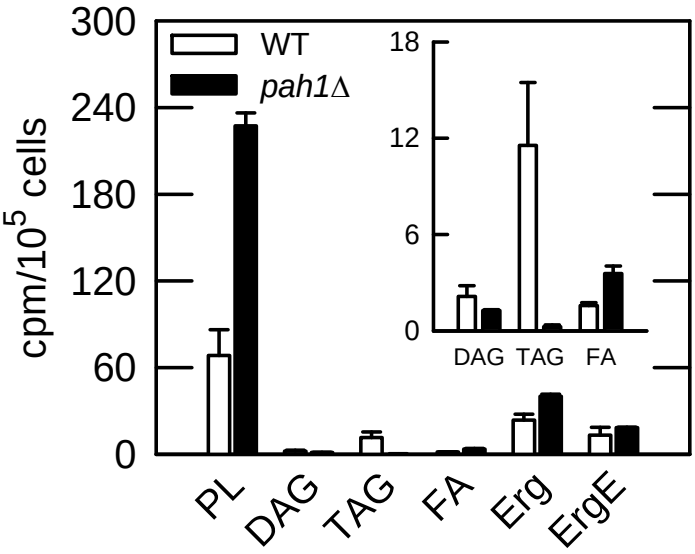
cpm/10^5 cells
0
60
120
180
240
300
WT
pah1Δ
18
12
6
0
DAG
TAG
FA
PL
DAG
TAG
FA
Erg
ErgE

The *pah1*Δ Mutant Exhibits an Increase in Superoxide Levels

Superoxide is generated by electron leaks as byproducts during oxidative phosphorylation, and unless removed react readily with other nearby molecules, causing a detrimental effect on the cellular structure and function (152-154). The lower levels of respiratory supercomplexes in the *pah1*Δ mutant raised a possibility that it produces more ROS than wild type. We first measured the mitochondrial superoxide levels in wild type and the *pah1*Δ mutant by staining with MitoSOX Red, a fluorescent indicator that permeates live cells where it is oxidized by mitochondrial superoxide to produce red fluorescence. The red fluorescence signals were measured with a flow cytometer. As a result, in the post-diauxic phase, wild type and the *pah1*Δ mutant showed similar mitochondrial superoxide level (Fig. 16). In the stationary phase, however, the *pah1*Δ mutant showed 2-fold higher mitochondrial superoxide level than wild type.

FIGURE 16. Mitochondrial superoxide levels in wild type, *dgk1*Δ, *pah1*Δ, *dgk1*Δ *pah1*Δ mutant cells. Wild type (W303-1A), the *dgk1*Δ mutant, the *pah1*Δ mutant, and the *dgk1*Δ *pah1*Δ mutant were grown at 30 °C in SC-glucose medium to the post-diauxic and the stationary phases. Cells corresponding to 1 $A_{600\ nm}$ were harvested, washed with PBS, and incubated for 30 min in the buffer containing MitoSOX Red. Fluorescence from the stained cells was measured with a flow cytometer.

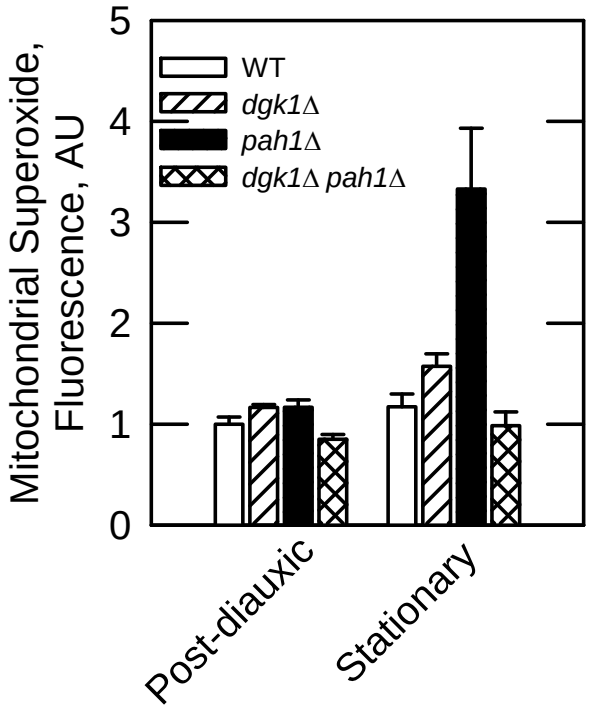
Mitochondrial Superoxide,
Fluorescence, AU
0
1
2
3
4
5
WT
dgk1Δ
pah1Δ
dgk1Δ pah1Δ
Post-diauxic
Stationary

The *pah1*Δ Mutant Exhibits an Increase in Lipid Hydroperoxides

The higher superoxide level in the *pah1*Δ mutant indicates the presence of elevated ROS level, which reacts with macromolecules (e.g., DNA, proteins, and lipids). The reaction of ROS with polyunsaturated fatty acids induces lipid peroxidation. In the stationary phase, the levels of total phospholipids and free fatty acids in the *pah1*Δ mutant were 60% and 77 % higher, respectively, than those in wild type (59). Accordingly, we measured lipid hydroperoxides in wild type and the *pah1*Δ mutant by a colorimetric assay using the ferrous oxidation-xylenol orange complex. Lipids were extracted the method of Bligh and Dyer from stationary phase cells, and then the amounts of lipids were measured by a chemical balance. After incubation with reagent for 30 min, the lipid hydroperoxides were measured. The *pah1*Δ mutant and wild type showed similar lipid hydroperoxides level per mg of lipid (Fig. 17A). However, compared with wild type, the *pah1*Δ mutant showed 3-fold higher lipid hydroperoxides level per cells because of its higher lipid contents (Fig. 17B).

FIGURE 17. Lipid hydroperoxides in wild type and the *pah1*Δ mutant. Wild type (W303-1A) and the *pah1*Δ mutant were grown at 30 °C in SC-glucose medium to the stationary phase. Lipids were extracted from the yeast cells in the stationary phase by the method of Bligh and Dyer, and the lipid hydroperoxides levels were measured with the ferric-xylenol orange complex reagent. *A*, lipid hydroperoxide content/mg lipid. *B*, lipid hydroperoxide content/g cells.

A.

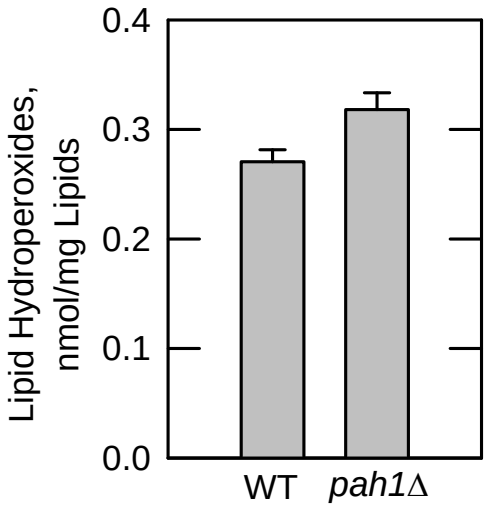
Lipid Hydroperoxides,
nmol/mg Lipids
0.4
0.3
0.2
0.1
0.0
WT
pah1Δ

B.

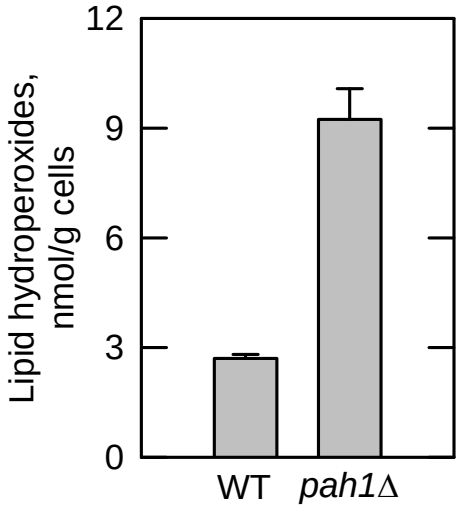
Lipid hydroperoxides,
nmol/g cells
12
9
6
3
0
WT
pah1Δ

The *pah1*Δ Mutant Exhibits a Decrease in Cta1 Catalase 1 and Sod2 Superoxide Dismutase Activities

The elevated mitochondrial superoxide level in the *pah1*Δ mutant and its increased sensitivity to hydrogen peroxide suggested a possibility that the ROS level in the *pah1*Δ mutant is increased by a deficiency in antioxidant enzymes. Accordingly, we examined the main antioxidant enzymes, SOD and catalase, for their catalytic activities. SOD catalyzes the conversion of superoxide to hydrogen peroxide, and catalase decomposes the reaction product hydrogen peroxide to water and oxygen.

To measure SOD activity, cell extracts from stationary phase cells were resolved by non-denaturing polyacrylamide gel electrophoresis, and then subjected to in-gel activity staining. Two different forms of SOD, Sod1 and Sod2, were distinguished by electrophoretic mobility in the polyacrylamide gel. This analysis showed that the Sod1activity, which is localized in the cytosol, was not significantly different in wild type and the *pah1*Δ mutant (Fig. 18). In the case of Sod2 activity, which is localized in mitochondria, was lower in the *pah1*Δ mutant when compared with the wild type.

Catalase activity in cell extract and purified mitochondria from the stationary phase was measured at $A_{240\ nm}$. In contrast to SOD activity, catalase activity was reduced by 30 % in the *pah1*Δ mutant (Fig. 19). Mitochondrial catalase activity was not different in wild type and the *pah1*Δ mutant, and was not considered to contribute to the decrease of the enzyme activity in the *pah1*Δ mutant (Fig. 19).

FIGURE 18. Superoxide dismutase activity of wild type and the *pah1*Δ mutant. Cell extracts (10 μg) were prepared from Wild type (W303-1A) and the *pah1*Δ mutant in the stationary phase, and were resolved by non-denaturing polyacrylamide gel electrophoresis with a 12% slab gel. After electrophoresis, the polyacrylamide gel was incubated for 20 min in the solution of nitro blue tetrazolium and for 15 min in the solution of riboflavin and TEMED, followed by exposure to white light. The unstained region, which indicates SOD activity, against a dark blue background of the gel was quantified by ImageQuant software.

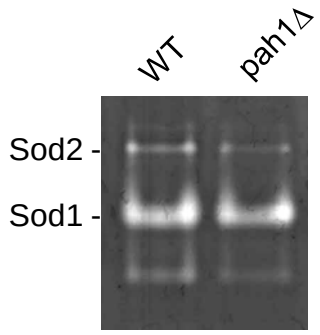
WT
pah1Δ
Sod2
Sod1

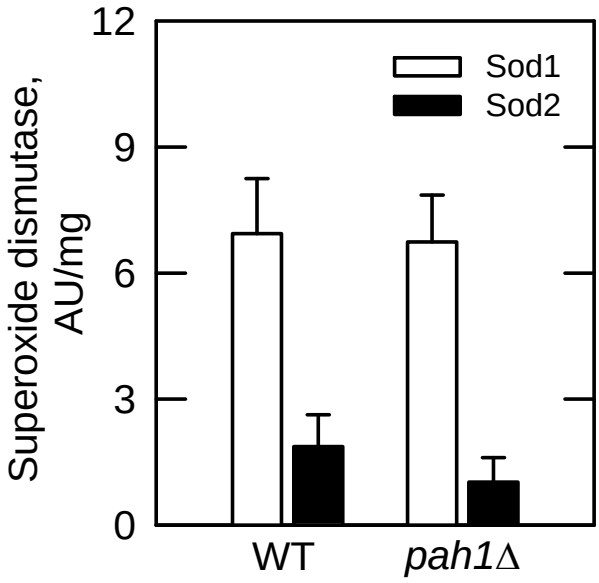
Superoxide dismutase, AU/mg
12
9
6
3
0
Sod1
Sod2
WT
pah1Δ

FIGURE 19. Catalase activity of wild type and the *pah1*Δ mutant. Cell extracts (20 μg) and mitochondrial fractions (20 μg) from stationary phase cells were prepared from wild type (W303-1A) and the *pah1*Δ mutant grown in SC-glucose medium, and were measured for catalase activity by the rate of hydrogen peroxide reduction at $A_{240\ nm}$. A unit of catalase activity was defined as 1 μmol hydrogen peroxide decomposition per min.

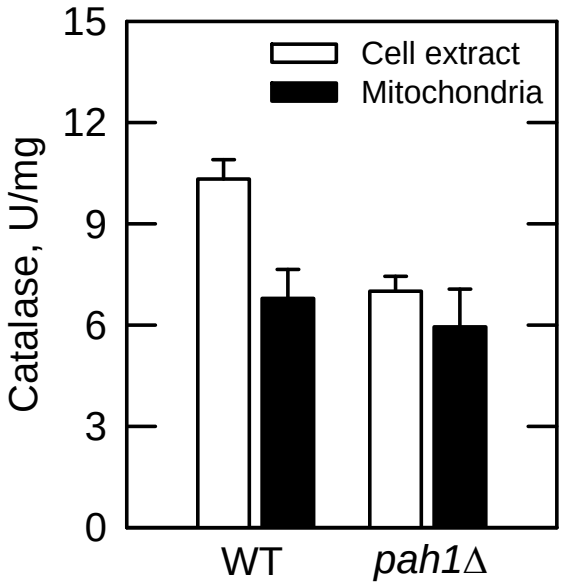
15
12
9
6
3
0
Catalase, U/mg
Cell extract
Mitochondria
WT
pah1Δ

The *pah1*Δ Mutant Is Sensitive to Hydrogen Peroxide

The *pah1*Δ mutant exhibiting a higher level of superoxide might be expected to be sensitive to hydrogen peroxide. To determine this possibility, we analyzed the growth of wild type and the *pah1*Δ mutant in culture medium containing various amounts of hydrogen peroxide. Compared with wild type, the *pah1*Δ mutant showed a growth defect that was dependent on the concentration of hydrogen peroxide (Fig. 20 A). At 1 mM hydrogen peroxide in SC-glucose medium, wild type showed no defect in growth, whereas the *pah1*Δ mutant showed almost no growth. The *pah1*Δ mutant exhibited less sensitivity to hydrogen peroxide on YEPD medium than on SC-glucose medium (Fig. 20B). The results showed that the *pah1*Δ mutant could not grow on YEPD plate containing 4 mM hydrogen peroxide, whereas the growth of wild type cells was not affected. We also tested whether the *pah1*Δ mutant is sensitive more in the non-fermentable carbon sources medium including 0.95% ethanol and 3% glycerol than the fermentable carbon source medium. Both wild type and the *pah1*Δ mutant displayed similar pattern to the result of YEPD medium but slightly increased sensitivity (3.5 mM H_2O_2) (Fig. 20C). These results support the conclusion that the *pah1*Δ mutant is vulnerable to oxidative stress.

FIGURE 20. Sensitivity to hydrogen peroxide. *A*, wild type (W303-1A) and the *dgk1*Δ mutant, the *pah1*Δ mutant, and the *dgk1*Δ *pah1*Δ mutant were grown to saturation in SC-glucose medium. The yeast cultures were harvested, washed with water, and adjusted to $A_{600\ nm} = 0.67$. After 10-fold serial dilutions, 5 μl of each cell suspension was spotted onto SC-glucose agar medium containing the indicated concentrations of hydrogen peroxide, followed by incubation for 3 days. *B*, wild type (W303-1A) and the *pah1*Δ mutant grown in YEPD medium were spotted onto YEPD medium containing the indicated concentrations of hydrogen peroxide. *C*, wild type (W303-1A) and the *pah1*Δ mutant grown in YEPD medium were spotted onto YPEG medium containing the indicated concentrations of hydrogen peroxide.

A.

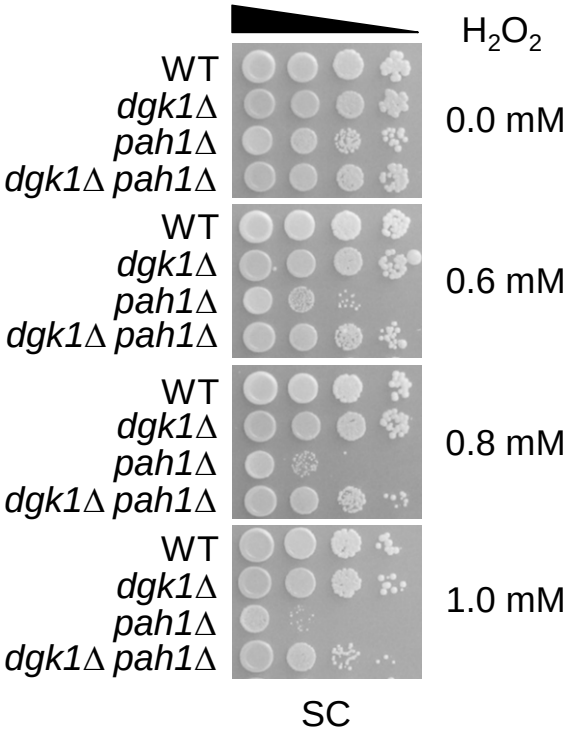
H2O2
WT
dgk1Δ
pah1Δ
dgk1Δ pah1Δ
0.0 mM
0.6 mM
0.8 mM
1.0 mM
SC

B.

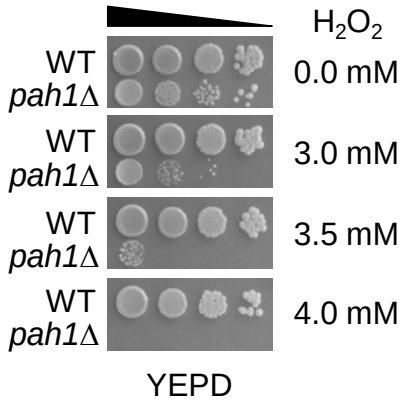
H2O2
WT
pah1Δ
0.0 mM
3.0 mM
3.5 mM
4.0 mM
YEPD

C.

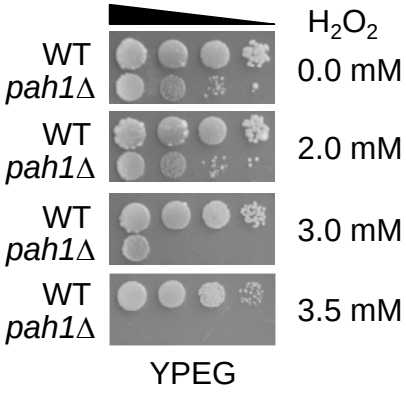
H2O2
WT
pah1Δ
0.0 mM
2.0 mM
3.0 mM
3.5 mM
YPEG

NADH-and FAD-dependent Glycerol-3-Phosphate Dehydrogenase Activities Are not Affected by the *pah1*Δ Mutation

Glycerol-3-phosphate which is a backbone of the lipid is produced from DHAP by NADH-dependent GPDH (Gpd1 and Gpd2) (233, 234). On the other hand, FAD-dependent GPDH (Gut2) found in mitochondria catalyzes the conversion of glycerol-3-phosphate to yield DHAP (235, 236). We questioned whether the activities of NADH- and FAD-dependent GPDH activities might be lower and higher, respectively, in the *pah1*Δ mutant than wild type cells, because glycerol-3-phosphate is needed for phospholipid synthesis. We monitored reduction in NADH substrate absorbance at $_{A340\ nm}$ to test the NADH-dependent GPDH activity from cell extracts. To test FAD-dependent GPDH activity, we purified mitochondria grown in SC-ethanol (2%) medium because the enzyme is activated in the presence of non-fermentable carbon sources (236, 237). We monitored decrease in FAD substrate absorbance at $A_{562\ nm}$ for 10 min.

The NADH-dependent GPDH activity was elevated in both wild type and the *pah1*Δ mutant in the post-diauxic phase than in the exponential phase (Fig. 21A). In the stationary phase, wild type cells exhibited ~ 30% lower activity than in the post-diauxic phase, whereas it was not decreased in the *pah1*Δ mutant. On the other hand, FAD-dependent GPDH activity was not changed by the *pah1*Δ mutation in the stationary phase (Fig. 21B).

FIGURE 21. NADH- and FAD-dependent glycerol-3-phosphate dehydrogenase activities of wild type and the *pah1*Δ mutant. *A***,** cell extracts (40 μg) were prepared from the exponential, the post-diauxic, and the stationary phases of wild type (W303-1A) and the *pah1*Δ mutant cells grown in SC-glucose medium. The NADH-dependent GPDH activity assay was conducted with 40 μg of cell extracts at $A_{340\ nm}$. A unit of NADH-dependent GPDH activity was defined as nmol of NADH oxidized per min. *B*, cells were grown in SC-ethanol medium at 30 °C. 50 μg purified mitochondria was used for FAD-dependent GPDH activity assay at $A_{562\ nm}$. A unit of FAD-dependent GPDH activity was defined as 1 nmol of MTT reduced per min.

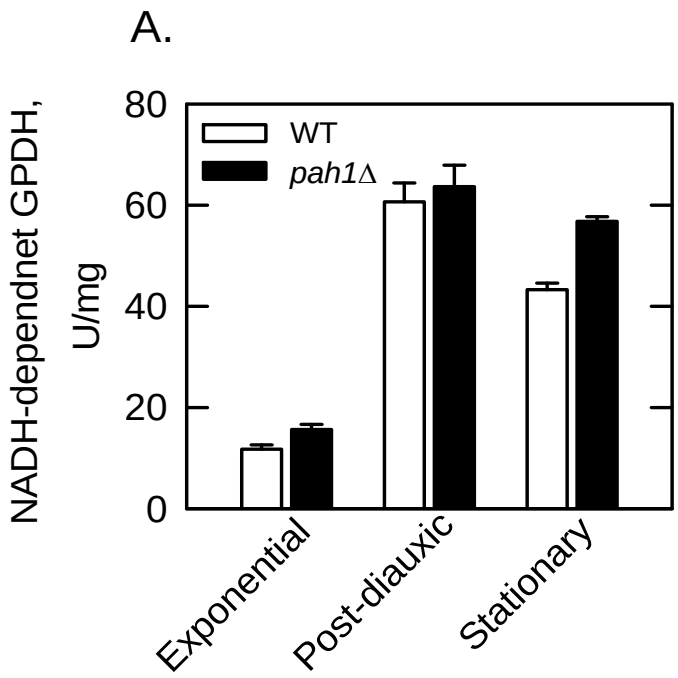
A.
NADH-dependnet GPDH, U/mg
80
60
40
20
0
WT
pah1Δ
Exponential
Post-diauxic
Stationary

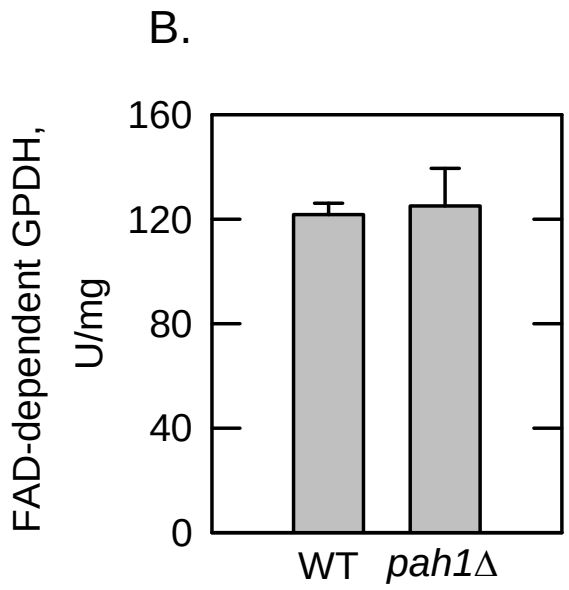
B.
FAD-dependent GPDH, U/mg
160
120
80
40
0
WT
pah1Δ

The *pah1*Δ Mutant Exhibits a Shortened Chronological Life Span

We analyzed the chronological life span of wild type and the *pah1*Δ mutant. In the viability assay, the yeast cells in the stationary phase were evaluated on their ability to form colonies on rich growth medium. Both wild type and the *pah1*Δ mutant exhibited a reduction in viability over time in the stationary phase (Fig. 22A). Compared with wild type, the *pah1*Δ mutant showed a rapid decrease in viability. Whereas wild type showed a 50% reduction of viability in 8 days, the *pah1*Δ mutant showed the same extent of reduced viability in 3 days with almost complete loss of viability in 7 days (Fig. 22A). The rapid decrease of the *pah1*Δ mutant viability indicates that the chronological life span is > 2-fold shorter than that of wild type. A similar reduction in chronological life span was also shown by the *pah1*Δ mutant derived from the BY4741 strain (Fig. 22B). The strain BY4741 exhibits a shorter life span than W303-1A, and it showed a 50% reduction of viability in 4 days. The *pah1*Δ mutant in the BY4741 background exhibited a 50% reduction of viability in less than one day, and showed no viability in 2 days.

FIGURE 22. Chronological life span. Yeast strains (*A*, wild type W303-1A and its mutant derivatives *dgk1*Δ, *pah1*Δ, and *dgk1*Δ *pah1*Δ; *B*, wild type BY4741and its mutant derivative *pah1*Δ) were grown in SC-glucose medium to the exponential phase, which were diluted at $A_{600\ nm}$ = 0.1 in the fresh medium and then grown for 48 h to the stationary phase (Day 0). The stationary phase cultures were continuously incubated, during which an aliquot was taken daily and plated onto YEPD agar plates. Colonies formed on the plates were scored after incubation for 2 days.

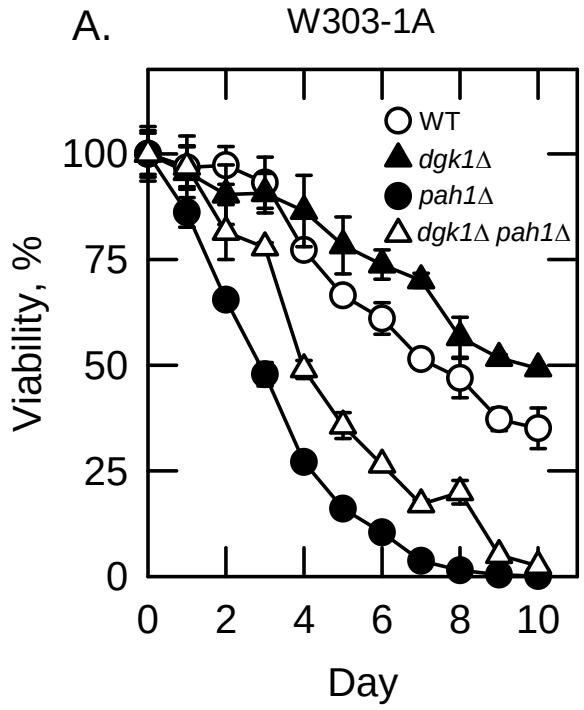
A.
W303-1A
WT
dgk1Δ
pah1Δ
dgk1Δ pah1Δ
Viability, %
100
75
50
25
0
0
2
4
6
8
10
Day

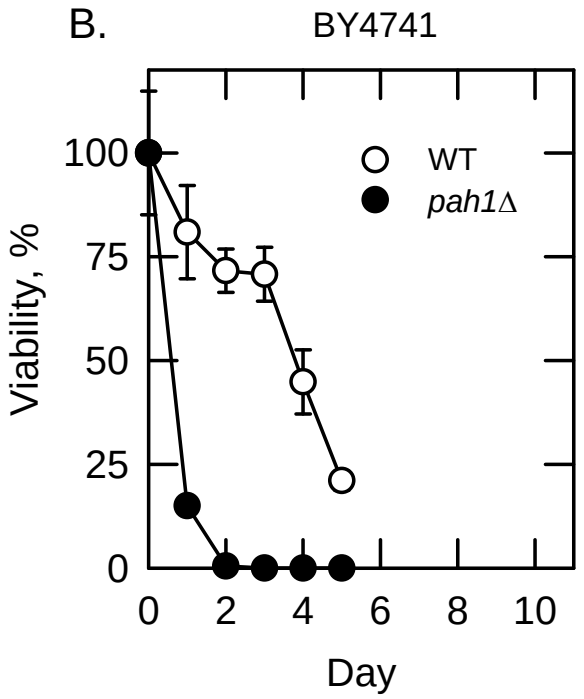
B.
BY4741
WT
pah1Δ
Viability, %
100
75
50
25
0
0
2
4
6
8
10
Day

The Deletion of *DGK1* Gene Complements Phenotypes of the *pah1*Δ Mutant

The *DGK1*-encoded DAG kinase counteracts Pah1 PAP by converting DAG to PA (87). Several phenotypes of the *pah1*Δ mutant which include nuclear/ER membrane expansion, reduced lipid droplet formation, and increased phospholipid content, are complemented by introduction of the *dgk1*Δ mutation indicating these phenotypes are related with the elevated level of PA in the *pah1*Δ mutant (87). Accordingly, we questioned whether introduction of the *DGK1* into *pah1*Δ rescues phenotypes that we found in this study.

At first, we performed growth on media containing non-fermentable carbon sources with wild type, *dgk1*Δ mutant, *pah1*Δ mutant, and *dgk1*Δ *pah1*Δ mutant cells (Fig. 5A). The mutation of the *DGK1* gene in the *pah1*Δ mutant improved the growth on non-fermentable carbon sources. Moreover, the growth of the double mutant was not limited in the presence of ethanol. However, the growth of the double mutant did not reach the level exhibited by wild type cells.

The *pah1*Δ mutant exhibited around 2-fold increase in the mitochondrial membrane potential in the post-diauxic phase. We wondered whether the deletion of the *DGK1* gene in the *pah1*Δ mutant affects the mitochondrial membrane potential (Fig. 12B). In the post-diauxic phase, the mitochondrial membrane potential was similar between the wild type and *dgk1*Δ mutant cells. The *dgk1*Δ *pah1*Δ double mutant exhibited about 1.5-fold increase in the mitochondrial membrane potential than wild type cells. However, comparing with the *pah1*Δ mutant, the double mutant exhibited 60 % decrease in the mitochondrial membrane potential in the post-diauxic phase.

We also measured the superoxide level in mitochondria using (Fig. 16B). In both the post-diauxic and the stationary phases, the superoxide level was not increased in the *dgk1*Δ mutant and the *dgk1*Δ *pah1*Δ mutant. Only the *pah1*Δ mutant exhibited highly increased superoxide level in the stationary phase.

Furthermore, the double mutant exhibited better growth than the *pah1*Δ mutant in the presence of hydrogen peroxide (Fig. 20A). In the presence of 0.6 mM hydrogen peroxide, the *pah1*Δ mutant exhibited sensitivity to the hydrogen peroxide, while the double mutant did not sensitive to the same concentration of the hydrogen peroxide. Even though the double mutant displayed sensitivity to the 1 mM hydrogen peroxide than wild type cells, the growth was improved over that of the *pah1*Δ mutant. The *dgk1*Δ single mutation did not exhibit the phenotype of the sensitivity to the hydrogen peroxide.

Finally, we examined the chronological life span of the *dgk1*Δ *pah1*Δ mutant (Fig. 22A). The *dgk1*Δ single mutation did not decrease the chronological life span. After day 4, the chronological life span of the *dgk1*Δ mutant was actually better than wild type cells. The chronological life span of the *dgk1*Δ *pah1*Δ double mutant exhibited viability of similar pattern with that of the *pah1*Δ mutant. However, the double mutant exhibited the increase in life span when compared with the *pah1*Δ mutant. Until day 3, the viability of the *dgk1*Δ *pah1*Δ mutant was not dramatically decreased within day 3, whereas, the *pah1*Δ mutant exhibited 50% viability at the same day.

DISCUSSION

In *S. cerevisiae*, Pah1 PAP, which catalyzes the dephosphorylation of PA to yield DAG, plays a crucial role in the synthesis of the storage lipid TAG (2, 10, 11). This evolutionarily conserved enzyme also plays a regulatory role in *de novo* phospholipid synthesis through the consumption of PA, a precursor of membrane phospholipids (2, 10, 11). The importance of Pah1 PAP in lipid metabolism is shown by the phenotypes of yeast cells containing altered levels of the enzyme activity. The lack of the enzyme activity causes phenotypes that are directly and indirectly associated with altered levels of PA and DAG, which include the aberrant nuclear/ER membrane expansion, reduced number of lipid droplets, and fatty acid induced-lipotoxicity (21, 24, 59, 82, 86). Conversely, the overexpression of Pah1 PAP has detrimental effects on cell viability, which include auxotrophic requirements for inositol and choline (95, 96), and DAG toxicity (69). In the case of mammalian cells, loss of lipin PAP enzymes result in metabolic disorders that include lipodystrophy, insulin resistance, peripheral neuropathy, rhabdomyolysis, and inflammation (28, 29, 88, 90, 92, 93, 238-244), whereas the overexpression of lipin-1 causes an obese phenotype and induces expression of genes involved in TCA cycle enzymes and oxidative phosphorylation (245).

In this study, we showed that the *pah1*Δ mutant is limited for ATP level, which correlated with an increase in lipid synthesis when cells progressed into the stationary phase (Fig. 23). Although the *pah1*Δ mutant is not defective in oxidative phosphorylation, it produced a higher mitochondrial superoxide level. The increased

FIGURE 23. Model for the loss of viability in the *pah1*Δ mutant. The *pah1*Δ mutant lacking PAP activity utilizes the PA precursor exclusively for the synthesis of membrane phospholipids. This process requires more ATP when compared with that of wild type cells that utilize PA for the synthesis of TAG. Therefore, the ATP synthesized by the mitochondria of *pah1*Δ cells is depleted due to the increased use for lipid synthesis. Furthermore, increased oxidative stress (high levels of ROS and lipid hydroperoxides) leads to cell damage in the stationary phase. Finally, ATP deletion and cell damage by toxic products decrease viability of the *pah1*Δ mutant in the stationary phase.

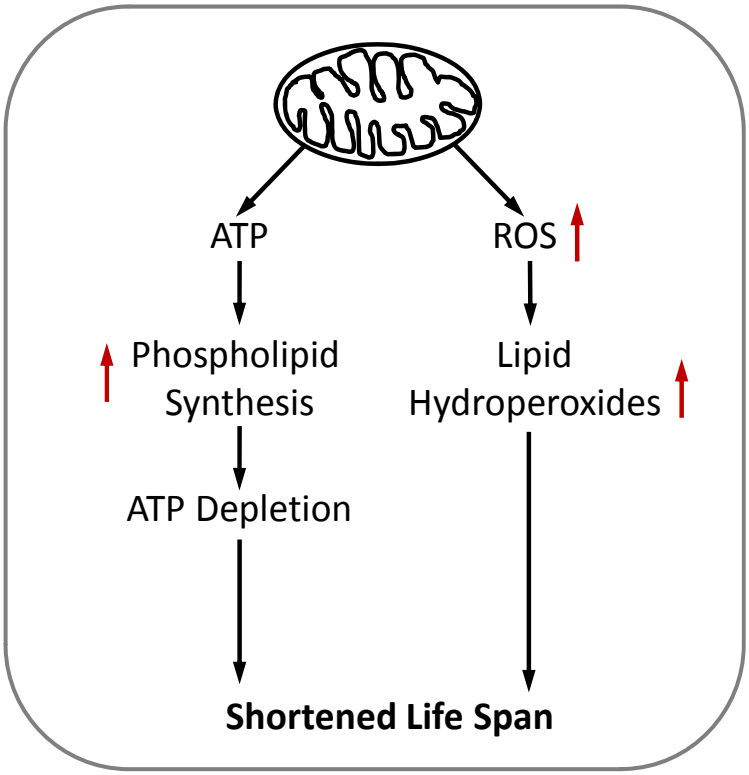
ATP
ROS
Phospholipid Synthesis
Lipid Hydroperoxides
ATP Depletion
Shortened Life Span

ATP consumption and higher ROS production contribute to a reduction of viability of the *pah1*Δ mutant in the stationary phase, i.e., shortens its chronological life span. We found that the ATP level was reduced in the post-diauxic phase *pah1*Δ mutant cells or in *pah1*Δ mutant cells grown with glycerol as a carbon source. We expected that the *pah1*Δ mutant is defective in oxidative phosphorylation and produces a reduced ATP level. However, in the exponential phase when mitochondrial function is not active as well as in the post-diauxic phase, the *pah1*Δ mutant was similar to wild type in regard to the components of oxidative phosphorylation, such as the oxygen consumption rate, mitochondrial membrane potential, and mitochondrial F_1F_O-ATP synthase activity. Unlike other respiratory deficient mutants (e.g., ρ^0, ρ^-, *PET* mutant), the *pah1*Δ mutant did not form petite colonies when grown on glucose medium. Based on these observations, we did not consider the *pah1*Δ mutant to be defective in the production of ATP by mitochondrial oxidative phosphorylation. Instead, we interpreted the decreased ATP level upon growth on a non-fermentable carbon source (or in the post-diauxic phase) was the result from the increased ATP consumption.

The *pah1*Δ mutant that is defective in the PA-to-DAG conversion and TAG synthesis (21), exhibits higher levels of the PA-derived phospholipids and the accumulation of fatty acids (59). The increased phospholipid synthesis caused by a defect in TAG synthesis and the resulting accumulation of fatty acids might not be expected to affect total cellular lipid levels. Yet, the increased phospholipid and fatty acid levels in the *pah1*Δ mutant resulted in the mutant having an elevated cellular lipid level when compared with the wild type control. The *pah1*Δ mutant grown with glucose to the late exponential phase and then transferred to glycerol-containing growth medium had a

two-fold greater amount of total lipid when compared with that of wild type. At the same time, the ATP level was 40% lower in the *pah1*Δ mutant when compared with the wild type. Since the increase is pronounced in the post-diauxic phase when otherwise TAG synthesis is higher, an increased demand for ATP make the *pah1*Δ mutant limited for its cellular levels, leading to a growth defect. Thus, we posit that the reduced level of ATP due to its over-consumption for phospholipid synthesis contributes to a reduction in cell viability in the stationary phase.

The *pah1*Δ mutation causes an elevation of Dgk1 DAG kinase activity leading to the elevation of PA levels (87). However, the deletion of the *DGK1* gene in the *pah1*Δ mutant does not increase the net cellular lipid levels (87). Fatty acid and PA levels in the *dgk1*Δ *pah1*Δ double mutant are similar to wild type but not slightly increased in major phospholipid levels because of blocking of TAG production from PA (87). We found that the *dgk1*Δ mutation improves viability of the *pah1*Δ mutant and growth on non-fermentable carbon sources, and decreases the mitochondrial membrane potential in the post-diauxic phase. Thus, the lower level of lipid in the *dgk1*Δ *pah1*Δ mutant alleviates the demand for ATP, resulting in the improved viability. These results indicated that the PA produced from DAG by Dgk1 DAG kinase is required for the phenotype exhibited by the *pah1*Δ mutant.

Nevertheless, we expect that other mechanisms are associated with the decreased viability of the *pah1*Δ mutant, because deletion of *DGK1* in the *pah1*Δ mutant did not completely rescue the phenotype of the *pah1*Δ mutant. Interestingly, the viability of cells is consistent with the TAG level. The *dgk1*Δ mutant, which exhibits the TAG level higher than that of wild type because DAG cannot be converted into PA, showed

increased viability in the late stationary phase when compared with wild type cells. The TAG level and viability were elevated in the *dgk1*Δ *pah1*Δ mutant than in the *pah1*Δ mutant. Mutants defective in the TAG synthesis exhibit apoptotic phenotypes, presumably because of increased levels of free fatty acid and DAG (246). The *pah1*Δ mutant also exhibits lipotoxicity induced by an increase in free fatty acids. Even though *dgk1*Δ mutation in the *pah1*Δ mutant decreased the level of free fatty acids than the *pah1*Δ mutant, the *dgk1*Δ *pah1*Δ mutant still exhibited the elevated level of free fatty acid than wild type cells in the stationary phase. These observations suggested that the reduced level of TAG in the *pah1*Δ is related to its reduced viability in the late stationary phase.

Mitochondria are involved in a wide variety of cellular processes, including ATP production, lipid synthesis and transfer, aging, and apoptosis (113-115). Many of these processes occur in the mitochondrial membrane, and phospholipids play important roles in mitochondrial morphology and respiratory capacity (116, 175, 177, 178, 186, 188). In particular, phospholipid composition in the mitochondrial inner-membrane significantly affects the formation of respiratory supercomplexes from ETC complexes (144, 186). The deletion of *PAH1* gene causes the expansion of nuclear/ER membrane because of the increased level of PA (95). Accordingly, we wondered whether the *pah1*Δ mutation affects the mitochondrial membrane, resulting in defects on the mitochondrial morphology and functions. However, we did not detect great changes in the composition of the major mitochondrial phospholipids in the *pah1*Δ mutant. We found that the *pah1*Δ mutant exhibited no defects in the levels of mitochondrial PE and CL, while supercomplexes levels were a bit lower in the *pah1*Δ mutant when compared with the

wild type control. Interestingly, we found a lower level of PA in the mitochondria of the *pah1*Δ mutant. The basis for this observation is unclear. In yeast, PE is primarily synthesized in the mitochondria and then transported to the ER for the synthesis of PC (36, 37). If the *pah1*Δ mutant is defective in mitochondrial function, then PE production and transfer to the ER to produce PC would not be efficiently carried out. Our data indicated that the *pah1*Δ mutation does not cause defects on lipid production and trafficking in mitochondria.

In mammalian cells, the level of PA in mitochondria is related to the mitochondrial fusion and fission. PA produced from CL via phospholipase D induces mitochondrial fusion leading to tubulated mitochondria, whereas a decrease in the level of PA through its conversion to DAG by lipin-1β causes mitochondrial fission leading to fragmented mitochondria (131, 247). HeLa cells depleted for PA due to phospholipase A_1–mediated hydrolysis exhibits fragmented mitochondria (248). Based on these observations, we expected that the *pah1*Δ mutant would exhibit a more fragmented mitochondrial morphology in the stationary phase. However, this was not observed in our studies. Overall, we did not find a relationship between the PA level in the mitochondria and mitochondrial morphology (e.g., fusion/fission).

The mitochondria are also a main organelle for the production of ROS, such as superoxide and hydrogen peroxide, which cause oxidative damage to the major classes of cellular molecules (nucleic acids, proteins, and lipids) and, eventually lead to reduced cell viability (217, 249-251). To generate ATP in mitochondria, electrons are transferred to oxygen through ETC and ROS is produced simultaneously. We found that stationary phase *pah1*Δ cells exhibited elevated superoxide and lipid hydroperoxides levels.

Moreover, the mitochondrial membrane potential was elevated in post-diauxic *pah1*Δ mutant cells. Even though we did not detect significant defects in CL and PC levels, which are important phospholipids for formation of respiratory supercomplexes, we found that the *pah1*Δ mutant exhibited the lower level of respiratory supercomplexes in non-fermentable carbon sources. We suggest that the increased oxidative phosphorylation in the *pah1*Δ mutant due to requirement of ATP for lipid production cause the elevated superoxide production, and then superoxide is readily react with high level of lipid in the *pah1*Δ mutant, leading to production of toxic byproducts. Apparently, a consequence was an increase in sensitivity to hydrogen peroxide. In addition, we suggest that lower levels of mitochondrial respiratory supercomplexes in the *pah1*Δ mutant affected the superoxide level. Even though the role of supercomplexes is still controversial, they could improve the efficiency of electron transfer among ETC.

The *dgk1*Δ *pah1*Δ mutant was less sensitive to the hydrogen peroxide than the *pah1*Δ mutant, because the *dgk1*Δ *pah1*Δ mutant exhibited similar level of superoxide with that of wild type. However, sensitivity to the hydrogen peroxide in the *dgk1*Δ *pah1*Δ mutant is higher than in wild type. We speculate that increased levels of phospholipids and fatty acids in the *dgk1*Δ *pah1*Δ mutant affect its sensitivity to hydrogen peroxide.

Even though the level of superoxide was higher in the *pah1*Δ mutant, SOD activity was not affected. Catalase activity from cytosol but not from mitochondria was even reduced in the *pah1*Δ mutant. Accordingly, these enzyme activities could not be sufficient to remove the increased level of superoxide in the *pah1*Δ mutant. Moreover, the *pah1*Δ mutation is synthetically lethal with the lack of the *TSA1* gene encoding

thioredoxin peroxidase, an antioxidant enzyme in yeast (252). This finding suggests that the *pah1*Δ mutant is under high oxidative stress.

CONCLUSIONS AND FUTURE DIRECTIONS

This work indicates that the *pah1*Δ mutant become deleted for energy in the stationary phase. The *dgk1*Δ *pah1*Δ double mutation does not affect total levels of cellular lipids, whereas the *pah1*Δ single mutation leads to the increase in it in the stationary phase (59, 87). The *dgk1*Δ mutation complements the *pah1*Δ mutation with respect to lipid hydroperoxidation, ATP demand, and increase in chronological life span. Accordingly, we speculate that the PA production from increased Dgk1 DAG kinase activity in the *pah1*Δ mutant is critical for the viability of the *pah1*Δ mutant. However, it is still unclear that PA level is used for the synthesis of phospholipids or participates in the activation of lipid production pathway signaling. We still need to figure out whether glycerol-3-phosphate and fatty acid productions are clearly induced to produce lipid in the stationary phase in the *pah1*Δ mutant.

In addition, the increase in total levels of cellular lipids in the *pah1*Δ mutant causes the secondary effect such as oxidative stress caused by superoxide and lipid hydroperoxides productions in the stationary phase. We found that anti-oxidant enzyme activities were not induced in the *pah1*Δ mutant than wild type, even though the *pah1*Δ mutant was exposed to the oxidative stress more than wild type. Transcription factors such as a zinc finger DNA-binding protein (encoded by *Msn2*/*Msn4*) and yeast AP-1, a member of the AP-1 family of transcription factors, are involved in the

expression of antioxidant enzymes. Msn2/Msn4 upon its activation translocates to the nucleus, and induces the expression of oxidative stress response genes containing stress response element (STRE) in the promoter (253, 254). For example, the *CTT1*gene encoding cytosolic catalase has been shown to be upregulated through the *cis*-acting element under oxidative stress (253, 255). In addition, upon activation by hydrogen peroxide, Yap1 translocates from the cytosol to the nucleus, and induces the expression of antioxidant genes including *GPX3* and *TRX2* (256, 257). Accordingly, additional studies to examine the effects of *pah1*Δ mutation on these oxidative stress response pathways are warranted. We also will examine whether overexpression of antioxidant enzymes including SOD, catalase, and thioredoxin peroxidase in the *pah1*Δ mutant and addition of antioxidants to the growth medium decrease the sensitivity to the hydrogen peroxide and/or improve the chronological life span.

Target of rapamycin (TOR), a Ser/Thr kinase, is associated with a wide range of cellular processing such as ribosome biogenesis, regulation of cell cycle and size, autophagy, and cell wall integrity pathway in yeast (258, 258-261). TOR, which is active in the presence of nutrient including glucose, promotes cell proliferation pathway, whereas TOR is inactive in the nutrient depletion (258, 259). Accordingly, TOR is active in the exponential phase, and then it is inactive in the stationary phase. The *tor1*Δ mutation extends chronological life span by changes of mitochondrial function and oxidative stress (262-264). Autophagy is also an important cellular processing when cells survive in the nutrient depletion for energy production. In mammals and bacteria, PA and DAG participate in TOR signaling, resulting in regulation of autophagy (265-268). The phenotypes of the *pah1*Δ mutant are similar to characteristics when TOR

signaling is malfunctioned considerably. Therefore, the investigation of TOR signaling in the *pah1*Δ mutant could be helpful to understand the mechanism the effects of Pah1 PAP on life span.

REFERENCES

1. Chang, Y.-F. and Carman, G. M. (2008) CTP synthetase and its role in phospholipid synthesis in the yeast *Saccharomyces cerevisiae*. *Prog. Lipid Res.* 333-339

2. Carman, G. M. and Han, G.-S. (2011) Regulation of phospholipid synthesis in the yeast *Saccharomyces cerevisiae*. *Ann. Rev. Biochem.* 80, 859-883

3. Henry, S. A., Kohlwein, S., and Carman, G. M. (2012) Metabolism and regulation of glycerolipids in the yeast *Saccharomyces cerevisiae*. *Genetics* 190, 317-349

4. Vance, D. E. Biochemistry of Lipids, Lipoproteins and Membranes,(Vance ,D.E., and Vance, J., eds). 153-181. 2004. Amsterdam, Elsecier Science publishers B.V. Ref Type: Generic

5. Carman, G. M. and Henry, S. A. (1999) Phospholipid biosynthesis in the yeast *Saccharomyces cerevisiae* and interrelationship with other metabolic processes. *Prog. Lipid Res.* 38, 361-399

6. Gaspar, M. L., Aregullin, M. A., Jesch, S. A., Nunez, L. R., Villa-Garcia, M., and Henry, S. A. (2007) The emergence of yeast lipidomics. *Biochim. Biophys. Acta* 1771, 241-254

7. Carman, G. M. and Han, G.-S. (2009) Regulation of phospholipid synthesis in yeast. *J. Lipid Res.* 50, S69-S73

8. Taylor, F. R. and Parks, L. W. (1979) Triacylglycerol metabolism in *Saccharomyces cerevisiae* relation to phospholipid synthesis. *Biochim. Biophys. Acta* 575, 204-214

9. Kennedy, E. P. (1961) Biosynthesis of complex lipids. *Federation Proceedings* 20, 934-940

10. Carman, G. M. and Han, G.-S. (2006) Roles of phosphatidate phosphatase enzymes in lipid metabolism. *Trends Biochem Sci* 31, 694-699

11. Carman, G. M. and Han, G.-S. (2009) Phosphatidic acid phosphatase, a key enzyme in the regulation of lipid synthesis. *J. Biol. Chem.* 284, 2593-2597

12. Pascual, F. and Carman, G. M. (2013) Phosphatidate phosphatase, a key regulator of lipid homeostasis. *Biochim. Biophys. Acta* 1831, 514-522

13. Smith, S. W., Weiss, S. B., and Kennedy, E. P. (1957) The enzymatic dephosphorylation of phosphatidic acids. *J. Biol. Chem.* 228, 915-922

14. Toke, D. A., Bennett, W. L., Dillon, D. A., Wu, W.-I., Chen, X., Ostrander, D. B., Oshiro, J., Cremesti, A., Voelker, D. R., Fischl, A. S., and Carman, G. M. (1998) Isolation and characterization of the *Saccharomyces cerevisiae DPP1* gene encoding for diacylglycerol pyrophosphate phosphatase. *J. Biol. Chem.* 273, 3278-3284

15. Toke, D. A., Bennett, W. L., Oshiro, J., Wu, W. I., Voelker, D. R., and Carman, G. M. (1999) Isolation and characterization of the *Saccharomyces cerevisiae LPP1* gene encoding a Mg^{2+}-independent phosphatidate phosphatase. *J. Biol. Chem.* 273, 14331-14338

16. Wu, W.-I., Liu, Y., Riedel, B., Wissing, J. B., Fischl, A. S., and Carman, G. M. (1996) Purification and characterization of diacylglycerol pyrophosphate phosphatase from *Saccharomyces cerevisiae*. *J. Biol. Chem.* 271, 1868-1876

17. Habeler, G., Natter, K., Thallinger, G. G., Crawford, M. E., Kohlwein, S. D., and Trajanoski, Z. (2002) YPL.db: the Yeast Protein Localization database. *Nucleic Acids Res.* 30, 80-83

18. Han, G.-S., Johnston, C. N., and Carman, G. M. (2004) Vacuole membrane topography of the *DPP1*-encoded diacylglycerol pyrophosphate phosphatase catalytic site from *Saccharomyces cerevisiae*. *J. Biol. Chem.* 279, 5338-5345

19. Furneisen, J. M. and Carman, G. M. (2000) Enzymological properties of the *LPP1*-encoded lipid phosphatase from *Saccharomyces cerevisiae*. *Biochim. Biophys. Acta* 1484, 71-82

20. Stukey, J. and Carman, G. M. (1997) Identification of a novel phosphatase sequence motif. *Protein Science* 6, 469-472

21. Han, G.-S., Wu, W.-I., and Carman, G. M. (2006) The *Saccharomyces cerevisiae* lipin homolog is a Mg^{2+}-dependent phosphatidate phosphatase enzyme. *J Biol. Chem.* 281, 9210-9218

22. Chae, M., Han, G.-S., and Carman, G. M. (2012) The *Saccharomyces cerevisiae* actin patch protein App1p is a phosphatidate phosphatase enzyme. *J. Biol. Chem.* 287, 40186-40196

23. Punta, M., Coggill, P. C., Eberhardt, R. Y., Mistry, J., Tate, J., Boursnell, C., Pang, N., Forslund, K., Ceric, G., Clements, J., Heger, A., Holm, L., Sonnhammer, E. L., Eddy, S. R., Bateman, A., and Finn, R. D. (2012) The Pfam protein families database. *Nucleic Acids Res.* 40, D290-D301

24. Han, G.-S., Siniossoglou, S., and Carman, G. M. (2007) The cellular functions of the yeast lipin homolog Pah1p are dependent on its phosphatidate phosphatase activity. *J. Biol. Chem.* 282, 37026-37035

25. Brindley, D. N. (1984) Intracellular translocation of phosphatidate

phosphohydrolase and its possible role in the control of glycerolipid synthesis. *Prog. Lipid Res.* 23, 115-133

26. Nanjundan, M. and Possmayer, F. (2003) Pulmonary phosphatidic acid phosphatase and lipid phosphate phosphohydrolase. *Am. J. Physiol Lung Cell Mol. Physiol* 284, L1-23

27. Brindley, D. N., Pilquil, C., Sariahmetoglu, M., and Reue, K. (2009) Phosphatidate degradation: phosphatidate phosphatases (lipins) and lipid phosphate phosphatases. *Biochim. Biophys. Acta* 1791, 956-961

28. Reue, K. and Brindley, D. N. (2008) Multiple roles for lipins/phosphatidate phosphatase enzymes in lipid metabolism. *J. Lipid Res.* 49, 2493-2503

29. Reue, K. and Dwyer, J. R. (2009) Lipin proteins and metabolic homeostasis. *J. Lipid Res.* 50 Suppl, S109-S114

30. Csaki, L. S. and Reue, K. (2010) Lipins: multifunctional lipid metabolism proteins. *Annu. Rev. Nutr.* 30, 257-272

31. Carter, J. R. and Kennedy, E. P. (1966) Enzymatic synthesis of cytidine diphosphate diglyceride. *J. Lipid Res.* 7, 678-683

32. Shen, H., Heacock, P. N., Clancey, C. J., and Dowhan, W. (1996) The *CDS1* gene encoding CDP-diacylglycerol synthase in *Saccharomyces cerevisiae* is essential for cell growth. *J. Biol. Chem.* 271, 789-795

33. Nikawa, J. and Yamashita, S. (1984) Molecular cloning of the gene encoding CDP-diacylglycerol- inositol 3-phosphatidyl transferase in *Saccharomyces cerevisiae*. *Eur. J. Biochem.* 143, 251-256

34. Nikawa, J., Kodaki, T., and Yamashita, S. (1987) Primary structure and disruption of the phosphatidylinositol synthase gene of *Saccharomyces cerevisiae*. *J. Biol. Chem.* 262, 4876-4881

35. Letts, V. A., Klig, L. S., Bae-Lee, M., Carman, G. M., and Henry, S. A. (1983) Isolation of the yeast structural gene for the membrane-associated enzyme phosphatidylserine synthase. *Proc. Natl. Acad. Sci. USA* 80, 7279-7283

36. Clancey, C. J., Chang, S.-C., and Dowhan, W. (1993) Cloning of a gene (*PSD1*) encoding phosphatidylserine decarboxylase from *Saccharomyces cerevisiae* by complementation of an *Escherichia coli* mutant. *J. Biol. Chem.* 268, 24580-24590

37. Kuchler, K., Daum, G., and Paltauf, F. (1986) Subcellular and submitochondrial localization of phospholipid- synthesizing enzymes in *Saccharomyces cerevisiae*. *J. Bacteriol.* 165, 901-910

38. Trotter, P. J. and Voelker, D. R. (1995) Identification of a non-mitochondrial phosphatidylserine decarboxylase activity (*PSD2*) in the yeast *Saccharomyces cerevisiae*. *J. Biol. Chem.* 270, 6062-6070

39. Gaynor, P. M. and Carman, G. M. (1990) Phosphatidylethanolamine methyltransferase and phospholipid methyltransferase activities from *Saccharomyces cerevisiae*. Enzymological and kinetic properties. *Biochim. Biophys. Acta* 1045, 156-163

40. Kodaki, T. and Yamashita, S. (1987) Yeast phosphatidylethanolamine methylation pathway: Cloning and characterization of two distinct methyltransferase genes. *J. Biol. Chem.* 262, 15428-15435

41. Summers, E. F., Letts, V. A., McGraw, P., and Henry, S. A. (1988) *Saccharomyces cerevisiae cho2* mutants are deficient in phospholipid methylation and cross-pathway regulation of inositol synthesis. *Genetics* 120, 909-922

42. Kodaki, T. and Yamashita, S. (1989) Characterization of the methyltransferases in the yeast phosphatidylethanolamine methylation pathway by selective gene disruption. *Eur. J. Biochem.* 185, 243-251

43. Kim, K., Kim, K.-H., Storey, M. K., Voelker, D. R., and Carman, G. M. (1999) Isolation and characterization of the *Saccharomyces cerevisiae EKI1* gene encoding ethanolamine kinase. *J. Biol. Chem.* 274, 14857-14866

44. Hosaka, K., Kodaki, T., and Yamashita, S. (1989) Cloning and characterization of the yeast *CKI* gene encoding choline kinase and its expression in *Escherichia coli*. *J. Biol. Chem.* 264, 2053-2059

45. Min-Seok, R., Kawamata, Y., Nakamura, H., Ohta, A., and Takagi, M. (1996) Isolation and characterization of *ECT1* gene encoding CTP:phosphoethanolamine cytidylyltransferase of *Saccharomyces cerevisiae*. *J. Biochem.* 120, 1040-1047

46. Tsukagoshi, Y., Nikawa, J., and Yamashita, S. (1987) Molecular cloning and characterization of the gene encoding cholinephosphate cytidylyltransferase in *Saccharomyces cerevisiae*. *Eur. J. Biochem.* 169, 477-486

47. Hjelmstad, R. H. and Bell, R. M. (1988) The sn-1,2-diacylglycerol ethanolaminephosphotransferase of *Saccharomyces cerevisiae*. Isolation of mutants and cloning of the *EPT1* gene. *J. Biol. Chem.* 263, 19748-19757

48. Hjelmstad, R. H. and Bell, R. M. (1987) Mutants of *Saccharomyces cerevisiae* defective in sn-1,2-diacylglycerol cholinephosphotransferase: Isolation, characterization, and cloning of the *CPT1* gene. *J. Biol. Chem.* 262, 3909-3917

49. Carman, G. M. and Henry, S. A. (1989) Phospholipid biosynthesis in yeast.

Annu. Rev. Biochem. 58, 635-669

50. Carman, G. M. (1989) in *Phosphatidylcholine metabolism* (Vance, D. E., eds) pp. 165-183, CRC Press, Inc., Boca Raton, Florida

51. Tamura, Y., Harada, Y., Nishikawa, S., Yamano, K., Kamiya, M., Shiota, T., Kuroda, T., Kuge, O., Sesaki, H., Imai, K., Tomii, K., and Endo, T. (2013) Tam41 is a CDP-diacylglycerol synthase required for cardiolipin biosynthesis in mitochondria. *Cell Metab* 17, 709-718

52. Carman, G. M. and Belunis, C. J. (1983) Phosphatidylglycerophosphate synthase activity in *Saccharomyces cerevisiae*. *Can. J. Microbiol.* 29, 1452-1457

53. Chang, S. C., Heacock, P. N., Clancey, C. J., and Dowhan, W. (1998) The *PEL1* gene (renamed *PGS1*) encodes the phosphatidylglycerophosphate synthase of *Saccharomyces cerevisiae*. *J. Biol. Chem.* 273, 9829-9836

54. Osman, C., Haag, M., Wieland, F. T., Brugger, B., and Langer, T. (2010) A mitochondrial phosphatase required for cardiolipin biosynthesis: the PGP phosphatase Gep4. *EMBO J.* 29, 1976-1987

55. Tamai, K. T. and Greenberg, M. L. (1990) Biochemical characterization and regulation of cardiolipin synthase in *Saccharomyces cerevisiae*. *Biochim. Biophys. Acta* 1046, 214-222

56. Kelly, B. L. and Greenberg, M. L. (1990) Characterization and regulation of phosphatidylglycerolphosphate phosphatase in *Saccharomyces cerevisiae*. *Biochim. Biophys. Acta* 1046, 144-150

57. Beranek, A., Rechberger, G., Knauer, H., Wolinski, H., Kohlwein, S. D., and Leber, R. (2009) Identification of a cardiolipin-specific phospholipase encoded by the gene *CLD1* (YGR110W) in yeast. *J. Biol. Chem.*

58. Vaz, F. M., Houtkooper, R. H., Valianpour, F., Barth, P. G., and Wanders, R. J. (2003) Only one splice variant of the human *TAZ* gene encodes a functional protein with a role in cardiolipin metabolism. *J. Biol. Chem.* 278, 43089-43094

59. Fakas, S., Qiu, Y., Dixon, J. L., Han, G.-S., Ruggles, K. V., Garbarino, J., Sturley, S. L., and Carman, G. M. (2011) Phosphatidate phosphatase activity plays a key role in protection against fatty acid-induced toxicity in yeast. *J. Biol. Chem.* 286, 29074-29085

60. Pascual, F., Soto-Cardalda, A., and Carman, G. M. (2013) *PAH1*-encoded phosphatidate phosphatase plays a role in the growth phase- and Inositol-mediated regulation of lipid synthesis in *Saccharomyces cerevisiae*. *J. Biol. Chem.*

61. Oelkers, P., Tinkelenberg, A., Erdeniz, N., Cromley, D., Billheimer, J. T., and Sturley, S. L. (2000) A lecithin cholesterol acyltransferase-like gene mediates diacylglycerol esterification in yeast. *J Biol. Chem.* 275, 15609-15612

62. Sorger, D. and Daum, G. (2002) Synthesis of triacylglycerols by the acyl-coenzyme A:diacyl-glycerol acyltransferase Dga1p in lipid particles of the yeast Saccharomyces cerevisiae. *J. Bacteriol.* 184, 519-524

63. Oelkers, P., Cromley, D., Padamsee, M., Billheimer, J. T., and Sturley, S. L. (2002) The *DGA1* gene determines a second triglyceride synthetic pathway in yeast. *J Biol. Chem.* 277, 8877-8881

64. Kohlwein, S. D. (2010) Triacylglycerol homeostasis: insights from yeast. *J. Biol. Chem.* 285, 15663-15667

65. Yang, H., Bard, M., Bruner, D. A., Gleeson, A., Deckelbaum, R. J., Aljinovic, G., Pohl, T. M., Rothstein, R., and Sturley, S. L. (1996) Sterol esterification in yeast: a two-gene process. *Science* 272, 1353-1356

66. Rajakumari, S., Grillitsch, K., and Daum, G. (2008) Synthesis and turnover of non-polar lipids in yeast. *Prog. Lipid Res.* 47, 157-171

67. Gaspar, M. L., Hofbauer, H. F., Kohlwein, S. D., and Henry, S. A. (2011) Coordination of Storage Lipid Synthesis and Membrane Biogenesis: EVIDENCE FOR CROSS-TALK BETWEEN TRIACYLGLYCEROL METABOLISM AND PHOSPHATIDYLINOSITOL SYNTHESIS. *J. Biol. Chem.* 286, 1696-1708

68. Han, G.-S., O'Hara, L., Siniossoglou, S., and Carman, G. M. (2008) Characterization of the yeast *DGK1*-encoded CTP-dependent diacylglycerol kinase. *J. Biol. Chem.* 283, 20443-20453

69. Fakas, S., Konstantinou, C., and Carman, G. M. (2011) *DGK1*-encoded diacylglycerol kinase activity is required for phospholipid synthesis during growth resumption from stationary phase in *Saccharomyces cerevisiae*. *J. Biol. Chem.* 286, 1464-1474

70. Waggoner, D. W., Xu, J., Singh, I., Jasinska, R., Zhang, Q. X., and Brindley, D. N. (1999) Structural organization of mammalian lipid phosphate phosphatases: implications for signal transduction. *Biochim. Biophys. Acta* 1439, 299-316

71. Sciorra, V. A. and Morris, A. J. (2002) Roles for lipid phosphate phosphatases in regulation of cellular signaling. *Biochim. Biophys. Acta* 1582, 45-51

72. Testerink, C. and Munnik, T. (2005) Phosphatidic acid: a multifunctional stress signaling lipid in plants. *Trends Plant Sci* 10, 368-375

73. Wang, X., Devaiah, S. P., Zhang, W., and Welti, R. (2006) Signaling functions

of phosphatidic acid. *Prog. Lipid Res.* 45, 250-278

74. Brindley, D. N. (2004) Lipid phosphate phosphatases and related proteins: signaling functions in development, cell division, and cancer. *J. Cell Biochem.* 92, 900-912

75. Howe, A. G. and McMaster, C. R. (2006) Regulation of phosphatidylcholine homeostasis by Sec14. *Can. J. Physiol. Pharmacol.* 84, 29-38

76. Foster, D. A. (2007) Regulation of mTOR by phosphatidic acid? *Cancer Res.* 67, 1-4

77. Bishop, W. R., Ganong, B. R., and Bell, R. M. (1986) Attenuation of sn-1,2-diacylglycerol second messengers by diacylglycerol kinase. *J. Biol. Chem.* 261, 6993-7000

78. Kearns, B. G., McGee, T. P., Mayinger, P., Gedvilaite, A., Phillips, S. E., Kagiwada, S., and Bankaitis, V. A. (1997) Essential role for diacylglycerol in protein transport from the yeast Golgi complex. *Nature* 387, 101-105

79. Carrasco, S. and Merida, I. (2007) Diacylglycerol, when simplicity becomes complex. *Trends Biochem. Sci.* 32, 27-36

80. Loewen, C. J. R., Gaspar, M. L., Jesch, S. A., Delon, C., Ktistakis, N. T., Henry, S. A., and Levine, T. P. (2004) Phospholipid metabolism regulated by a transcription factor sensing phosphatidic acid. *Science* 304, 1644-1647

81. Carman, G. M. and Henry, S. A. (2007) Phosphatidic acid plays a central role in the transcriptional regulation of glycerophospholipid synthesis in *Saccharomyces cerevisiae*. *J. Biol. Chem.* 282, 37293-37297

82. Santos-Rosa, H., Leung, J., Grimsey, N., Peak-Chew, S., and Siniossoglou, S. (2005) The yeast lipin Smp2 couples phospholipid biosynthesis to nuclear membrane growth. *EMBO J* 24, 1931-1941

83. Adeyo, O., Horn, P. J., Lee, S., Binns, D. D., Chandrahas, A., Chapman, K. D., and Goodman, J. M. (2011) The yeast lipin orthologue Pah1p is important for biogenesis of lipid droplets. *J. Cell Biol.* 192, 1043-1055

84. Lussier, M., White, A. M., Sheraton, J., di, P. T., Treadwell, J., Southard, S. B., Horenstein, C. I., Chen-Weiner, J., Ram, A. F., Kapteyn, J. C., Roemer, T. W., Vo, D. H., Bondoc, D. C., Hall, J., Zhong, W. W., Sdicu, A. M., Davies, J., Klis, F. M., Robbins, P. W., and Bussey, H. (1997) Large scale identification of genes involved in cell surface biosynthesis and architecture in *Saccharomyces cerevisiae*. *Genetics* 147, 435-450

85. Ruiz, C., Cid, V. J., Lussier, M., Molina, M., and Nombela, C. (1999) A large-scale sonication assay for cell wall mutant analysis in yeast. *Yeast* 15, 1001-

1008

86. Sasser, T., Qiu, Q. S., Karunakaran, S., Padolina, M., Reyes, A., Flood, B., Smith, S., Gonzales, C., and Fratti, R. A. (2011) The yeast lipin 1 orthologue Pah1p regulates vacuole homeostasis and membrane fusion. *J. Biol. Chem.* 287, 2221-2236

87. Han, G.-S., O'Hara, L., Carman, G. M., and Siniossoglou, S. (2008) An unconventional diacylglycerol kinase that regulates phospholipid synthesis and nuclear membrane growth. *J. Biol. Chem.* 283, 20433-20442

88. P?erfy, M., Phan, J., Xu, P., and Reue, K. (2001) Lipodystrophy in the *fld* mouse results from mutation of a new gene encoding a nuclear protein, lipin. *Nat. Genet.* 27, 121-124

89. Donkor, J., Sariahmetoglu, M., Dewald, J., Brindley, D. N., and Reue, K. (2007) Three mammalian lipins act as phosphatidate phosphatases with distinct tissue expression patterns. *J. Biol. Chem.* 282, 3450-3457

90. Phan, J. and Reue, K. (2005) Lipin, a lipodystrophy and obesity gene. *Cell Metab* 1, 73-83

91. Langner, C. A., Birkenmeier, E. H., Roth, K. A., Bronson, R. T., and Gordon, J. I. (1991) Characterization of the peripheral neuropathy in neonatal and adult mice that are homozygous for the fatty liver dystrophy (fld) mutation. *J. Biol. Chem.* 266, 11955-11964

92. Nadra, K., De Preux Charles, A.-S., Medard, J.-J., Hendriks, W. T., Han, G.-S., Gres, S., Carman, G. M., Saulnier-Blache, J.-S., Verheijen, M. H. G., and Chrast, R. (2008) Phosphatidic acid mediates demyelination in *Lpin1* mutant mice. *Genes Dev.* 22, 1647-1661

93. Zeharia, A., Shaag, A., Houtkooper, R. H., Hindi, T., de, L. P., Erez, G., Hubert, L., Saada, A., de, K. Y., Eshel, G., Vaz, F. M., Pines, O., and Elpeleg, O. (2008) Mutations in *LPIN1* cause recurrent acute myoglobinuria in childhood. *Am. J. Hum. Genet.* 83, 489-494

94. Bergounioux, J., Brassier, A., Rambaud, C., Bustarret, O., Michot, C., Hubert, L., Arnoux, J. B., Laquerriere, A., Bekri, S., Galene-Gromez, S., Bonnet, D., Hubert, P., and de, L. P. (2012) Fatal rhabdomyolysis in 2 children with *LPIN1* mutations. *J. Pediatr.* 160, 1052-1054

95. O'Hara, L., Han, G.-S., Peak-Chew, S., Grimsey, N., Carman, G. M., and Siniossoglou, S. (2006) Control of phospholipid synthesis by phosphorylation of the yeast lipin Pah1p/Smp2p $Mg2^{+-}$dependent phosphatidate phosphatase. *J Biol. Chem.* 281, 34537-34548

96. Choi, H.-S., Su, W.-M., Morgan, J. M., Han, G.-S., Xu, Z., Karanasios, E.,

Siniossoglou, S., and Carman, G. M. (2011) Phosphorylation of phosphatidate phosphatase regulates its membrane association and physiological functions in S*accharomyces cerevisiae.* Identification of Ser6^{02,} Thr7^{23,} and Ser7^{44} as the sites phosphorylated by *CDC28* (*CDK1)*-encoded cyclin-dependent kinase. *J. Biol. Chem.* 286, 1486-1498

97. Choi, H.-S., Su, W.-M., Han, G.-S., Plote, D., Xu, Z., and Carman, G. M. (2012) Pho85p-Pho80p phosphorylation of yeast Pah1p phosphatidate phosphatase regulates its activity, location, abundance, and function in lipid metabolism. *J. Biol. Chem.* 287, 11290-11301

98. Su, W.-M., Han, G.-S., Casciano, J., and Carman, G. M. (2012) Protein kinase A-mediated phosphorylation of Pah1p phosphatidate phosphatase functions in conjunction with the Pho85p-Pho80p and Cdc28p-cyclin B kinases to regulate lipid synthesis in yeast. *J. Biol. Chem.* 287, 33364-33376

99. Su, W. M., Han, G. S., and Carman, G. M. (2014) Cross-talk phosphorylations by protein kinase C and Pho85p-Pho80p protein kinase regulate Pah1p phosphatidate phosphatase abundance in *Saccharomyces cerevisiae.* J. *Biol. Chem.* 289, 18818-18830

100. Karanasios, E., Han, G.-S., Xu, Z., Carman, G. M., and Siniossoglou, S. (2010) A phosphorylation-regulated amphipathic helix controls the membrane translocation and function of the yeast phosphatidate phosphatase. *Proc. Natl. Acad. Sci. U. S. A.* 107, 17539-17544

101. Karanasios, E., Barbosa, A. D., Sembongi, H., Mari, M., Han, G.-S., Reggiori, F., Carman, G. M., and Siniossoglou, S. (2013) Regulation of lipid droplet and membrane biogenesis by the acidic tail of the phosphatidate phosphatase Pah1p. *Mol. Biol. Cell* 24, 2124-2133

102. Pascual, F., Hsieh, L.-S., Soto-Cardalda, A., and Carman, G. M. (2014) Yeast Pah1p phosphatidate phosphatase is regulated by proteasome-mediated degradation. *J. Biol. Chem.* 289, 9811-9822

103. Blom, N., Sicheritz-Ponten, T., Gupta, R., Gammeltoft, S., and Brunak, S. (2004) Prediction of post-translational glycosylation and phosphorylation of proteins from the amino acid sequence. *Proteomics.* 4, 1633-1649

104. Siniossoglou, S., Santos-Rosa, H., Rappsilber, J., Mann, M., and Hurt, E. (1998) A novel complex of membrane proteins required for formation of a spherical nucleus. *EMBO J.* 17, 6449-6464

105. Madera, M., Vogel, C., Kummerfeld, S. K., Chothia, C., and Gough, J. (2004) The SUPERFAMILY database in 2004: additions and improvements. *Nucleic Acids Res.* 32, D235-D239

106. Koonin, E. V. and Tatusov, R. L. (1994) Computer analysis of bacterial

haloacid dehalogenases defines a large superfamily of hydrolases with diverse specificity. Application of an iterative approach to database search. *J. Mol. Biol.* 244, 125-132

107. Wu, W.-I. and Carman, G. M. (1996) Regulation of phosphatidate phosphatase activity from the yeast *Saccharomyces cerevisiae b*y phospholipids. *Biochemistry* 35, 3790-3796

108. Wu, W.-I., Lin, Y.-P., Wang, E., Merrill, A. H., Jr., and Carman, G. M. (1993) Regulation of phosphatidate phosphatase activity from the yeast *Saccharomyces cerevisiae b*y sphingoid bases. *J. Biol. Chem.* 268, 13830-13837

109. Wu, W.-I. and Carman, G. M. (1994) Regulation of phosphatidate phosphatase activity from the yeast *Saccharomyces cerevisiae b*y nucleotides. *J. Biol. Chem.* 269, 29495-29501

110. Ostrander, D. B., O'Brien, D. J., Gorman, J. A., and Carman, G. M. (1998) Effect of CTP synthetase regulation by CTP on phospholipid synthesis in *Saccharomyces cerevisiae. J. Biol. Chem.* 273, 18992-19001

111. Soto-Cardalda, A., Fakas, S., Pascual, F., Choi, H. S., and Carman, G. M. (2011) Phosphatidate phosphatase plays role in zinc-mediated regulation of phospholipid synthesis in yeast. *J. Biol. Chem.* 287, 968-977

112. Vallee, B. L. and Falchuk, K. H. (1993) The biochemical basis of zinc physiology. *Physiol Rev.* 73, 79-118

113. Perkins, G., Bossy-Wetzel, E., and Ellisman, M. H. (2009) New insights into mitochondrial structure during cell death. *Exp. Neurol.* 218, 183-192

114. Osman, C., Voelker, D. R., and Langer, T. (2011) Making heads or tails of phospholipids in mitochondria. *The Journal of Cell Biology* 192, 7-16

115. Ocampo, A., Liu, J., Schroeder, E. A., Shadel, G. S., and Barrientos, A. (2012) Mitochondrial respiratory thresholds regulate yeast chronological life span and its extension by caloric restriction. *Cell Metab* 16, 55-67

116. Okamoto, K. and Shaw, J. M. (2005) Mitochondrial morphology and dynamics in yeast and multicellular eukaryotes. *Annu. Rev. Genet.* 39, 503-536

117. DiMauro, S. and Schon, E. A. (2003) Mitochondrial respiratory-chain diseases. *N. Engl. J. Med.* 348, 2656-2668

118. Ren, J., Pulakat, L., Whaley-Connell, A., and Sowers, J. R. (2010) Mitochondrial biogenesis in the metabolic syndrome and cardiovascular disease. *J. Mol. Med. (Berl)* 88, 993-1001

119. Supale, S., Li, N., Brun, T., and Maechler, P. (2012) Mitochondrial dysfunction

in pancreatic beta cells. *Trends Endocrinol. Metab* 23, 477-487

120. de, V. S. and Grivell, L. A. (1988) Purification and characterization of a rotenone-insensitive NADH:Q6 oxidoreductase from mitochondria of S*accharomyces cerevisiae. Eur. J. Biochem.* 176, 377-384

121. Saraste, M. (1999) Oxidative phosphorylation at the fin de siecle. *Science* 283, 1488-1493

122. Luttik, M. A., Overkamp, K. M., Kotter, P., de, V. S., van Dijken, J. P., and Pronk, J. T. (1998) The *Saccharomyces cerevisiae NDE1* and *NDE2* genes encode separate mitochondrial NADH dehydrogenases catalyzing the oxidation of cytosolic NADH. *J. Biol. Chem.* 273, 24529-24534

123. Small, W. C. and ister-Henn, L. (1998) Identification of a cytosolically directed NADH dehydrogenase in mitochondria of *Saccharomyces cerevisiae. J. Bacteriol.* 180, 4051-4055

124. Bakker, B. M., Overkamp, K. M., van Maris, A. J., Kotter, P., Luttik, M. A., van Dijken, J. P., and Pronk, J. T. (2001) Stoichiometry and compartmentation of NADH metabolism in *Saccharomyces cerevisiae. FEMS Microbiol. Rev.* 25, 15-37

125. Larsson, C., Pahlman, I. L., Ansell, R., Rigoulet, M., Adler, L., and Gustafsson, L. (1998) The importance of the glycerol 3-phosphate shuttle during aerobic growth of *Saccharomyces cerevisiae. Yeast* 14, 347-357

126. Rigoulet, M., Aguilaniu, H., Averet, N., Bunoust, O., Camougrand, N., Grandier-Vazeille, X., Larsson, C., Pahlman, I. L., Manon, S., and Gustafsson, L. (2004) Organization and regulation of the cytosolic NADH metabolism in the yeast *Saccharomyces cerevisiae. Mol. Cell Biochem.* 256-257, 73-81

127. Bakker, B. M., Bro, C., Kotter, P., Luttik, M. A., van Dijken, J. P., and Pronk, J. T. (2000) The mitochondrial alcohol dehydrogenase Adh3p is involved in a redox shuttle in *Saccharomyces cerevisiae. J. Bacteriol.* 182, 4730-4737

128. Robinson, K. M., von Kieckebusch-Guck, A., and Lemire, B. D. (1991) Isolation and characterization of a *Saccharomyces cerevisiae* mutant disrupted for the succinate dehydrogenase flavoprotein subunit. *J. Biol. Chem.* 266, 21347-21350

129. Hauber, J. and Singer, T. P. (1967) Studies on succinate dehydrogenase. 14. Intracellular distribution, catalytic properties and regulation of fumarate reductases in yeast. *Eur. J. Biochem.* 3, 107-116

130. Beattie, D. S., Japa, S., Howton, M., and Zhu, Q. S. (1992) Direct interaction between the internal NADH: ubiquinone oxidoreductase and ubiquinol:cytochrome *c* oxidoreductase in the reduction of exogenous quinones

by yeast mitochondria. *Arch. Biochem. Biophys.* 292, 499-505

131. Kagawa, Y. and Racker, E. (1966) Partial resolution of the enzymes catalyzing oxidative phosphorylation. X. Correlation of morphology and function in submitochondrial particles. *J. Biol. Chem.* 241, 2475-2482

132. Macino, G. and Tzagoloff, A. (1979) Assembly of the mitochondrial membrane system. The DNA sequence of a mitochondrial ATPase gene in *Saccharomyces cerevisiae. J. Biol. Chem.* 254, 4617-4623

133. Todd, R. D., Griesenbeck, T. A., and Douglas, M. G. (1980) The yeast mitochondrial adenosine triphosphatase complex. Subunit stoichiometry and physical characterization. *J. Biol. Chem.* 255, 5461-5467

134. Heinemeyer, J., Braun, H. P., Boekema, E. J., and Kouril, R. (2007) A structural model of the cytochrome *C* reductase/oxidase supercomplex from yeast mitochondria. *J. Biol. Chem.* 282, 12240-12248

135. Cruciat, C. M., Brunner, S., Baumann, F., Neupert, W., and Stuart, R. A. (2000) The cytochrome bc1 and cytochrome *c* oxidase complexes associate to form a single supracomplex in yeast mitochondria. *J. Biol. Chem.* 275, 18093-18098

136. Krause, F., Scheckhuber, C. Q., Werner, A., Rexroth, S., Reifschneider, N. H., Dencher, N. A., and Osiewacz, H. D. (2004) Supramolecular organization of cytochrome *c* oxidase- and alternative oxidase-dependent respiratory chains in the filamentous fungus Podospora anserina. *J. Biol. Chem.* 279, 26453-26461

137. Dudkina, N. V., Eubel, H., Keegstra, W., Boekema, E. J., and Braun, H. P. (2005) Structure of a mitochondrial supercomplex formed by respiratory-chain complexes I and III. *Proc. Natl. Acad. Sci. U. S. A* 102, 3225-3229

138. Eubel, H., Jansch, L., and Braun, H. P. (2003) New insights into the respiratory chain of plant mitochondria. Supercomplexes and a unique composition of complex II. *Plant Physiol* 133, 274-286

139. Schagger, H. and Pfeiffer, K. (2000) Supercomplexes in the respiratory chains of yeast and mammalian mitochondria. *EMBO J.* 19, 1777-1783

140. Gomez, L. A., Monette, J. S., Chavez, J. D., Maier, C. S., and Hagen, T. M. (2009) Supercomplexes of the mitochondrial electron transport chain decline in the aging rat heart. *Arch. Biochem. Biophys.* 490, 30-35

141. Vartak, R., Porras, C. A., and Bai, Y. (2013) Respiratory supercomplexes: structure, function and assembly. *Protein Cell* 4, 582-590

142. Genova, M. L. and Lenaz, G. (2014) Functional role of mitochondrial respiratory supercomplexes. *Biochim. Biophys. Acta* 1837, 427-443

143. cin-Perez, R. and Enriquez, J. A. (2014) The function of the respiratory supercomplexes: the plasticity model. *Biochim. Biophys. Acta* 1837, 444-450

144. McKenzie, M., Lazarou, M., Thorburn, D. R., and Ryan, M. T. (2006) Mitochondrial respiratory chain supercomplexes are destabilized in Barth Syndrome patients. *J. Mol. BIol.* 361, 462-469

145. Paumard, P., Vaillier, J., Coulary, B., Schaeffer, J., Soubannier, V., Mueller, D. M., Brethes, D., di Rago, J. P., and Velours, J. (2002) The ATP synthase is involved in generating mitochondrial cristae morphology. *EMBO J.* 21, 221-230

146. Wanders, R. J. and Waterham, H. R. (2006) Biochemistry of mammalian peroxisomes revisited. *Annu. Rev. Biochem.* 75, 295-332

147. Starkov, A. A. (2008) The role of mitochondria in reactive oxygen species metabolism and signaling. *Ann. N. Y. Acad. Sci.* 1147, 37-52

148. Brown, G. C. and Borutaite, V. (2012) There is no evidence that mitochondria are the main source of reactive oxygen species in mammalian cells. *Mitochondrion.* 12, 1-4

149. Beckman, K. B. and Ames, B. N. (1998) The free radical theory of aging matures. *Physiol Rev.* 78, 547-581

150. Chen, Q., Vazquez, E. J., Moghaddas, S., Hoppel, C. L., and Lesnefsky, E. J. (2003) Production of reactive oxygen species by mitochondria: central role of complex III. *J. Biol. Chem.* 278, 36027-36031

151. Murphy, M. P. (2009) How mitochondria produce reactive oxygen species. *Biochem. J.* 417, 1-13

152. Balaban, R. S., Nemoto, S., and Finkel, T. (2005) Mitochondria, oxidants, and aging. *Cell* 120, 483-495

153. Fridovich, I. (1978) The biology of oxygen radicals. *Science* 201, 875-880

154. Jamieson, D. J. (1998) Oxidative stress responses of the yeast *Saccharomyces cerevisiae. Yeast* 14, 1511-1527

155. Perrone, G. G., Tan, S. X., and Dawes, I. W. (2008) Reactive oxygen species and yeast apoptosis. *Biochim. Biophys. Acta* 1783, 1354-1368

156. Steinman, H. M. (1980) The amino acid sequence of copper-zinc superoxide dismutase from bakers' yeast. *J. Biol. Chem.* 255, 6758-6765

157. Sturtz, L. A., Diekert, K., Jensen, L. T., Lill, R., and Culotta, V. C. (2001) A fraction of yeast Cu,Zn-superoxide dismutase and its metallochaperone, CCS, localize to the intermembrane space of mitochondria. A physiological role for

SOD1 in guarding against mitochondrial oxidative damage. *J. Biol. Chem.* 276, 38084-38089

158. Ravindranath, S. D. and Fridovich, I. (1975) Isolation and characterization of a manganese-containing superoxide dismutase from yeast. *J. Biol. Chem.* 250, 6107-6112

159. Cohen, G., Rapatz, W., and Ruis, H. (1988) Sequence of the *Saccharomyces cerevisiae* C*TA1* gene and amino acid sequence of catalase A derived from it. *Eur. J. Biochem.* 176, 159-163

160. Seah, T. C. and Kaplan, J. G. (1973) Purification and properties of the catalase of bakers' yeast. *J. Biol. Chem.* 248, 2889-2893

161. Petrova, V. Y., Drescher, D., Kujumdzieva, A. V., and Schmitt, M. J. (2004) Dual targeting of yeast catalase A to peroxisomes and mitochondria. *Biochem. J.* 380, 393-400

162. Seah, T. C., Bhatti, A. R., and Kaplan, J. G. (1973) Novel catalatic proteins of bakers' yeast. I. An atypical catalase. *Can. J. Biochem.* 51, 1551-1555

163. Avery, A. M. and Avery, S. V. (2001) *Saccharomyces cerevisiae* expresses three phospholipid hydroperoxide glutathione peroxidases. *J. Biol. Chem.* 276, 33730-33735

164. Herrero, E., Ros, J., Belli, G., and Cabiscol, E. (2008) Redox control and oxidative stress in yeast cells. *Biochim. Biophys. Acta* 1780, 1217-1235

165. Gralla, E. B. and Valentine, J. S. (1991) Null mutants of *Saccharomyces cerevisiae* Cu,Zn superoxide dismutase: characterization and spontaneous mutation rates. *J. Bacteriol.* 173, 5918-5920

166. Longo, V. D., Gralla, E. B., and Valentine, J. S. (1996) Superoxide dismutase activity is essential for stationary phase survival in *Saccharomyces cerevisiae.* Mitochondrial production of toxic oxygen species i*n vivo. J. Biol. Chem.* 271, 12275-12280

167. Corson, L. B., Folmer, J., Strain, J. J., Culotta, V. C., and Cleveland, D. W. (1999) Oxidative stress and iron are implicated in fragmenting vacuoles of *Saccharomyces* c*erevisiae* lacking Cu,Zn-superoxide dismutase. *J. Biol. Chem.* 274, 27590-27596

168. van Loon, A. P., Pesold-Hurt, B., and Schatz, G. (1986) A yeast mutant lacking mitochondrial manganese-superoxide dismutase is hypersensitive to oxygen. *Proc. Natl. Acad. Sci. U. S. A* 83, 3820-3824

169. Cortes-Rojo, C., Estrada-Villagomez, M., Calderon-Cortes, E., Clemente-Guerrero, M., Mejia-Zepeda, R., Boldogh, I., and Saavedra-Molina, A. (2011)

Electron transport chain dysfunction by H_2O_2 is linked to increased reactive oxygen species production and iron mobilization by lipoperoxidation: studies using *Saccharomyces cerevisiae* mitochondria. *J. Bioenerg. Biomembr.* 43, 135-147

170. Izawa, S., Inoue, Y., and Kimura, A. (1996) Importance of catalase in the adaptive response to hydrogen peroxide: analysis of acatalasaemic *Saccharomyces cerevisiae*. *Biochem. J.* 320 (Pt 1), 61-67

171. Lee, H. Y., Choi, C. S., Birkenfeld, A. L., Alves, T. C., Jornayvaz, F. R., Jurczak, M. J., Zhang, D., Woo, D. K., Shadel, G. S., Ladiges, W., Rabinovitch, P. S., Santos, J. H., Petersen, K. F., Samuel, V. T., and Shulman, G. I. (2010) Targeted expression of catalase to mitochondria prevents age-associated reductions in mitochondrial function and insulin resistance. *Cell Metab* 12, 668-674

172. Mesquita, A., Weinberger, M., Silva, A., Sampaio-Marques, B., Almeida, B., Leao, C., Costa, V., Rodrigues, F., Burhans, W. C., and Ludovico, P. (2010) Caloric restriction or catalase inactivation extends yeast chronological lifespan by inducing H_2O_2 and superoxide dismutase activity. *Proc. Natl. Acad. Sci. U. S. A* 107, 15123-15128

173. van, M. G., Voelker, D. R., and Feigenson, G. W. (2008) Membrane lipids: where they are and how they behave. *Nat. Rev. Mol. Cell Biol.* 9, 112-124

174. Gohil, V. M. and Greenberg, M. L. (2009) Mitochondrial membrane biogenesis: phospholipids and proteins go hand in hand. *J. Cell Biol.* 184, 469-472

175. Zhang, M., Mileykovskaya, E., and Dowhan, W. (2005) Cardiolipin is essential for organization of complexes III and IV into a supercomplex in intact yeast mitochondria. *J. Biol. Chem.* 280, 29403-29408

176. Chen, S., Tarsio, M., Kane, P. M., and Greenberg, M. L. (2008) Cardiolipin mediates cross-talk between mitochondria and the vacuole. *Mol. Biol. Cell* 19, 5047-5058

177. Zhou, J., Zhong, Q., Li, G., and Greenberg, M. L. (2009) Loss of cardiolipin leads to longevity defects that are alleviated by alterations in stress response signaling. *J. Biol. Chem.* 284, 18106-18114

178. Joshi, A. S., Zhou, J., Gohil, V. M., Chen, S., and Greenberg, M. L. (2009) Cellular functions of cardiolipin in yeast. *Biochim. Biophys. Acta* 1793, 212-218

179. Zhong, Q., Gvozdenovic-Jeremic, J., Webster, P., Zhou, J., and Greenberg, M. L. (2005) Loss of function of KRE5 suppresses temperature sensitivity of mutants lacking mitochondrial anionic lipids. *Mol. Biol. Cell* 16, 665-675

180. Jiang, F., Gu, Z., Granger, J. M., and Greenberg, M. L. (1999) Cardiolipin

synthase expression is essential for growth at elevated temperature and is regulated by factors affecting mitochondrial development. *Mol Microbiol* 31, 373-379

181. Zhong, Q., Gohil, V. M., Ma, L., and Greenberg, M. L. (2004) Absence of cardiolipin results in temperature sensitivity, respiratory defects, and mitochondrial DNA instability independent of pet56. *J. Biol. Chem.* 279, 32294-32300

182. Ye, C., Lou, W., Li, Y., Chatzispyrou, I. A., Huttemann, M., Lee, I., Houtkooper, R. H., Vaz, F. M., Chen, S., and Greenberg, M. L. (2014) Deletion of the cardiolipin-specific phospholipase Cld1 rescues growth and life span defects in the tafazzin mutant: implications for Barth syndrome. *J. Biol. Chem.* 289, 3114-3125

183. Serricchio, M. and Butikofer, P. (2013) Phosphatidylglycerophosphate synthase associates with a mitochondrial inner membrane complex and is essential for growth of Trypanosoma brucei. *Mol. Microbiol.* 87, 569-579

184. Baile, M. G., Sathappa, M., Lu, Y. W., Pryce, E., Whited, K., McCaffery, J. M., Han, X., Alder, N. N., and Claypool, S. M. (2014) Unremodeled and remodeled cardiolipin are functionally indistinguishable in yeast. *J. Biol. Chem.* 289, 1768-1778

185. Joshi, A. S., Thompson, M. N., Fei, N., Huttemann, M., and Greenberg, M. L. (2012) Cardiolipin and mitochondrial phosphatidylethanolamine have overlapping functions in mitochondrial fusion in *Saccharomyces cerevisiae. J. Biol. Chem.* 287, 17589-17597

186. Tasseva, G., Bai, H. D., Davidescu, M., Haromy, A., Michelakis, E., and Vance, J. E. (2013) Phosphatidylethanolamine deficiency in Mammalian mitochondria impairs oxidative phosphorylation and alters mitochondrial morphology. *J. Biol. Chem.* 288, 4158-4173

187. Steenbergen, R., Nanowski, T. S., Beigneux, A., Kulinski, A., Young, S. G., and Vance, J. E. (2005) Disruption of the phosphatidylserine decarboxylase gene in mice causes embryonic lethality and mitochondrial defects. *J. Biol. Chem.* 280, 40032-40040

188. Yang, C. Y. and Frohman, M. A. (2012) Mitochondria: Signaling with phosphatidic acid. *Int. J. Biochem. Cell Biol.* 44, 1346-1350

189. Twig, G., Elorza, A., Molina, A. J., Mohamed, H., Wikstrom, J. D., Walzer, G., Stiles, L., Haigh, S. E., Katz, S., Las, G., Alroy, J., Wu, M., Py, B. F., Yuan, J., Deeney, J. T., Corkey, B. E., and Shirihai, O. S. (2008) Fission and selective fusion govern mitochondrial segregation and elimination by autophagy. *EMBO J.* 27, 433-446

190. Westermann, B. (2010) Mitochondrial fusion and fission in cell life and death. *Nat. Rev. Mol. Cell Biol.* 11, 872-884

191. Altmann, K., Frank, M., Neumann, D., Jakobs, S., and Westermann, B. (2008) The class V myosin motor protein, Myo2, plays a major role in mitochondrial motility in *Saccharomyces cerevisiae. J. Cell Biol.* 181, 119-130

192. Tondera, D., Grandemange, S., Jourdain, A., Karbowski, M., Mattenberger, Y., Herzig, S., Da, C. S., Clerc, P., Raschke, I., Merkwirth, C., Ehses, S., Krause, F., Chan, D. C., Alexander, C., Bauer, C., Youle, R., Langer, T., and Martinou, J. C. (2009) SLP-2 is required for stress-induced mitochondrial hyperfusion. *EMBO J.* 28, 1589-1600

193. Karbowski, M., Lee, Y. J., Gaume, B., Jeong, S. Y., Frank, S., Nechushtan, A., Santel, A., Fuller, M., Smith, C. L., and Youle, R. J. (2002) Spatial and temporal association of Bax with mitochondrial fission sites, Drp1, and Mfn2 during apoptosis. J. *Cell Biol.* 159, 931-938

194. Chan, D. C. (2006) Mitochondria: dynamic organelles in disease, aging, and development. *Cell* 125, 1241-1252

195. Karbowski, M. (2010) Mitochondria on guard: role of mitochondrial fusion and fission in the regulation of apoptosis. *Adv. Exp. Med. Biol.* 687, 131-142

196. Sang, Y., Cui, D., and Wang, X. (2001) Phospholipase D and phosphatidic acid-mediated generation of superoxide in Arabidopsis. *Plant Physiol* 126, 1449-1458

197. Li, M., Hong, Y., and Wang, X. (2009) Phospholipase D- and phosphatidic acid-mediated signaling in plants. *Biochim. Biophys. Acta* 1791, 927-935

198. Hanscho, M., Ruckerbauer, D. E., Chauhan, N., Hofbauer, H. F., Krahulec, S., Nidetzky, B., Kohlwein, S. D., Zanghellini, J., and Natter, K. (2012) Nutritional requirements of the BY series of *Saccharomyces cerevisiae* strains for optimum growth. *FEMS Yeast Res.* 12, 796-808

199. Sambrook, J., Fritsch, E. F., and Maniatis, T. (1989) *Molecular Cloning, A Laboratory Manual,* 2nd Ed., Cold Spring Harbor Laboratory, Cold Spring Harbor, N.Y.

200. Thomas, B. and Rothstein, R. (1989) Elevated recombination rates in transcriptionally active DNA. *Cell* 56, 619-630

201. Brachmann, C. B., Davies, A., Cost, G. J., Caputo, E., Li, J., Hieter, P., and Boeke, J. D. (1998) Designer deletion strains derived from *Saccharomyces cerevisiae* S288C: a useful set of strains and plasmids for PCR-mediated gene disruption and other applications. *Yeast* 14, 115-132

202. Westermann, B. and Neupert, W. (2000) Mitochondria-targeted green fluorescent proteins: convenient tools for the study of organelle biogenesis in *Saccharomyces cerevisiae*. *Yeast* 16, 1421-1427

203. Innis, M. A. and Gelfand, D. H. (1990) in *PCR Protocols. A Guide to Methods and Applications* (Innis, M. A., Gelfand, D. H., Sninsky, J. J., and White, T. J., eds) pp. 3-12, Academic Press, Inc., San Diego

204. Ito, H., Fukuda, Y., Murata, K., and Kimura, A. (1983) Transformation of intact yeast cells treated with alkali cations. *J. Bacteriol.* 153, 163-168

205. Rothstein, R. (1991) Targeting, disruption, replacement, and allele rescue: Integrative DNA transformation in yeast. *Methods Enzymol.* 194, 281-301

206. Carman, G. M. and Lin, Y.-P. (1991) Phosphatidate phosphatase from yeast. *Methods Enzymol.* 197, 548-553

207. Bradford, M. M. (1976) A rapid and sensitive method for the quantitation of microgram quantities of protein utilizing the principle of protein-dye binding. *Anal. Biochem.* 72, 248-254

208. Meisinger, C., Pfanner, N., and Truscott, K. N. (2006) Isolation of yeast mitochondria. *Methods Mol. Biol.* 313, 33-39

209. Laemmli, U. K. (1970) Cleavage of structural proteins during the assembly of the head of bacteriophage T4. *Nature (London)* 227, 680-685

210. Burnette, W. (1981) Western blotting: Electrophoretic transfer of proteins from sodium dodecyl sulfate-polyacrylamide gels to unmodified nitrocellulose and radiographic detection with antibody and radioiodinated protein A. *Anal. Biochem.* 112, 195-203

211. Haid, A. and Suissa, M. (1983) Immunochemical identification of membrane proteins after sodium dodecyl sulfate-polyacrylamide gel electrophoresis. *Methods Enzymol.* 96, 192-205

212. Schagger, H. and von, J. G. (1991) Blue native electrophoresis for isolation of membrane protein complexes in enzymatically active form. *Anal. Biochem.* 199, 223-231

213. Bozzola, J. J. and Russell, L. D. (1999) *Electron microscopy: Principles and techniques for biologists.,* 2nd Ed., Jones and Bartlett Publisher, Boston

214. Bligh, E. G. and Dyer, W. J. (1959) A rapid method of total lipid extraction and purification. *Can. J. Biochem. Physiol.* 37, 911-917

215. Esko, J. D. and Raetz, C. R. H. (1980) Mutants of Chinese hamster ovary cells with altered membrane phospholipid composition. Replacement of

phosphatidylinositol by phosphatidylglycerol in a *myo*-inositol auxotroph. *J. Biol. Chem.* 255, 4474-4480

216. Henderson, R. J. and Tocher, D. R. (1992) in *Lipid Analysis* (Hamilton, R. J. and Hamilton, S., eds) pp. 65-111, IRL Press, New York

217. Bonawitz, N. D., Rodeheffer, M. S., and Shadel, G. S. (2006) Defective mitochondrial gene expression results in reactive oxygen species-mediated inhibition of respiration and reduction of yeast life span. *Mol. Cell Biol.* 26, 4818-4829

218. Jiang, Z. Y., Hunt, J. V., and Wolff, S. P. (1992) Ferrous ion oxidation in the presence of xylenol orange for detection of lipid hydroperoxide in low density lipoprotein. A*nal. Biochem.* 202, 384-389

219. Beauchamp, C. and Fridovich, I. (1971) Superoxide dismutase: improved assays and an assay applicable to acrylamide gels. *Anal. Biochem.* 44, 276-287

220. Goldsteins, G., Keksa-Goldsteine, V., Ahtoniemi, T., Jaronen, M., Arens, E., Akerman, K., Chan, P. H., and Koistinaho, J. (2008) Deleterious role of superoxide dismutase in the mitochondrial intermembrane space. *J. Biol. Chem.* 283, 8446-8452

221. BEERS, R. F., Jr. and SIZER, I. W. (1952) A spectrophotometric method for measuring the breakdown of hydrogen peroxide by catalase. *J. Biol. Chem.* 195, 133-140

222. Blomberg, A. and Adler, L. (1989) Roles of glycerol and glycerol-3-phosphate dehydrogenase (NAD^+) in acquired osmotolerance of *Saccharomyces cerevisiae*. *J. Bacteriol.* 171, 1087-1092

223. Guerra, D. G., Decottignies, A., Bakker, B. M., and Michels, P. A. (2006) The mitochondrial FAD-dependent glycerol-3-phosphate dehydrogenase of Trypanosomatidae and the glycosomal redox balance of insect stages of Trypanosoma brucei and Leishmania spp. *Mol. Biochem. Parasitol.* 149, 155-169

224. Gardner, R. S. (1974) A sensitive colorimetric assay for mitochondrial alpha-glycerophosphate dehydrogenase. *Anal. Biochem.* 59, 272-276

225. Parrella, E. and Longo, V. D. (2008) The chronological life span of Saccharomyces cerevisiae to study mitochondrial dysfunction and disease. *Methods* 46, 256-262

226. Ocampo, A. and Barrientos, A. (2011) Quick and reliable assessment of chronological life span in yeast cell populations by flow cytometry. *Mech. Ageing Dev.* 132, 315-323

227. Huang, H. and Frohman, M. A. (2009) Lipid signaling on the mitochondrial surface. *Biochim. Biophys. Acta* 1791, 839-844

228. Shaw, J. M. and Nunnari, J. (2002) Mitochondrial dynamics and division in budding yeast. *Trends Cell Biol.* 12, 178-184

229. Skulachev, V. P. (2001) Mitochondrial filaments and clusters as intracellular power-transmitting cables. *Trends Biochem. Sci.* 26, 23-29

230. Ehrenberg, B., Montana, V., Wei, M. D., Wuskell, J. P., and Loew, L. M. (1988) Membrane potential can be determined in individual cells from the nernstian distribution of cationic dyes. *Biophys. J.* 53, 785-794

231. Ludovico, P., Sansonetty, F., and Corte-Real, M. (2001) Assessment of mitochondrial membrane potential in yeast cell populations by flow cytometry. *Microbiology* 147, 3335-3343

232. Pullman, M. E., Penefsky, H. S., Datta, A., and Racker, E. (1960) Partial resolution of the enzymes catalyzing oxidative phosphorylation. I. Purification and properties of soluble dinitrophenol-stimulated adenosine triphosphatase. *J. Biol. Chem.* 235, 3322-3329

233. Albertyn, J., Hohmann, S., Thevelein, J. M., and Prior, B. A. (1994) *GPD1,* which encodes glycerol-3-phosphate dehydrogenase, is essential for growth under osmotic stress in *Saccharomyces cerevisiae,* and its expression is regulated by the high-osmolarity glycerol response pathway. *Mol. Cell Biol.* 14, 4135-4144

234. Ansell, R., Granath, K., Hohmann, S., Thevelein, J. M., and Adler, L. (1997) The two isoenzymes for yeast NAD^+-dependent glycerol 3-phosphate dehydrogenase encoded by *GPD1* and *GPD2* have distinct roles in osmoadaptation and redox regulation. *EMBO J.* 16, 2179-2187

235. Ronnow, B. and Kielland-Brandt, M. C. (1993) *GUT2,* a gene for mitochondrial glycerol 3-phosphate dehydrogenase of *Saccharomyces cerevisiae. Yeast* 9, 1121-1130

236. Sprague, G. F. and Cronan, J. E. (1977) Isolation and characterization of *Saccharomyces cerevisiae* mutants defective in glycerol catabolism. *J. Bacteriol.* 129, 1335-1342

237. Grauslund, M. and Ronnow, B. (2000) Carbon source-dependent transcriptional regulation of the mitochondrial glycerol-3-phosphate dehydrogenase gene, *GUT2,* from *Saccharomyces cerevisiae. Can. J. Microbiol.* 46, 1096-1100

238. Lindegaard, B., Larsen, L. F., Hansen, A. B., Gerstoft, J., Pedersen, B. K., and Reue, K. (2007) Adipose tissue lipin expression levels distinguish HIV patients with and without lipodystrophy. *Int. J. Obes. (Lond)* 31, 449-456

239. Donkor, J., Zhang, P., Wong, S., O'Loughlin, L., Dewald, J., Kok, B. P., Brindley, D. N., and Reue, K. (2009) A conserved serine residue is required for the phosphatidate phosphatase activity but not transcriptional coactivator functions of lipin-1 and lipin-2. *J. Biol. Chem.* 284, 29968-29978

240. Kim, H. B., Kumar, A., Wang, L., Liu, G. H., Keller, S. R., Lawrence, J. C., Jr., Finck, B. N., and Harris, T. E. (2010) Lipin 1 represses NFATc4 transcriptional activity in adipocytes to inhibit secretion of inflammatory factors. *Mol. Cell Biol.* 30, 3126-3139

241. Grkovich, A. and Dennis, E. A. (2009) Phosphatidic acid phosphohydrolase in the regulation of inflammatory signaling. *Adv. Enzyme Regul.* 49, 114-120

242. Mul, J. D., Nadra, K., Jagalur, N. B., Nijman, I. J., Toonen, P. W., Medard, J. J., Gres, S., de, B. A., Han, G.-S., Brouwers, J. F., Carman, G. M., Saulnier-Blache, J. S., Meijer, D., Chrast, R., and Cuppen, E. (2011) A hypomorphic mutation in *Lpin1* induces progressively improving neuropathy and lipodystrophy in the rat. *J. Biol. Chem.* 286, 26781-26793

243. Nadra, K., Medard, J. J., Mul, J. D., Han, G.-S., Gres, S., Pende, M., Metzger, D., Chambon, P., Cuppen, E., Saulnier-Blache, J. S., Carman, G. M., Desvergne, B., and Chrast, R. (2012) Cell autonomous lipin 1 function is essential for development and maintenance of white and brown adipose tissue. *Mol. Cell Biol.* 32, 4794-4810

244. Michot, C., Mamoune, A., Vamecq, J., Viou, M. T., Hsieh, L.-S., Testet, E., Laine, J., Hubert, L., Dessein, A. F., Fontaine, M., Ottolenghi, C., Fouillen, L., Nadra, K., Blanc, E., Bastin, J., Candon, S., Pende, M., Munnich, A., Smahi, A., Djouadi, F., Carman, G. M., Romero, N., de, K. Y., and de, L. P. (2013) Combination of lipid metabolism alterations and their sensitivity to inflammatory cytokines in human lipin-1-deficient myoblasts. *Biochim. Biophys. Acta* 1832, 2103-2114

245. Finck, B. N., Gropler, M. C., Chen, Z., Leone, T. C., Croce, M. A., Harris, T. E., Lawrence, J. C., Jr., and Kelly, D. P. (2006) Lipin 1 is an inducible amplifier of the hepatic PGC-1alpha/PPARalpha regulatory pathway. *Cell Metab* 4, 199-210

246. Zhang, Q., Chieu, H. K., Low, C. P., Zhang, S., Heng, C. K., and Yang, H. (2003) Schizosaccharomyces pombe cells deficient in triacylglycerols synthesis undergo apoptosis upon entry into the stationary phase. *J. Biol. Chem.* 278, 47145-47155

247. Richard, A. J., mini-Vaughan, Z., Ribnicky, D. M., and Stephens, J. M. (2013) Naringenin inhibits adipogenesis and reduces insulin sensitivity and adiponectin expression in adipocytes. *Evid. Based. Complement Alternat. Med.* 2013, 549750

248. Swanson, W. H. and Clifton, C. E. (1948) Growth and Assimilation in Cultures of *Saccharomyces cerevisiae. J. Bacteriol.* 56, 115-124

249. Boveris, A., Oshino, N., and Chance, B. (1972) The cellular production of hydrogen peroxide. *Biochem. J.* 128, 617-630

250. Finkel, T. and Holbrook, N. J. (2000) Oxidants, oxidative stress and the biology of ageing. *Nature* 408, 239-247

251. Feng, J., Bussiere, F., and Hekimi, S. (2001) Mitochondrial electron transport is a key determinant of life span in Caenorhabditis elegans. *Dev. Cell* 1, 633-644

252. Arnold, I., Pfeiffer, K., Neupert, W., Stuart, R. A., and Schagger, H. (1998) Yeast mitochondrial F_1F_0-ATP synthase exists as a dimer: identification of three dimer-specific subunits. *EMBO J.* 17, 7170-7178

253. Schmitt, A. P. and McEntee, K. (1996) Msn2p, a zinc finger DNA-binding protein, is the transcriptional activator of the multistress response in *Saccharomyces cerevisiae. Proc. Natl. Acad. Sci. U. S. A* 93, 5777-5782

254. Martinez-Pastor, M. T., Marchler, G., Schuller, C., Marchler-Bauer, A., Ruis, H., and Estruch, F. (1996) The *Saccharomyces cerevisiae* zinc finger proteins Msn2p and Msn4p are required for transcriptional induction through the stress response element (STRE). *EMBO J.* 15, 2227-2235

255. Bissinger, P. H., Wieser, R., Hamilton, B., and Ruis, H. (1989) Control of *Saccharomyces cerevisiae* catalase T gene (CTT1) expression by nutrient supply via the RAS-cyclic AMP pathway. *Mol. Cell Biol.* 9, 1309-1315

256. Wood, M. J., Storz, G., and Tjandra, N. (2004) Structural basis for redox regulation of Yap1 transcription factor localization. *Nature* 430, 917-921

257. Moye-Rowley, W. S., Harshman, K. D., and Parker, C. S. (1989) Yeast *YAP1* encodes a novel form of the jun family of transcriptional activator proteins. *Genes Dev.* 3, 283-292

258. Loewith, R. and Hall, M. N. (2011) Target of rapamycin (TOR) in nutrient signaling and growth control. *Genetics* 189, 1177-1201

259. Wullschleger, S., Loewith, R., and Hall, M. N. (2006) TOR signaling in growth and metabolism. *Cell* 124, 471-484

260. Zheng, X. F. and Schreiber, S. L. (1997) Target of rapamycin proteins and their kinase activities are required for meiosis. *Proc. Natl. Acad. Sci. U. S. A* 94, 3070-3075

261. Torres, J., Di Como, C. J., Herrero, E., and De La Torre-Ruiz MA (2002) Regulation of the cell integrity pathway by rapamycin-sensitive TOR function

in budding yeast. *J. Biol. Chem.* 277, 43495-43504

262. Powers, R. W., III, Kaeberlein, M., Caldwell, S. D., Kennedy, B. K., and Fields, S. (2006) Extension of chronological life span in yeast by decreased TOR pathway signaling. *Genes Dev.* 20, 174-184

263. Bonawitz, N. D., Chatenay-Lapointe, M., Pan, Y., and Shadel, G. S. (2007) Reduced TOR signaling extends chronological life span via increased respiration and upregulation of mitochondrial gene expression. *Cell Metab* 5, 265-277

264. Pan, Y., Schroeder, E. A., Ocampo, A., Barrientos, A., and Shadel, G. S. (2011) Regulation of yeast chronological life span by TORC1 via adaptive mitochondrial ROS signaling. *Cell Metab* 13, 668-678

265. vila-Flores, A., Santos, T., Rincon, E., and Merida, I. (2005) Modulation of the mammalian target of rapamycin pathway by diacylglycerol kinase-produced phosphatidic acid. *J. Biol. Chem.* 280, 10091-10099

266. Knaevelsrud, H. and Simonsen, A. (2012) Lipids in autophagy: constituents, signaling molecules and cargo with relevance to disease. *Biochim. Biophys. Acta* 1821, 1133-1145

267. Fang, Y., Vilella-Bach, M., Bachmann, R., Flanigan, A., and Chen, J. (2001) Phosphatidic acid-mediated mitogenic activation of mTOR signaling. *Science* 294, 1942-1945

268. Shahnazari, S., Yen, W. L., Birmingham, C. L., Shiu, J., Namolovan, A., Zheng, Y. T., Nakayama, K., Klionsky, D. J., and Brumell, J. H. (2010) A diacylglycerol-dependent signaling pathway contributes to regulation of antibacterial autophagy. *Cell Host. Microbe* 8, 137-146